

https://dspace.org/

The effect of the hydrothermal alteration associated with the Saffy East Fault on the UG2 reef at Saffy Shaft of Lonmin Platinum, Western Limb of the Bushveld Complex

Kondlo, Lusanda

2021

https://hdl.handle.net/10539/32293

Downloaded from a DSpace repository. https://dspace.org/

The effect of the hydrothermal alteration associated with the Saffy East Fault on the UG2 reef at Saffy Shaft of Lonmin Platinum, Western Limb of the Bushveld Complex

MSc Economic Geology



UNIVERSITY OF THE
WITWATERSRAND,
JOHANNESBURG

Student name: Lusanda Kondlo

Student No: 1405264

Supervisor: Prof P. Nex

Co-Supervisor: Mrs R. Knipe

Thesis submitted for partial fulfilment of the requirements for the MSc degree

I hereby declare that this research report is my own work and my own interpretation from the data I have collected and analysed for the purpose of this study. It is being submitted for the MSc Economic Geology (CW) degree from the University of the Witwatersrand, School of Geoscience, Johannesburg. It has not been submitted before for any degree or examination in any other institution.

Author: Mr. L. Kondlo

Signature: .

Date: Month of **August** on this **20th** day of **2020**

Acknowledgement

The following individuals are highly appreciated and thanked for all their contribution towards the success of this project. Firstly my supervisor Prof Paul Nex who always guided and offered me his academic knowledge with an open heart, even after I have taken a 2 year gap due to personal commitments; My co-supervisor Mrs Riana Knipe, who is the Geology manager from Saffy Shaft at Lonmin Platinum (now known as Sibanye Stillwater). Mrs Knipe has been not just a co-supervisor but a mother and a mentor to me, she always shown patience and belief in me. I would also like to thank Lonmin Platinum and Saffy Shaft staff for their assistance and for granting me an access to their resources even after I left the company to pursue my MSc degree.

- To MSc program course co-ordinator, Prof Judith Kinnaird for all her guidance and selfless advice, Prof you have taught me to learn from constructive criticism.
- To Dr. Ben Hayes and Dr. Peter Horvath for their assistance with microprobe analysis.
- To PhD candidates Leo and Kirsten for their assistance in Petrographic analysis.
- To Mr Caiphus Majola and Mr Sam for preparing the thin sections for my study.
- To my family who have been with me physically and emotionally giving me parenthood advice and guidance.
- Finally I would like to thank my wife Mrs C.L Jiyana Kondlo for all her support, encouragement and love she has shown to me and to our son and daughter.

Abstract

The UG2 chromitite layer of the western limb of the Bushveld Complex has been mined extensively and studied for its economic importance. The UG2 is defined as a fine-grained dark grey to black in colour, chromitite layer of approximately 1.2 m in thickness, consisting mainly of chromite, orthopyroxene and plagioclase. The UG2 chromitite layer is well-known as the world's largest platinum group elements (PGEs) bearing horizon. Most studies that have been conducted on this economic horizon focus on the normal UG2 chromitite layer and little research on the hydrothermal altered UG2 chromitite has been documented. The presence of hydrothermal altered UG2 at Saffy Shaft at Lonmin Platinum is prevalent within the eastern block of the Lonmin Mining Area and it is associated with known major faults. Sampling for the study has been collected from both Saffy East and Saffy West UG2 chromitite layers at Lonmin Platinum, to study any correlation or differences between the two chromitite layers on the east and west of Saffy Shaft. Channel sampling analysis, surface borehole analysis and underground mapping were all studied and interpreted for any differences that might have led to grade reduction or possible change in the ideal grade distribution. Underground mapping and observations have shown that areas affected by hydrothermal alteration dominate in linear geological structures such as minor faulting, intense jointing and thin veins. It has been observed that top contact of UG2 chromitite layer often exhibits shearing, which is associated with secondary mineralisation. In areas where the UG2 chromitite package is split by pyroxenite lenses, these pyroxenite lenses tends to show the effects of the hydrothermal alteration, such as discolouring and brittle behaviour. The channel sampling data from Saffy East altered chromitite areas contains approximately 2% less total PGE grade compared to less altered chromitite at Saffy West. The altered chromitite areas show less unintentional waste mining than less altered areas. Electron microprobe, scanning electron microscope analysis and petrography were conducted to analyse chemical variation in chromite grains, textural as well as mineralogical changes respectively. The petrographic analysis showed that plagioclase and orthopyroxene are the dominant minerals surrounding the chromite grains with clinopyroxenes in some Saffy East samples. Secondary minerals in Saffy East chromitite such as serpentine, biotite and talc are dominant especially within microstructures. Electron microprobe analysis of chromite showed an increase in aluminium and magnesium at Saffy East, where hydrothermal alteration is known to be prevalent; whereas Cr_2O_3 content is higher at Saffy West. The TiO_2 from both Saffy East and Saffy West shows similar values of approximately 1%, whereas the FeO is higher at Saffy East where the hydrothermal alteration is prevalent. The Cr# and Mg# of Saffy West and Saffy East chromite display slight variation with Saffy East chromite grains showing lower Cr# and higher Mg#; while the Saffy West chromite grains shows a slightly higher Cr# and lower Mg#. SEM studies have shown presence of PGM's from both Saffy East

and West chromite; the observed PGM's are intercumulus to the matrix, they do not occur on the chromite grains.

Table of contents

Chapter one

1. Introduction

1.1 Regional Geology……1

1.2 Local Geology of Lonmin Marikana Operations……6

1.3 The Geology of Saffy Shaft……10

1.4 Aims and objective of the study……13

1.5 Methodology……14

Chapter two

2. Underground observations and borehole data from Saffy Block

2.1 Underground observations and mapping ……16

2.2 Grade and contamination……21

2.2.1 Underground grade contamination and grade distribution……21

2.2.2 Surface Borehole grade and grade distribution……27

Chapter three

3. Petrography and chromite mineral chemistry from Saffy Block

3.1 The formation of chromitite layers……33

3.1.1 The UG2 chromitite layer at Lonmin lease area……33

3.2 Chromitite petrography……33

3.2.1 Similarities and the differences from Saffy East and West samples……34

3.3 Chromite mineral chemistry analysis using Electron Microprobe……37

3.3.1 Chromium and Magnesium number……44

3.4 Bright Phase Scanning Electron Microscopy (SEM)……46

Chapter four

4. Discussion

4.1 The effect of hydrothermal alteration and grade distribution……53

4.2 Chromite petrography interpretation……58

4.3 Electron Microprobe analysis interpretation……59

4.3.1 Cr# and Mg# interpretation……61

4.4 Scanning Electron Microscope interpretation……62

Chapter five

5. Conclusion ……64

References……66

Appendices

Appendice A: Surface borehole showing PGE grade per ton……70

Appendice B: Microprobe analysis (wt. %) from Saffy West samples……72

Appendice C: Microprobe analysis (wt. %) of Saffy East samples……74

Appendice D: Channel sampling of PGE grade results……76

Appendice E: Cr# and Mg#……78

Appendice F: Thin section images from Saffy East and West chromitite samples……80

Appendice G: Saffy East and West bright phase search……85

List of Figures

Figure 1: Simplified geological map showing the five limbs of the Bushveld Complex as well as the Thabazimbi-Murchison Lineament with Platinum reefs sub-crop indicated as a dashed red line (Maier *et al*, 2012).

Figure 2: Simplified stratigraphic column of the Bushveld Comlex showing the main stratigraphic zones (Maier & Barnes, 2008).

Figure 3: Simplified map of Lonmin lease area showing all the shafts at Lonmin Marikana Operations with east and west lease areas indicated (Lonmin, 2014).

Figure 4: A simplified stratigraphic column showing the Merensky and UG2 reefs at Lonmin lease area with stratigraphic interval between the two economic horizons (Lonmin, 2009).

Figure 5: Lonmin Marikana Operation shafts and all major faults throughout the lease area (Hartzenberg, 2019).

Figure 6: Saffy Shaft plan with major geological structures including Saffy East Fault, Turffontein West Fault, Turffontein East Faults and Saffy West Fault; The vertical (north-south) blue dashed line is the boundary between Saffy East and West (Lonmin Saffy Shaft database).

Figure 7: Saffy Shaft plan indicating the mapped underground areas, the red stars indicates the areas mapped at Saffy East side (Lonmin Saffy Shaft database).

Figure 8: Typical stratigraphic column below and above UG2 horizon (Latypov *et al*.2017).

Figure 9: Typical UG2 chromitite split reef, showing two bands of chromitite horizon separated by pyroxenite, letter "C" indicates split chromitite (UG2 split reef), (Latypov *et al*.2017).

Figure 10: Typical underground mapping showing undulating chromitite package, minor faults, infill joints, veinlets and pyroxenite lenses in a stoping area affected hydrothermal alteration at Saffy Shaft.

Figure 11: Typical underground mapping presented on MineCad software showing undulating UG2, minor faults, infill joints and deteriorated ground condition in a stoping area affected hydrothermal alteration (Lonmin Saffy Shaft database).

Figure 12: Mineral resource department channel sampling localities and spatial distribution (Lonmin Saffy Shaft database).

Figure 13: The Saffy Shaft West PGE grade and grade distribution of UG2 chromitite layer from the existing channel sampling data.

Figure 14: The Saffy Shaft East PGE grade and grade distribution of UG2 chromitite layer from the existing channel sampling data.

Figure 15: The combined histogram for Saffy Shaft East and West PGE grade and grade distribution of UG2 chromitite layer from the existing channel sampling data of mineral resource department.

Figure 16: Plan view showing the surface boreholes drilled at Saffy Shaft (Lonmin Saffy Shaft database).

Figure 17 (a): Typical east of Saffy Shaft stope panel photo, showing the hydrothermal alteration above the UG2 reef horizon (Hartzenberg, 2019).

Figure 17 (b): Photo grab of borehole core showing the UG2 chromitite (UG2) with the sheared upper contact (Lonmin Saffy Shaft database).

Figure 18: Surface borehole histograms showing PGE grade and grade distribution of UG2 chromitite layer from Saffy West.

Figure 19: Surface borehole histograms showing PGE grade and grade distribution of UG2 chromitite layer from Saffy East.

Figure 20: Plan showing the spatial distribution of the prepared thin sections from underground channel sampling at Saffy East and cover drilled boreholes at Saffy West (Lonmin Saffy Shaft database).

Figure 21: Photomicrographs illustrating polished thin sections from Saffy West and East samples of chromitite layer of Saffy Shaft.

Figure 22 (a): Graph showing the concentration of Ti_2O vs MgO from Saffy East and Saffy West chromite grains.

Figure 22 (b): Graph showing the concentration of Ti_2O vs Al_2O_3 from Saffy East and Saffy West chromite grains.

Figure 22 (c): Graph showing the concentration of FeO vs Al_2O_3 from Saffy East and Saffy West chromite grains.

Figure 22 (d): Graph showing the concentration of FeO vs MgO from Saffy East and Saffy West chromite grains.

Figure 22 (e): Graph showing the concentration of Al_2O_3 vs MgO from Saffy East and Saffy West chromite grains.

Figure 22 (f): Graph showing the concentration of Al_2O_3 vs Cr_2O_3 from Saffy East and Saffy West chromite grains.

Figure 22 (g): Graph showing the concentration of TiO_2 vs Cr_2O_3 from Saffy East and Saffy West chromite grains.

Figure 22 (h): Graph showing the concentration of MgO vs Cr_2O_3 from Saffy East and Saffy West chromite grains.

Figure 22 (i): Graph showing the concentration of Fe0 vs Cr_2O_3 from Saffy East chromite grains.

Figure 22 (j): Graph showing the Cr# versus Mg# of chromite grains from the east side of Saffy Shaft.

Figure 22 (k): Graph showing the Cr# versus Mg# of chromite grains from the west side of Saffy Shaft.

Figure 23 (a): Photomicrographs showing bright particle 1 from Saffy East thin section, with a zoomed-in view of the same particle on the right.

Figure 23 (b): Photomicrographs showing bright particle 2 from Saffy East thin section with a zoomed-in view of the same particle on the right.

Figure 24: Typical mineral spectra for Saffy East bright particle 1, indicating the dominating elements; where platinum (Pt) and gold (Au) show significant peaks.

Figure 25: Spectra for particle 1, indicating the dominating elements within the bright particle of Saffy East, where iron (Fe), potassium (K), nickel (Ni) and sulphur (S) are present.

Figure 26: Photomicrographs showing the identified six particles from Saffy West thin section

Figure 27: Spectra for particle 3, indicating the dominating elements within the bright particle of Saffy West, where tantalum (Ta), tungsten (W) and gold (Au) are present.

Figure 28: The presence of talc, serpentine and shearing in chromitite layers at Lonmin Platinum (Hartzenberg, 2019).

Figure 29: Plot of Pt, Pd and Pt/Pd ratio in 2cm thick samples of the UG2 chromitite from Lonplats Mines (Hiemstra, 1985).

Figure 30: Vertical distribution of the PGE concentration, nickel and copper in the UG2 chromitite layer at Lonmin (Lonmin pub, 2009).

Figure 31: Analysis showing the Cr# and Mg# of seven chemical group layers, showing variation in host rock units (after Junge *et al.* 2014).

List of Tables

Table 1: Lonmin mineral resource department data showing difference in grade with both footwall and hangingwall unintentional waste mining at Saffy Shaft in areas where PGE (4E's) channel sampling has been analysed.

Table 2: Typical mineral composition of the samples from Saffy East and West.

Table 3: Saffy East average compositions of the chromite grains from the UG2 chromitite.

Table 4: Saffy West average compositions of the chromite grains from the UG2 chromitite.

Table 5: Average compositions of the chromite crystals from the lower and upper chromitite layer from the Merensky Reef, (Vukmanovic *et al*.2013).

Keywords

Bushveld Complex

Chromite composition

Hydrothermal Alteration

Lonmin Platinum

Saffy Shaft

UG2 Reef

Chapter 1

1. Introduction

The Bushveld Complex is made up of ultramafic, mafic, granitic and granophyre rocks. The ultramafic and mafic rocks are known as Rustenburg Layered Suite (RLS), while the granitic rocks are known as the Lebowa Granite Suite (Barnes and Maier, 2002). The Bushveld Complex is the large layered mafic intrusion, subdivided stratigraphically into five major units and they are the Marginal, Lower, Critical, Main, and Upper Zones, which comprise a total thickness of about 7–9 km (Latypov *et al*.2017). Bushveld Complex is greater than 350 km in diameter and was emplaced at approximately 2.05 billion years ago into the Transvaal Supergroup sequence (Latypov *et al*.2017 and Zeh *et al.*2015). The Bushveld Complex was formed by the repeated injection of magma into the crust from possibly a crustal staging chamber (Cawthorn, 1999). The Bushveld Complex is the world's largest layered mafic intrusion in which products of crystallisation and fractionation can be observed, and the large-scale processes giving rise to the layered rocks with its associated mineralisation are well preserved (Cawthorn and Walraven, 1998).

During the formation of Bushveld Complex, cooling and crystallization was relatively slow. The silicate minerals crystallised and accumulated forming igneous rocks and the temperature decrease and changes in magma composition resulted in changes in mineral compositions. The minerals formed accumulated in sub-horizontal layers occurring from the base to the top of the magma chamber, producing cyclic units of the mineral layering (Schouwstra *et al*., 2000). The layering in the complex is disturbed by several major geological structures such as faults, potholes, intrusive iron rich ultramafic pegmatite (IRUP), dykes and sills.

This study will focus on the effect of the hydrothermal alteration associated with the Saffy East Fault on the Upper Group 2 (UG2) chromitite at Saffy Shaft of Lonmin Platinum Marikana Operations in the western limb of the Bushveld Complex. This hydrothermal alteration is often disruptive to mining as the areas affected by alteration are characterised by low PGE grade and a crumbling hangingwall pyroxenite which causes geotechnical concerns.

1.1 Regional Geology

The Bushveld Complex includes one of the world's largest A-type granites and rhyolites and constitutes some of the world's most valuable mineral deposits, hosting the bulk of global resources in PGE, Cr and V, with significant Cu, Ni, Au, Sn, fluorite and dimension stone (Wilson *et al.,* 1998). The Bushveld Complex intruded as a flat, sill-like sheet typically at the boundary between the felsic rocks

of the Rooiberg Group and the underlying Pretoria Group. Despite the overall sill-like character, some features of a funnel-shaped intrusion are evident. The Lower Zone outcrop is discontinuous, and the upper Critical Zone and Main Zone transgress the floor-rocks in places as shown in the Eastern Bushveld Complex (Kruger, 2005). The bulk of the Bushveld Complex and most of the world's other substantial PGE- mineralised intrusions are in stabilised cratons (Maier and Groves, 2011).

The Bushveld Complex was emplaced into the Kaapvaal craton and generally intruded into the Transvaal Supergroup, which comprises a very thick package of intracratonic chemical and clastic sedimentary rocks, ranging in age from 2551 to 2204 Ma (Walraven *et al.*, 1990). The Bushveld Complex is divided into the Eastern, Western, Northern and Bethal limb (Fig.1). An extension known as the far Western limb has also been identified (Cawthorn and Walraven, 1998). The Western limb extends +-200 km along an arc from Thabazimbi to near Pretoria. The Eastern limb strikes more than 200 km from Stoffberg to Chuniespoort and underlies a more rugged terrain where surface exposure is better.

The Bushveld Complex extends 288 km along strike (E-W axis) and from Pretoria ~153 km north-south. It consists broadly of continuous layers of igneous rocks which extend laterally for 300 km with an approximated thickness of 9 km (Kinnaird *et al.*, 2002). The Thabazimbi-Murchison Lineament (TML) is central to the tectonics of the Bushveld Complex, as it is a long lived continuously reactivated fault, which was active before, during and after the intrusion of the Bushveld Complex (Good and de Wit, 1997). The Bushveld complex is sub-divided into five stratigraphic zones, which are the Marginal Zone, Lower Zone, Critical Zone (lower and upper), Main Zone and Upper Zone (Fig. 2). Within the Lower Critical Zone there are a number of chromitite layers divided into Lower Group (LG) 1 to 7 and Middle Group (MG) 1 and 2. The Upper Critical Zone includes the MG 3 and 4, as well as UG 1 and 2. In the northern part of the Eastern Bushveld Complex the Upper Group 2 (UG2) splits, such that the upper part of UG2 forms the Upper Group 3 (UG3), (Kruger, 2005). The Lower and Middle Group chromitites are extracted for chromite, while the UG2 layer is mined for platinum group elements (PGE) (Lee, 1996). Different models have been suggested explaining the formation of chromitite layers in the Bushveld Complex which include: magma mixing, gravitational settling, liquid immiscibility, oxygen fugacity changes and increase in pressure (Kinnaird *et al*., 2002). However Latypov *et al*.2017, suggest that Bushveld Complex chromitites formed from magma emplaced along the floor of the chamber, from which crystallization took place essentially in situ, on the magma cumulate interface.

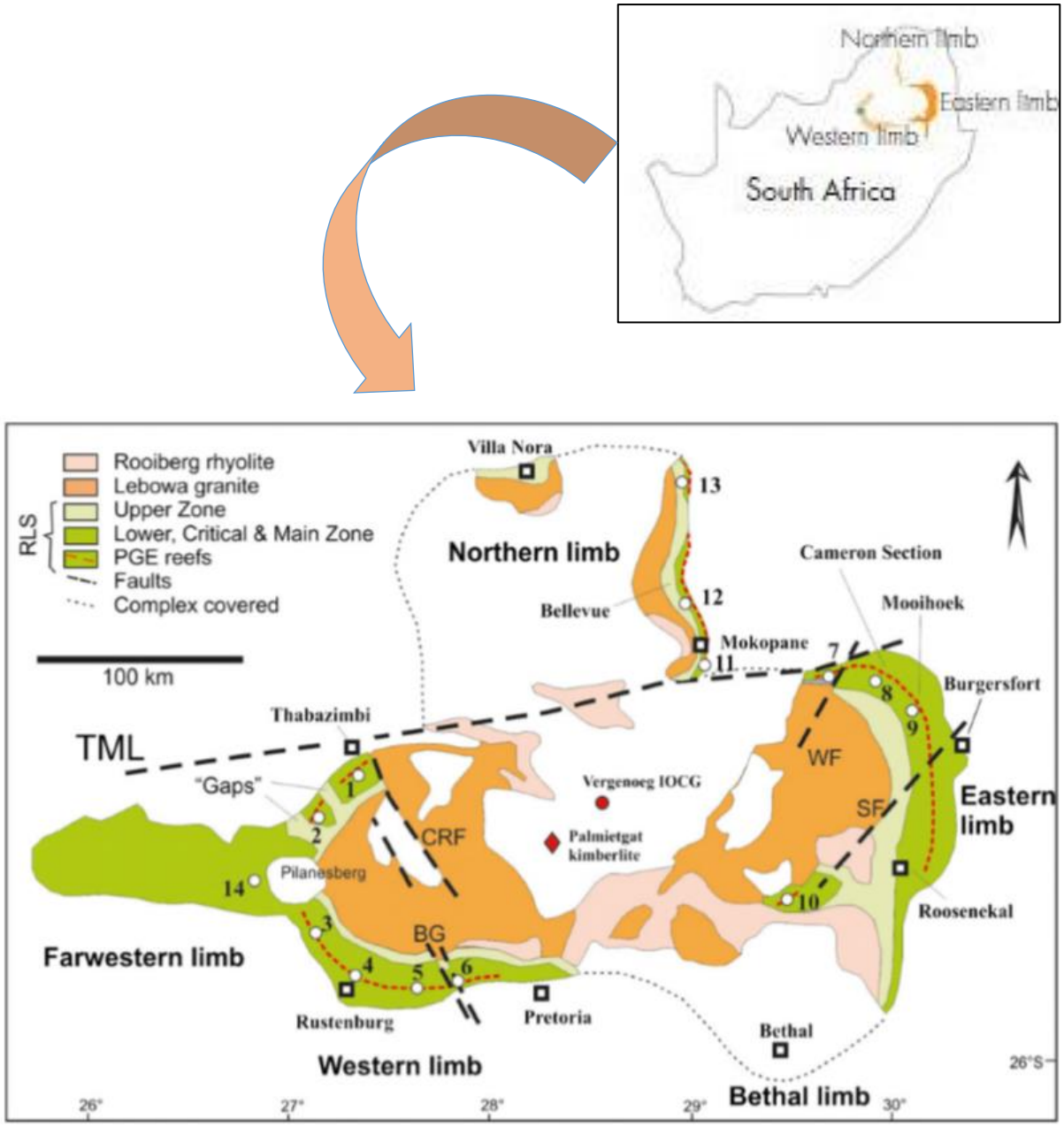


Fig 1: Simplified geological map showing the five limbs of the Bushveld Complex as well as the Thabazimbi-Murchison Lineament (TML) with Platinum reefs sub-crop indicated as a dashed red line (Maier *et al*, 2012).

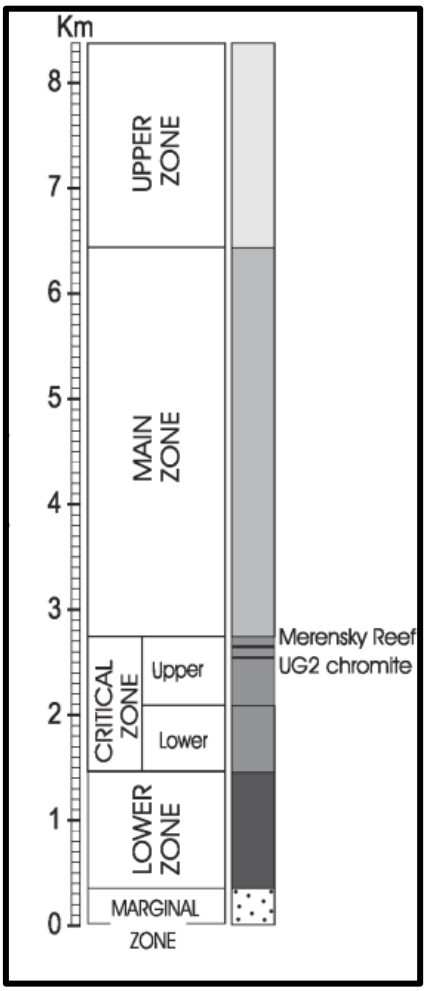


Fig 2: Simplified stratigraphic column of the Bushveld Comlex showing the main stratigraphic zones (Maier & Barnes, 2008)

Location of the study area

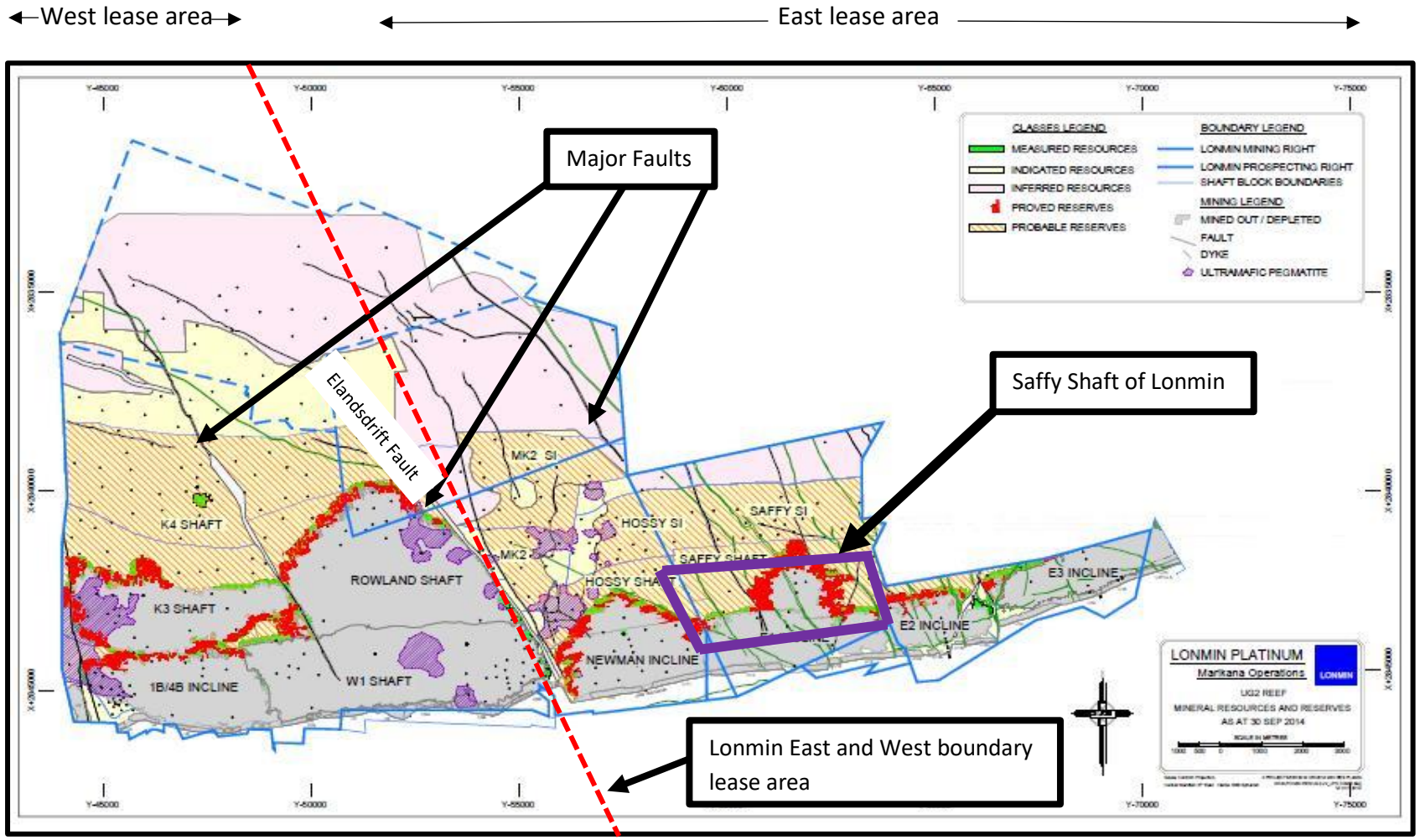


Fig 3: Simplified map of Lonmin lease area showing all the shafts at Lonmin Marikana Operations with east and west lease areas indicated, red dashed sub-vertical line indicates the east and west boundary of Lonmin lease area in Marikana Operations (Lonmin, 2014).

1.2 Local Geology of Lonmin Marikana Operations

Lonmin Platinum was previously the third largest primary producer of platinum in the world before the takeover by Sibanye Stillwater in the year 2019. The Marikana operations of Lonmin are situated in the Western Limb of Bushveld Complex; 30 km to 60 km east of Rustenburg in the North-West Province. Lonmin exploits the Merensky and Upper Group 2 (UG2) reefs for their platinum group element (PGE) contents; both reefs are located in upper Critical Zone of the Bushveld Complex (Fig.2). These economic horizons (Merensky and UG2) outcrop along the 27 km strike of the Lonmin Marikana lease area, are exploited extensively both in open cast and underground mining. The ore bodies strike in a general east-west direction and dip between 9° and 14°north. All the shafts located on the eastern side of Lonmin lease area or east of the Elandsdrift Fault (Fig.3 and Fig.5) are currently extracting PGE from the UG2 chromitite layer only, while all the shafts allocated on the western side of Lonmin lease area are extracting both UG2 and Merensky reefs (Fig. 3 and Fig.5). The stratigraphic interval between the Merensky and UG2 reefs increases from ~ 130 m at Karee mine in the west to more than 210 m at East 3 Incline shaft (Fig. 4).

Geological disturbances such as faults, joints, potholes, IRUP's and thrust planes affect the ore bodies at Lonmin Marikana operations (Van der Merwe *et al*, 1998). The shaft boundaries are mostly separated by the major faults (Fig. 5), which have between 30 m and -150 m displacement (Lonmin, 2009); however, some of the incline shafts on the eastern side of the lease area at Lonmin Platinum are separated by sub-vertical dolerite dykes of approximately 40m thickness. It has been observed that some of the major faults and major dolerite dykes on the Lonmin lease area are associated with significant volumes of meteoric ground water; this impacts on mining as it delays extraction processes and the associated structures and secondary minerals, which might impact on the ground conditions.

The UG2 chromitite varies from 1m - 1.2m thick in the Marikana Operations lease area, where the immediate footwall to the UG2 is a medium grained mottled anorthosite in the western side of Lonmin lease area and a coarse grained pegmatoidal pyroxenite in the eastern side of the Lonmin lease area; whereas immediate hangingwall to the UG2 is a barren brownish medium-grained pyroxenite with sharp contacts. The footwall contact to the UG2 chromitite layer from west to east of the lease area is sharp and undulating while the top contact is sharp and planar (Fig: 4).

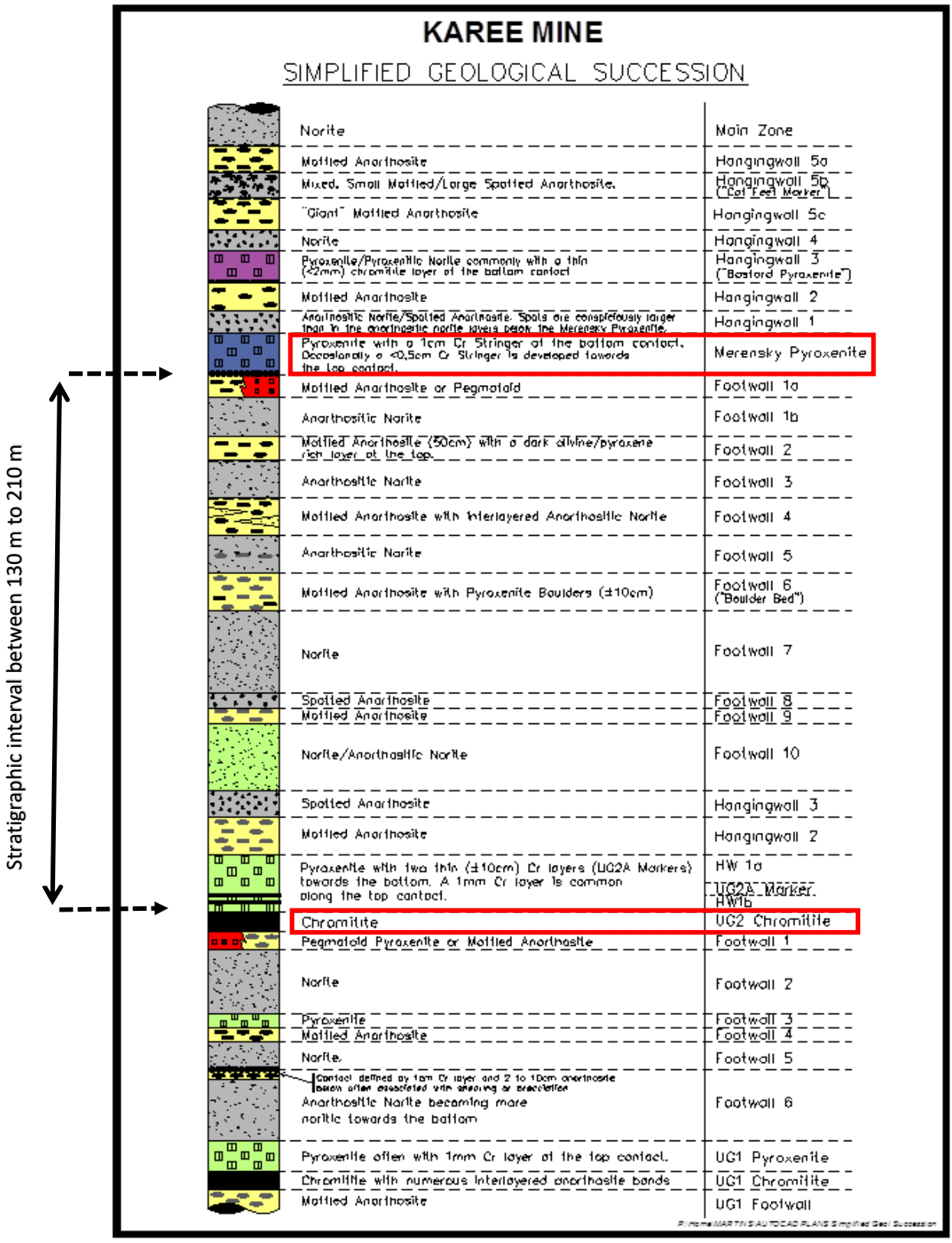
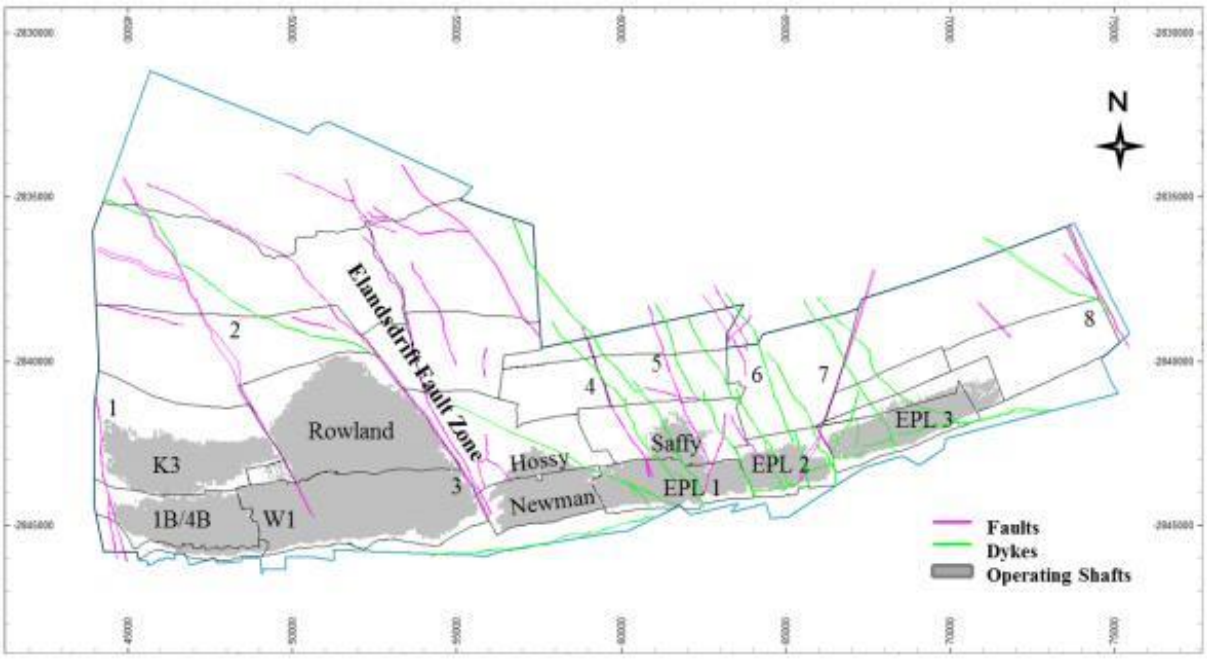


Fig 4: A simplified stratigraphic column showing the Merensky and UG2 reefs at Lonmin lease area with stratigraphic interval between the two economic horizons. Merensky and UG2 horizons are bordered red (Lonmin, 2009).



1-Spruitfontein Fault
2-Marikana Fault
3-Elandsdrift Fault Zone
4-Saffy West Fault
5-Saffy East Fault
6-Turffontein Faults
7-Harties West Fault
8- Roodekopjes Fault

Fig 5: Lonmin Marikana Operation shafts and all major faults throughout the lease area (Hartzenberg, 2019).

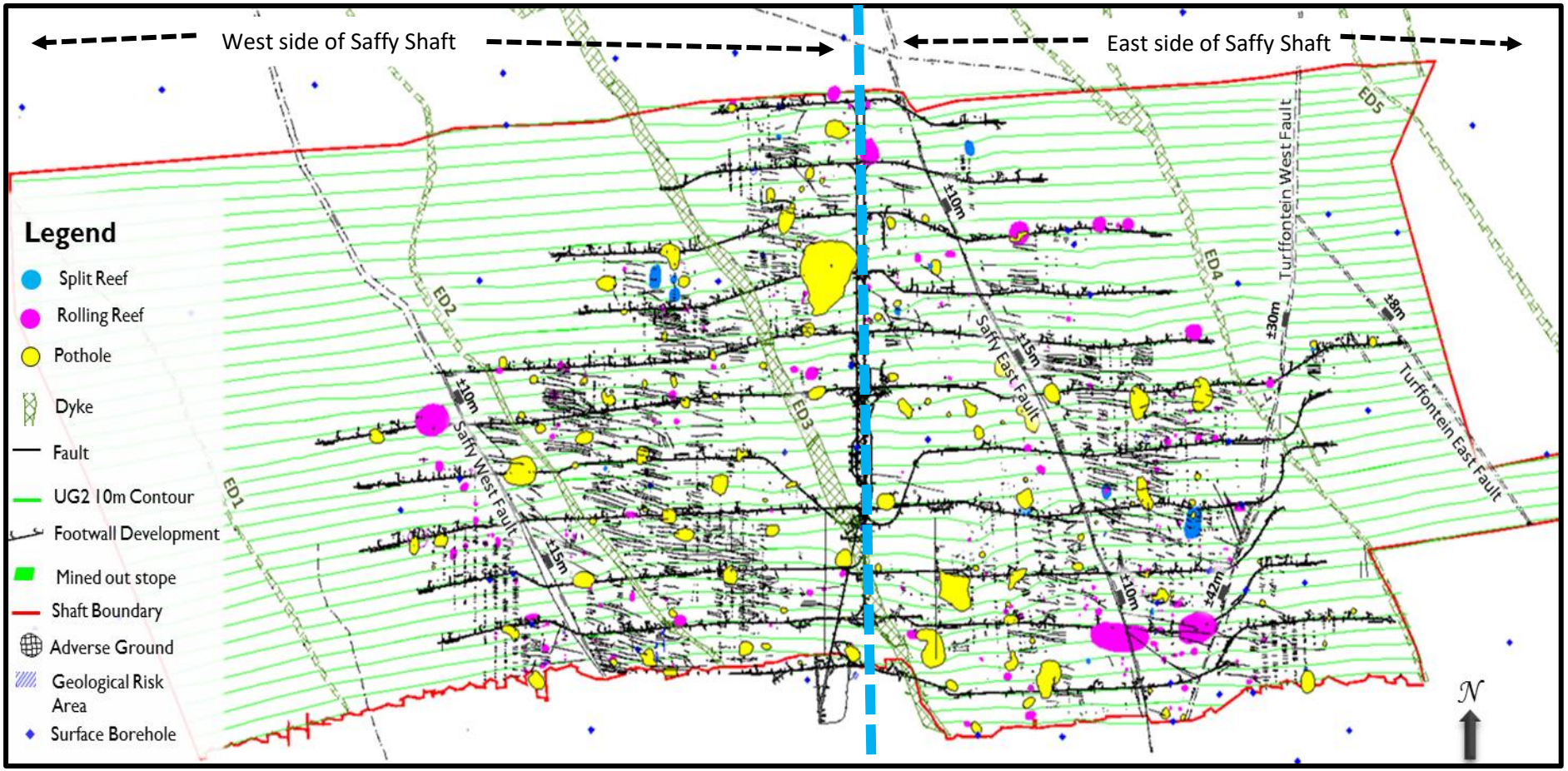


Fig 6: Saffy Shaft plan with major geological structures including Saffy East Fault, Turffontein West Fault, Turffontein East Faults and Saffy West Fault; The vertical (north-south) blue dashed line is the boundary between Saffy East and West (Lonmin Saffy Shaft database).

1.3 The Geology of Saffy Shaft

The Saffy Shaft block is situated on farm Turffontein 462JQ, immediately down dip of the East-1 Incline Shaft block. Surface elevation in Saffy Shaft area varies between 1148 m and 1158 m above mean sea level (amsl); however the UG2 chromitite layer is situated between 870 m and 450 m amsl, which equates to between 291 m and 711 m below surface elevation (Lonmin, 2009). The Saffy Shaft operations exploit the UG2 chromitite layer only, which forms a narrow tabular layer approximately 1.2 m thick, striking east-west and dipping at an average of 11.5° north (Lonmin, 2009). The underlying layer to the UG2 is pegmatoidal pyroxenite and norite respectively; while above the UG2 is pyroxenite. The UG2 chromitite at Saffy Shaft is known to be disturbed and modified by geological features including faults, joints, potholes, rolling reefs, dykes, internal waste lenses (pyroxenite and anorthosite) and hangingwall hydrothermal alteration (Fig.6) which has caused some areas containing UG2 reserves to be abandoned**.** Saffy Shaft is characterised by prominent NW to NNW striking faults and dolerite dykes, and by the low- angle layer parallel and sub-parallel faults and shear structures on the top contact of chromitite layer as well as in the overlying pyroxenite. The underground observations indicate that similar layer parallel structures occur on the east shafts (east of Elandsdrift Fault) such as Newman, Hossy, East 1, East 2 and East 3 incline Shafts.

Another layer parallel fault best developed on the footwall 4-footwall 5 contact (FW4-FW5) and footwall 5-footwall 6 contact (FW5-FW6) (Fig 4) is locally referred to as the footwall shear (FW shear) which is more prominent on the eastern shafts, compared to the western shafts on Lonmin Platinum. The low angle faulting is also observed directly above and below the prominent Upper Group 2A chromitite layers (UG2A chromitite layers). The hydrothermal alteration at Saffy Shaft is associated with more intense structural deformation associated with the Saffy East Fault, where intense jointing, random veinlets associated with secondary mineralisation, brittle rock behaviour and discolouring of the hangingwall pyroxenite is identified (Davis, 2013). There are mineralogical differences between the UG2 chromitite at shafts on east of Lonmin compared to the UG2 chromitite at shafts on west of Lonmin, causing the ore to react differently during flotation process with emphasis on Pt, Pd and Rh. This difference is in the abundance of base metal sulphides and PGM mineral assemblages (Penberthy *et al*. 1999).

Flotation test work done in year 2012 at Lonmin confirmed there is difference in bulk modal base metal sulphides abundance and the difference in PGM association between east and west shafts of Lonmin Platinum. The slightly lower recovery of PGM's from UG2 chromitite at Saffy Shaft and slightly higher mass pull during flotation separation compared to K 3 and Rowland Shaft on the western lease area of Lonmin Marikana Operations. This could be the effect of secondary minerals in the hangingwall

pyroxenite directly above the UG2 chromitite layer and also the presence of these secondary minerals on the UG2 layer could contribute to this effect.

The presence of hangingwall hydrothermal alteration is highly prevalent adjacent to the Saffy East Fault and Turffontein West Faults (Davis, 2013). In areas affected by hydrothermal alteration, hangingwall conditions tend to deteriorate due to intense jointing and poor cohesion, resulting in additional unplanned unintentional waste mining in both development and stoping areas. There has been no formal study conducted to describe the reaction and characteristics of the UG2 chromitite layers in areas affected by hangingwall hydrothermal alteration at Saffy Shaft of Lonmin Platinum. However, Davis, 2013 described and documented the change in mineralogy in the immediate hangingwall of UG2 chromitite layer.

The hangingwall deformation and different UG2 mineralogy at Saffy Shaft and other shafts in east of Lonmin lease area, together with the evidence of low temperature hydrothermal alteration in an area adjacent to the Saffy East Fault suggest that there is a requirement to understand the spatial extent of immediate hangingwall pyroxenite to the UG2; and if the UG2 chromitite east of Lonmin especially at Saffy Shaft is itself affected by hydrothermal alteration. There is a general perception from Technical Service Departments at Saffy Shaft that the UG2 immediate hangingwall pyroxenite on east side of Saffy Shaft is more altered than on the west side, this is based on the hangingwall pyroxenite conditions adjacent to the Saffy East Fault. However recently more intense deformation and areas with possible hydrothermally altered hangingwall pyroxenite has been identified on the west side of Saffy Shaft.

The purpose of this study is to determine the effect of the hydrothermal alteration associated with the Saffy East Fault on the UG2 chromitite layer at Saffy Shaft of Lonmin Platinum Marikana Operations in the western limb of the Bushveld complex. The hydrothermal alteration at Saffy Shaft where the study is conducted is known to be significant on the immediate UG2 hangingwall pyroxenite of eastern side of the shaft adjacent to sub vertical faults (Davis, 2013). At Saffy Shaft there is no formal study that has been conducted to determine if the hydrothermal alteration has any effect in overall UG2 chromitite PGE grade, or possibly in changes of grade distribution in the UG2 chromitite layer or perhaps if the hydrothermal alteration contributes to relatively slightly lower Platinum Group Metal (PGM) recoveries and slightly higher mass pull compared to the UG2 on the western side of the Marikana Operations.

It is expected that the UG2 chromitite layer adjacent to Saffy East Fault from the east side of Saffy Shaft will show a different mineralogical composition, PGE grade, grade distribution, and geochemical

composition, compared to the UG2 chromitite layer from the western side of Saffy Shaft, as Saffy East is perceived by Technical Service Departments to be affected by hydrothermal alteration. Lonmin surface borehole database and underground channel sampling data are analysed for PGE grade variation, whereas underground mapping is conducted for the determination of geological structures associated with hydrothermal alteration. Surface boreholes and channel sampling data is expected to show variation in PGE grade and grade distribution between Saffy East adjacent to Saffy East Fault and Saffy West.

1.4 Aims and Objectives of the study

Previous research indicated that the base metal sulphide mineralogy and PGM mineralogy as well as the mineral association in the UG2 chromitite layers at the shafts east of the Elandsdrift Fault (east of Lonmin) differ from the shafts west of Elandsdrift Fault (west of Lonmin), (Penberthy *et al*.1999). The more abundant, prominent low-angle layer as well as the sub-parallel structures with the proven hydrothermal alteration associated with the Saffy East Fault will be investigated. The effect influencing slightly higher mass pull during flotation separation will also be studied, as to determine if the mineralogical variation in the UG2 chromitite layer could be the result of hydrothermal alteration associated with more intense structural deformation east of the Elandsdrift Fault.

Aim

The aim of this research is to compare a degree of hydrothermal alteration of the UG2 chromitite east and west of the Saffy Shaft as well as to determine relationships between alteration and faulting or other deformations.

Objectives

- To determine if there is a difference in the mineralogical composition of the UG2 chromitite from an area with known hydrothermally altered hangingwall (HW) pyroxenite compared to an area with no visual evidence of alteration in the hangingwall.
- To determine if there are secondary minerals in the UG2 chromitite layer which could potentially have an influence on flotation separation of the PGMs, such as clay minerals formed from the breakdown of plagioclase.
- To determine if there is a difference in the PGE grade or grade distribution in the UG2 chromitite in an area with known hydrothermally altered hangingwall pyroxenite compared to an area with no visual evidence of alteration in the hangingwall.
- To determine if there is any chromite grain morphological difference between Saffy East and Saffy West.
- To study and analyse the UG2 chromitite from Saffy West and compare it with UG2 chromitite from Saffy East adjacent to Saffy East Fault and Turffontein Fault.

1.5 Methodology

The study area is at Saffy Shaft, in particular the area between the Saffy East Fault and Turffontein West Fault at Saffy Shaft of Lonmin Platinum Marikana Operations. Underground mapping was conducted from both Saffy East and Saffy West and it was conducted to constrain the geology and structural deformation in the sampled areas.

<u>Saffy East underground mapped and studied areas are as follows</u>

- 15 East 35 02 West Panel
- 15 East 35 01 West Panel
- 11 East 23 04 West Panel
- 14 East 32 Raise
- 11 East 23 5West Advanced Strike Gully (ASG)
- 20 East 03 East Panel
- 20 East 03 East Advanced Strike Gully (ASG)
- 20 East 02 East Advanced Strike Gully (ASG)

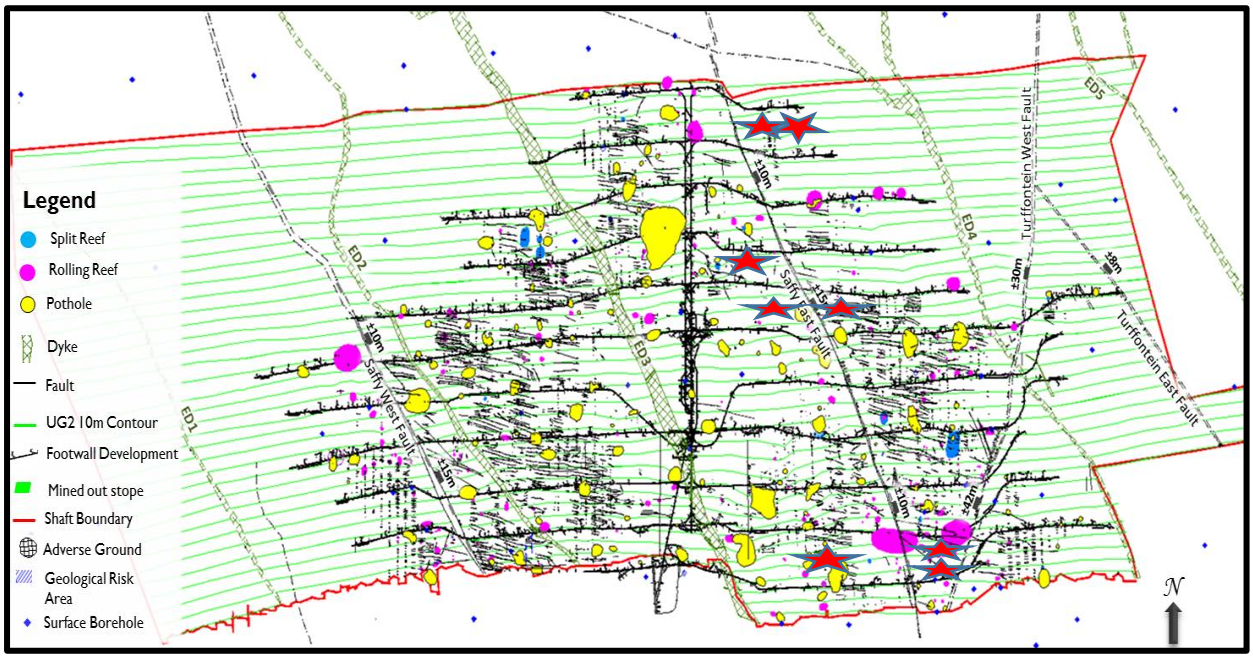


Fig 7: Saffy Shaft plan indicating the mapped underground areas, the red stars indicates the areas mapped at Saffy East side (Lonmin Saffy Shaft database).

UG2 chromitite sampling has been conducted from underground mining areas, from areas with visual indication of immediate altered hangingwall pyroxenite, this sampling has been done for mineralogical purposes and chromite composition analysis. Whereas for the areas with no visual indication of

altered hangingwall pyroxenite, the UG2 chromitite sampling has been done from the diamond drilled boreholes from Saffy Shaft core yard. A total of 22 samples have been prepared for polished thin sections, which are utilised for petrography, microprobe analysis and scanning electron microprobe (SEM).

The existing PGE grade and grade distribution from Lonmin's surface borehole database from Saffy East side has been compared with borehole information from Saffy West. Random surface borehole selection has been done from areas adjacent to Saffy East Fault and also from areas in the west side of the shaft to compare any possible variation from grade or grade distribution. Also the existing PGE grade and grade distribution with identified contamination from Lonmin's underground routine daily sampling database from areas with visual altered hangingwall pyroxenite on the east is compared with areas with no visual altered hangingwall pyroxenite on the west.

Chapter 2

2. Underground observations and borehole data from Saffy Block

2.1 Underground observations and mapping

Davis (2013) identified hydrothermal alteration in the pyroxenite which overlies the UG2 chromitite layer and concluded that areas adjacent to the Saffy East Fault are characterised by a very brittle pyroxenite which crumbles when exposed in underground operations and this is primarily caused by the low temperature hydrothermal alteration of the pyroxenite hangingwall above the UG2 chromitite layer. These areas with altered hangingwall pyroxenite can also be identified on the mine plans, due to excessive mined barren pyroxenite which varies between tens of centimetres to couple of metres. The areas affected by the hydrothermal alteration are also identified from underground working areas at Saffy Shaft from underground observation and routine mine mapping.

Therefore for the purpose of this study, is to analyse the areas on the west of Saffy Shaft and areas on the east adjacent to Saffy East Fault and Turffontein Fault are mapped in order to compare and analyse any variations in the UG2 chromitite and its associated geological structures. The typical overlying pyroxenite which is UHW1b at Saffy Shaft is brownish grey in colour with medium grain size and has a planar sharp contact with the underlying UG2 chromitite (Fig.8). The UG2 chromitite immediate hangingwall is split into two units by approximately two to three 5 cm thin chromitite layers known as Upper Group 2A makers (UG2A markers or triplets), where below the chromitite markers it is called hangingwall 1B pyroxenite (i.e. UHW1B), whereas above the chromitite markers it is called hangingwall 1A pyroxenite (i.e. UHW1A),Fig.8.

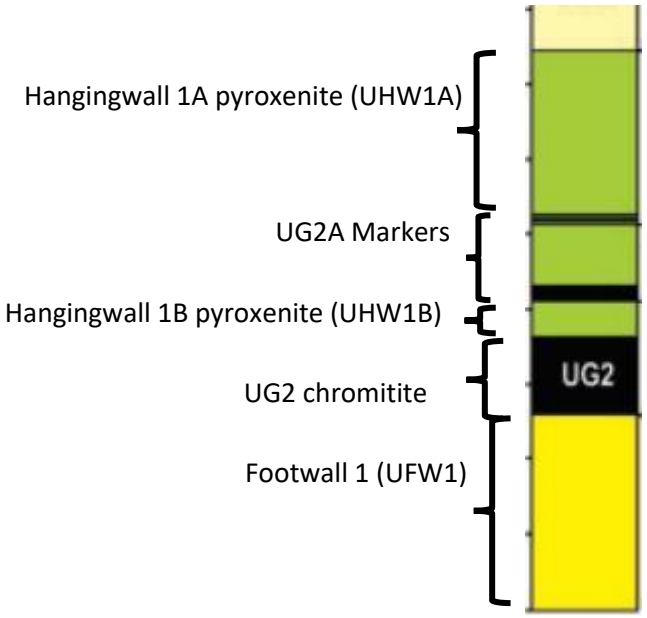


Fig 8: Typical stratigraphic column below and above UG2 horizon (Latypov *et al*.2017)

It is of fundamental importance to note that the UG2A markers or triplets are not exposed in mining areas on the far east shafts of Lonmin (i.e. Hossy and Saffy Shafts, as well as at Newman, E1, E2 and E3 incline shafts) as they are approximately 8 m above the mineralised UG2 chromitite layer. On the west shafts of Lonmin (i.e. Rowland and Karee Shafts) the UG2A markers or triplets are often mined with the UG2 chromitite as they lie directly above the UG2 chromitite horizon. At Saffy Shaft the ~1.2 m UG2 chromitite (mineralised zone) is grey to black in colour with fine grained minerals, with a sharp undulating contact with its underlying pegmatitic pyroxenite, locally anorthosite rock type underlies the UG2 chromitite horizon. The underlying 20 to 90 cm pegmatitic pyroxenite or anorthosite is locally known as footwall 1 (UFW1), (Fig.8). Pegmatitic pyroxenite is brownish in colour with coarse grains, whereas in a case if its anorthosite it is normally white in colour with pyroxene patches forming a gradational contact to its underlying norite rock type layer known as footwall 2 (UFW2). In some areas, lenses or sublayers of barren silicate rocks which are either anorthosite or pyroxenite splits the UG2 chromitite horizon into two bands (Fig.9).

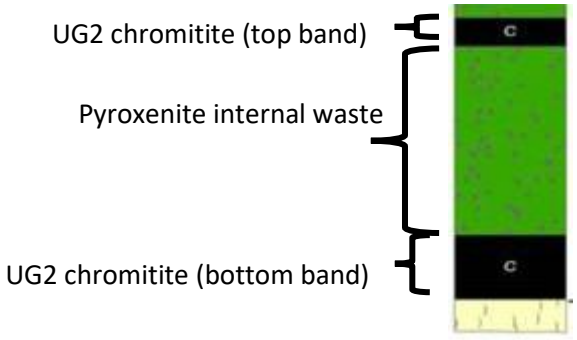


Fig 9: Typical UG2 chromitite split reef, showing two bands of chromitite horizon separated by pyroxenite sublayer, letter "C" indicates split chromitites (Latypov *et al*.2017).

It has been observed from the underground mine mappings that on the west of Saffy Shaft the rock units shows the typical and expected characteristics. On the east of Saffy Shaft especially adjacent to Saffy East Fault, a change in colour, texture with joints and minor faults is observed on the rock layers/units. The pyroxenite colour adjacent to Saffy East Fault changes from brownish colour to dark greenish, giving the pyroxenite a crumbling character. Adjacent to Saffy East Fault, geological structures such as minor faulting with an approximate 5 - 45 cm displacement and the moderate to intense jointing with an average dip of 40°-80° is observed (Fig.10). The introduction of thin veins filled with secondary white minerals has been also observed on the east side of the shaft especially adjacent to Saffy East Fault. Whereas the rolling or undulating UG2 chromitite layer is observed from both east

and west of Saffy Shaft, however on the east of Saffy Shaft the UG2 overlying barren hangingwall pyroxenite is excessively mined in underground mined areas for up to 1.35 m in development areas, this is probably because of crumbling behaviour and compromised strength of the immediate hangingwall pyroxenite, which is effected by hydrothermal alteration compromising the rock strength.

On the east of the shaft the horizontal pyroxenite lenses or internal waste, which separates the UG2 chromitite package into at least two bands or even three bands, also assumes the greenish colour and become more brittle. In mining areas at Saffy Shaft where the UG2 is separated by pyroxenite lenses into two bands, the top UG2 band becomes thinner (+-35 cm) while the bottom UG2 band tend to be the thicker (+-70 cm), Fig.9. The consistent thrust plane, with is evidence of horizontal movement on top contact of UG2 chromitite package on east of Saffy Shaft has been observed at Saffy East drilled core (Fig.17b), whereas it seems to be rare on the west side of Saffy Shaft.

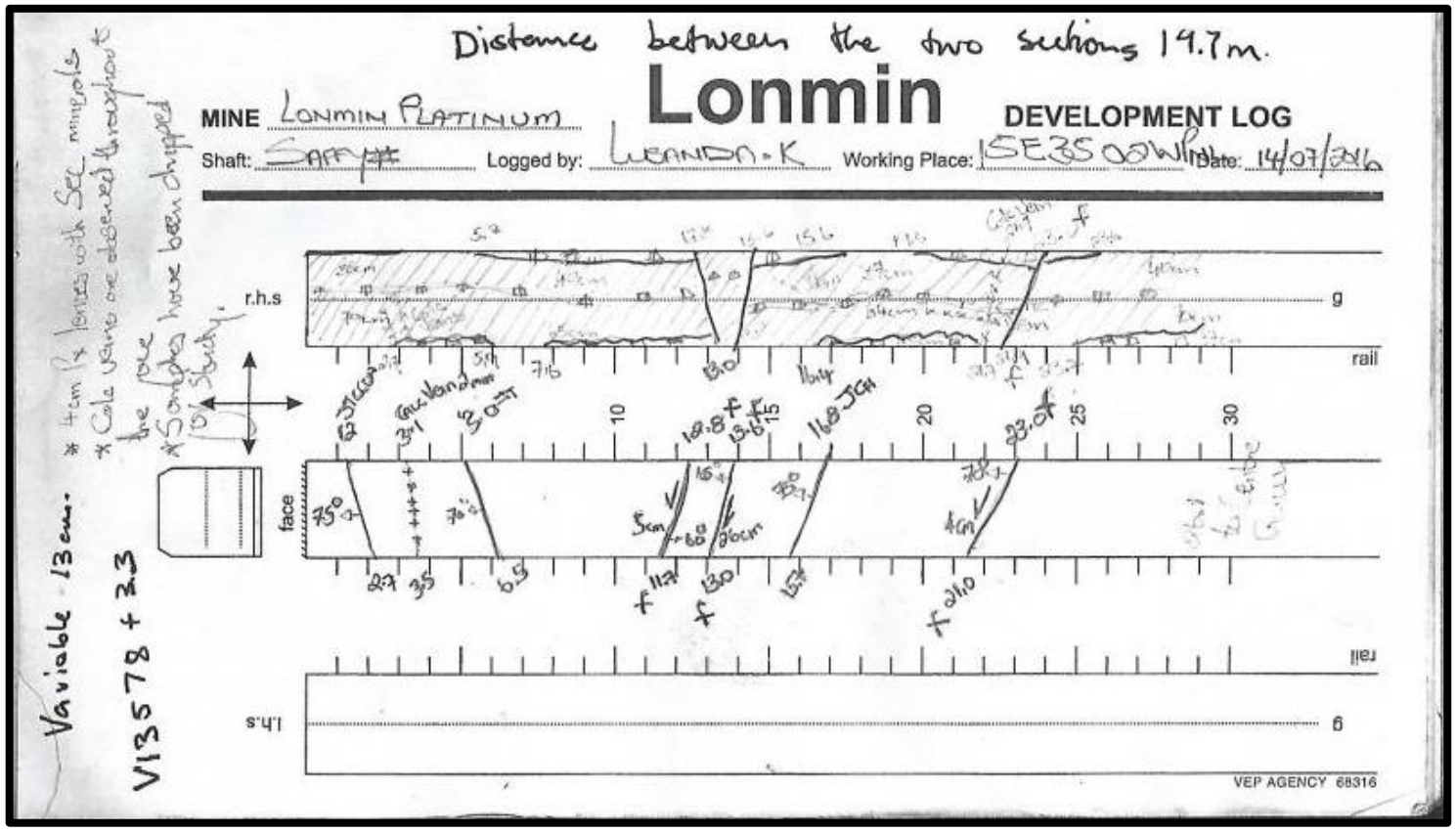


Fig 10: Typical underground mapping showing undulating chromitite package, minor faults, infill joints, veinlets and pyroxenite lenses in a stoping area affected hydrothermal alteration at Saffy Shaft.

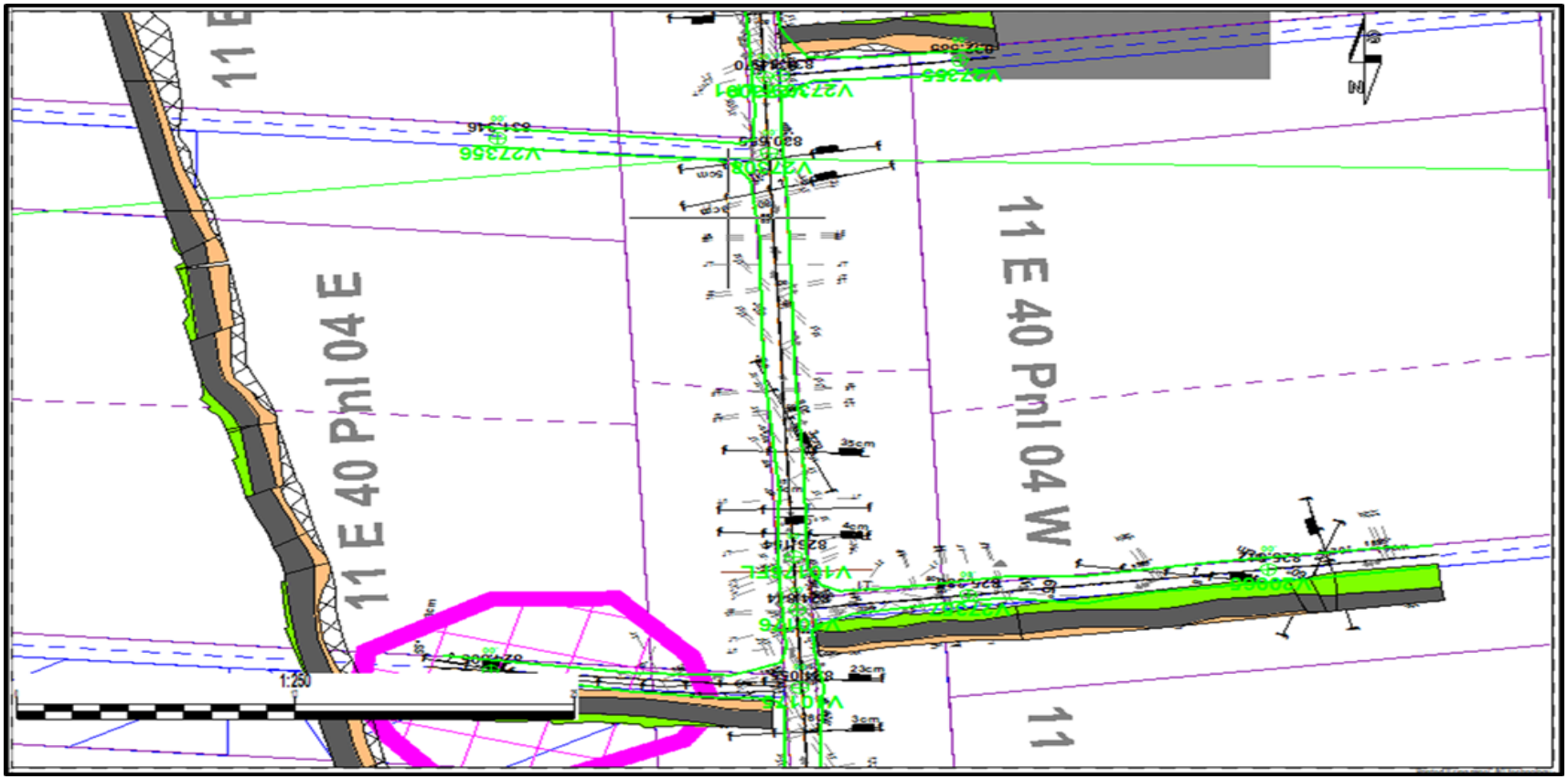


Fig 11: Typical underground mapping presented on MineCad software showing undulating UG2, minor faults, infill joints and deteriorated ground condition in a stoping area affected hydrothermal alteration (Lonmin Saffy Shaft database).

On the MineCad plottings above in Fig.11 green colour indicates hangingwall pyroxenite, grey is UG2, orange is footwall pegmatitic pyroxenite, net-like plottings below pegmatitic pyroxenite presents the norite footwall, while pink net indicates rolling of UG2 package and the black lines plotted East-West and North-South crossing across the section are joints and minor faults, and they are the indication the ground deterioration.

2.2 Grade and contamination

2.2.1 Underground grade contamination and grade distribution

At Lonmin Platinum the routine sampling of the mineralised UG2 chromitite is continually conducted in all underground active development mining areas as per company's sampling standard. The UG2 chromitite samples that are cut are locally known as "channel samples" and as per company sampling standard, each UG2 chromitite sample should be 20 cm in length and 5 cm breadth. The routine channel samples are cut perpendicular from the UG2 chromitite top contact to the bottom contact through pyroxenite lenses/internal waste if there is any, with 2 cm overlapping into the overlying pyroxenite and another 2 cm overlapping into the UG2 chromitite underlying pegmatitic pyroxenite footwall. The samples are cut at every 30 m interval along the UG2 chromitite horizon and analysed at the Lonmin laboratory for 4E fire assay with lead collection (i.e. platinum, palladium, rhodium and gold), all this process is for mine planning and metal accounting purposes.

Lonmin Platinum also conducts the routine diamond drilling in all of its shafts including at Saffy Shaft and the diamond drilling is mostly done in main underground on strike travelling tunnels known as "haulages", making use of the hydraulic diamond machine with an "AXT bit size" which is 48 mm diameter bit size with 32.5 mm in diameter of core recovered. The main purpose of diamond drilling is to prospect ahead from the current tunnels, in case there is unknown geological structure or water present. The diamond drilling is mostly done at 0° (cover boreholes), whereas the ore body prospect boreholes are drilled at an inclination of +90° from the haulage walls up to the hangingwall of the UG2 chromitite layer.

The 120 m long cover boreholes ideally do not intersect the ore body, if that happens then the haulage (on strike tunnel) direction has to be adjusted in order to maintain the ideal distance between the haulage and the overlying ore body. The cover holes are drilled at every 120 m intervals in the haulage to prospect any unforeseen geological issues such water pockets, potholes, strike swings, faults etc. The ~40 m long ore body prospect boreholes intersects the ore body with both underlying and overlying rock layers and they are drilled at every 50 m interval in the haulage to confirm the ore body elevation, ore body thickness and any other possible deformation that might affect the UG2 chromitite ore body from being efficiently mined.

For the purpose of the study the existing 4E (Pt+Pd+Rh+Au, g/t) channel sampling data and existing ore body prospect borehole data from Lonmin mineral resource department have been analysed for grade, grade distribution and possible grade contamination (Table 1). The analysed channel samples were cut as per Lonmin sampling standard, eight chromitite sampling channels from the east side of

Saffy Shaft close to the Saffy East Fault where the overlying hangingwall pyroxenite is affected by hydrothermal alteration have been analysed. Another eight UG2 chromitite ore body prospect boreholes from the west side of Saffy Shaft where the hangingwall is not known to be affected by hydrothermal alteration have also been analysed.

Saffy West channel sampling localities	**Footwall waste mining (centimetres)**	**Hangingwall waste mining (centimetres)**	**Saffy East channel sampling localities**	**Footwall over breaking (centimetres)**	**Hangingwall over breaking (centimetres)**
11W31 Raise	118.8	234.0	10E19 Raise	84.9	39.0
11W32 Raise	113.7	163.3	10E24 Raise	107.0	73.8
11W33 Raise	119.0	153.4	11E24 Raise	86.8	102.9
12W34 Raise	113.1	195.8	12E22 Raise	126.7	27.2
12W35 Raise	108.2	223.7	12E23 Raise	107.5	202.4
12W36 Raise	113.1	239.0	12E24 Raise	104.2	115.4
12W37 Raise	116.0	239.0	15E16 Raise	69.2	0.0
13W35 Raise	101.8	99.3	20E 01 Raise	88.4	10.0
Saffy West average PGE grade (4 E's) is 4.64 g/ton			**Saffy East average PGE grade (4 E's) is 4.56 g/ton**		

Table 1: Lonmin mineral resource department data showing difference in grade with both footwall and hangingwall unintentional waste mining at Saffy Shaft in areas where PGE 4E's (Pt+Pd+Rh+Au) channel sampling has been analysed.

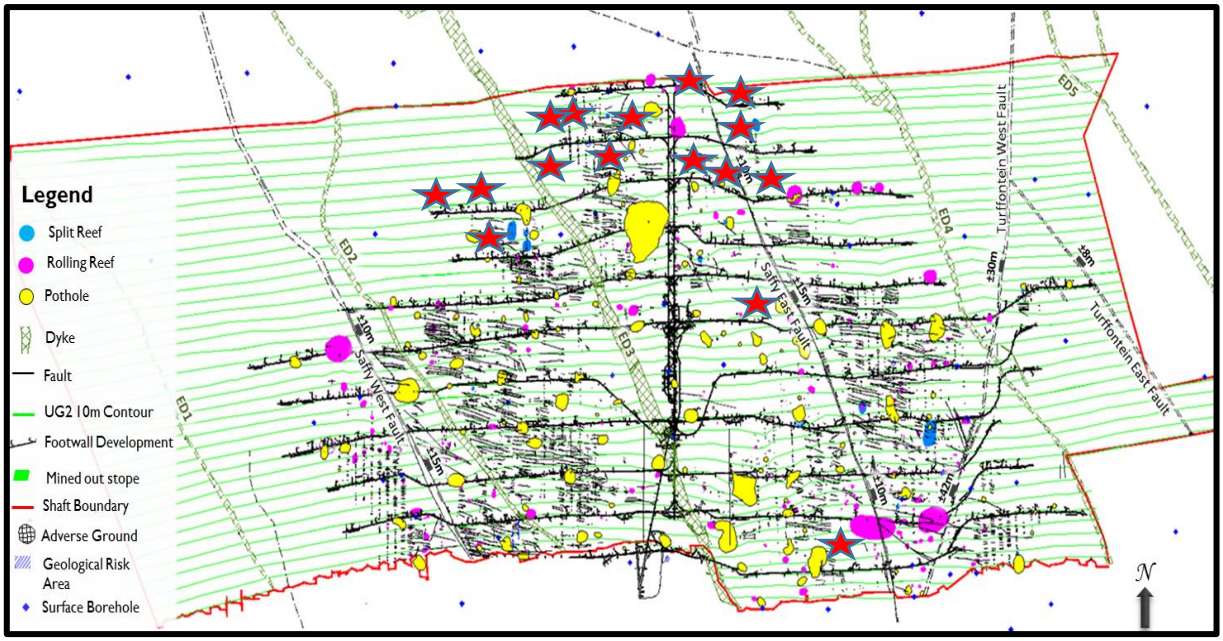


Fig 12: Mineral resource department channel sampling localities and spatial distribution (Lonmin Saffy Shaft database).

It is observed that the above development channel sampling data from mineral resource department (Table.1), shows an average grade per tonne from the east UG2 chromitite layer to be approximately 2% lower than west chromitite layer. The other possible contributing factor on grade difference such as waste mining (i.e. unintentional waste mining) is not ignored. The sampling data also shows average of 63.43 cm of UG2 overlying hangingwall pyroxenite and average of 86.07 cm of UG2 underlying pegmatitic pyroxenite/norite footwall waste mining mined on the east of Saffy Shaft.

On the west of Saffy Shaft in development areas, the waste mining is approximately 192.42 cm and 110.75 cm of overlying hangingwall pyroxenite and underlying footwall pegmatitic pyroxenite/norite mined respectively. This simply means there's more waste mined from Saffy West UG2 chromitite areas, however the PGE grade per tonne from Saffy West UG2 chromitite remains 2% higher than Saffy East UG2 chromitite. This grade difference might seem insignificant but it is noticeable, taking into consideration that the waste mining from Saffy West areas has definitely contributed on the observed grade reduction. The analysed grade distribution histograms derived from the existing mineral resource channel sampling database (Fig.13, Fig.14 and Fig.15), presents a slight different grade distribution from the histograms plotted from surface borehole data (Fig.18 and Fig.19).

Saffy Shaft West channel samples

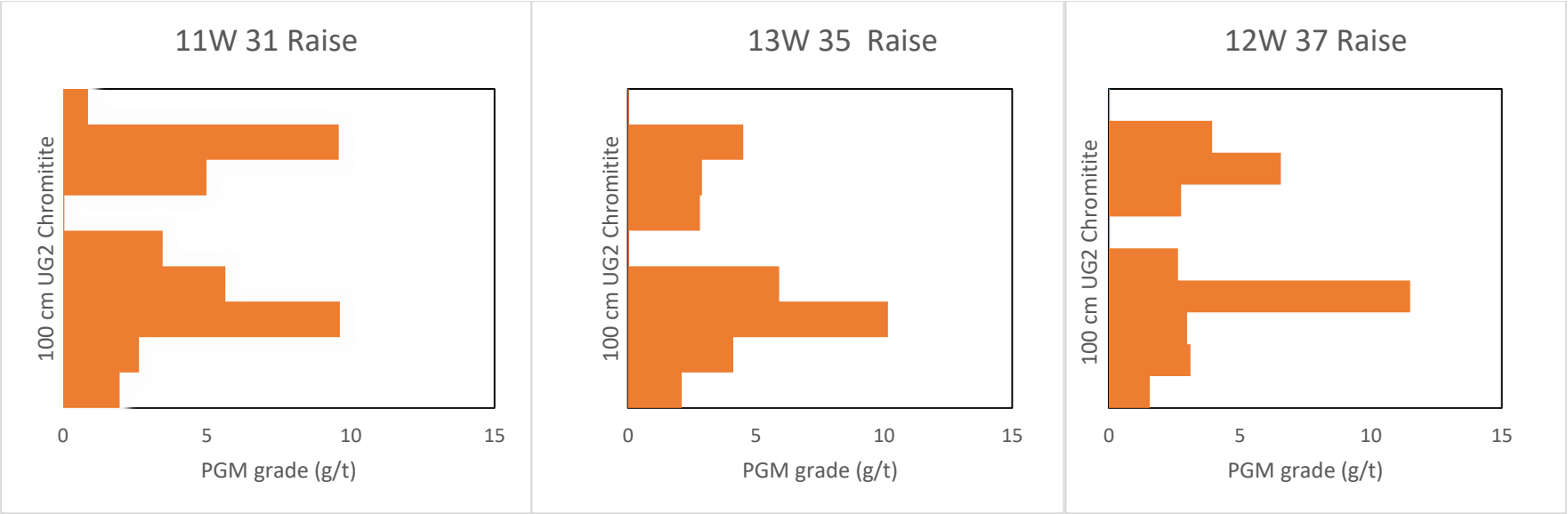


Fig 13: The Saffy Shaft West PGE grade and grade distribution of UG2 chromitite layer from the existing channel sampling data.

Saffy Shaft East channel samples

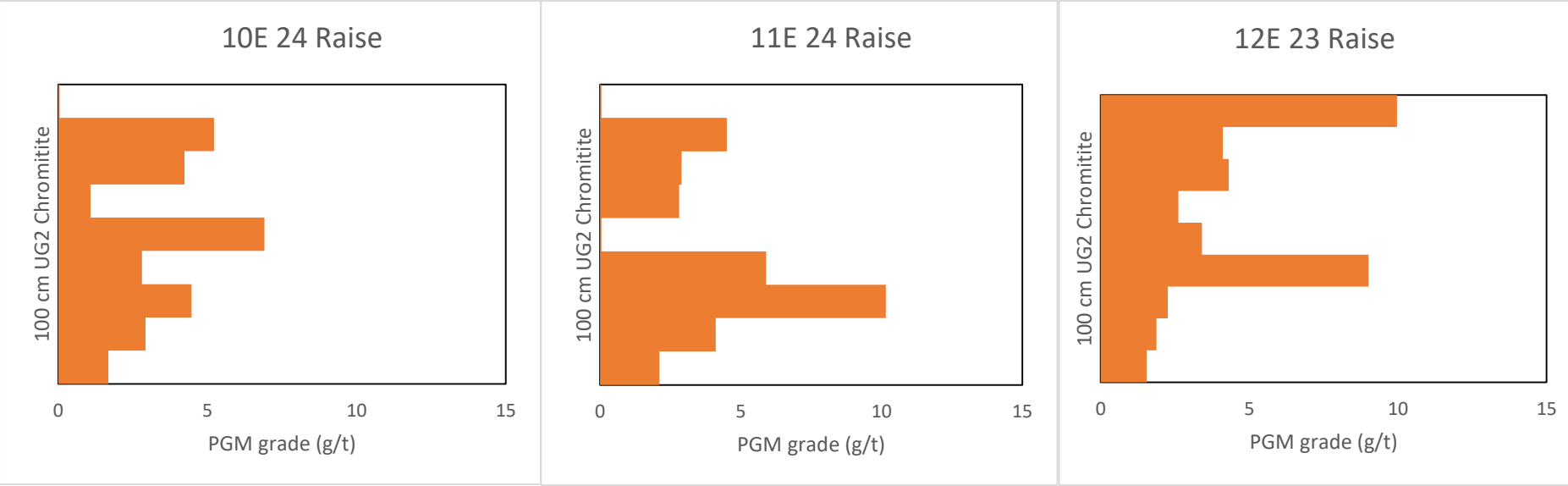


Fig 14: The Saffy Shaft East PGE grade and grade distribution of UG2 chromitite layer from the existing channel sampling data.

Combined histograms from both east and west of Saffy Shaft

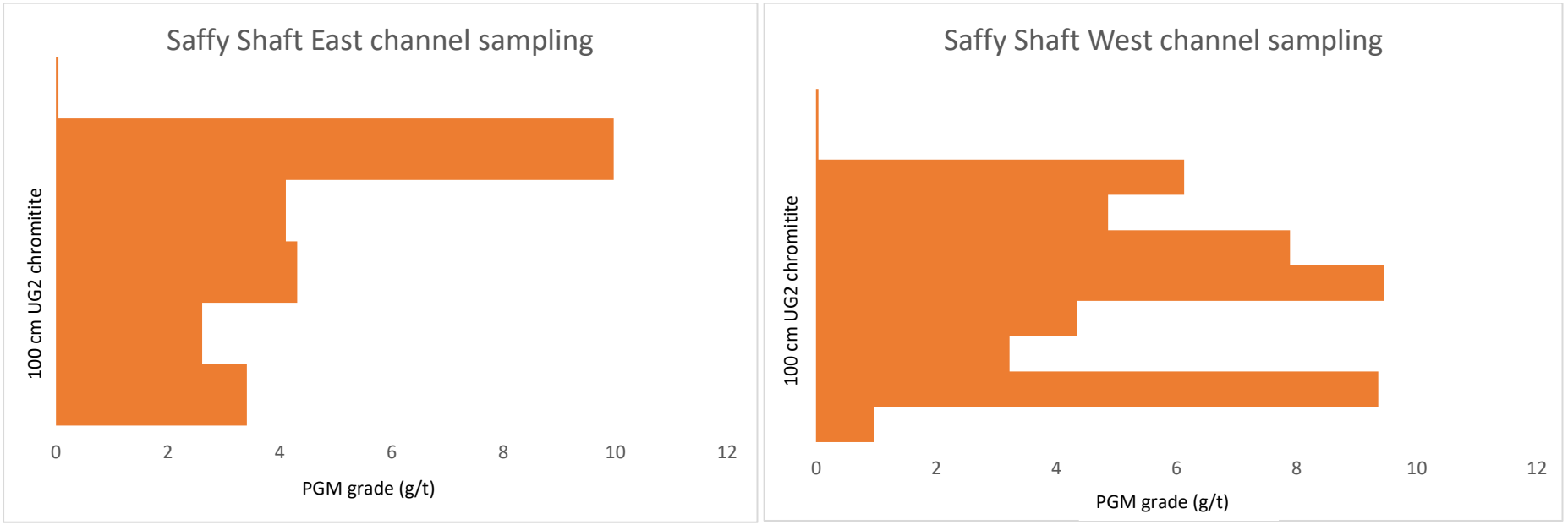


Fig 15: The combined histogram for Saffy Shaft East and West PGE grade and grade distribution of UG2 chromitite layer from the existing channel sampling data of mineral resource department.

2.2.2 Surface borehole grade and grade distribution

Lonmin Platinum has the existing surface boreholes on the database which were drilled for exploration purpose for all the shafts that are currently being mined or planned to be mined. These surface boreholes are drilled through the ore body from surface (-90°) prior sinking the shaft, the primary purpose for these surface core boreholes is to increase the confidence level on the grade, grade distribution and structural modelling of the shafts. In each surface borehole drilled, the UG2 ore intersections and deflections are sampled and analysed for 6 elements known as "6E" (platinum, palladium, rhodium, ruthenium, iridium and gold). Each surface boreholes core is logged by a competent geologist strictly following the Lonmin core logging standard, upon core logging the data is captured and stored safely on Sable Warehouse Software under the supervision and approval of a responsible senior geologist/resource geologist.

For the purpose of this study Saffy Shaft East and West surface exploration borehole data stored from Sable Warehouse Software is selected for analysis; the surface boreholes selected on the east of Saffy Shaft are the ones close to the sub-vertical Saffy East Fault (Fig.16) as the UG2 overlying altered pyroxenite hangingwall is known in the vicinity (Davis,2013). The surface boreholes selected on the west of Saffy Shaft are in the vicinity of Saffy West Fault (Fig.16). All the surface boreholes selected from both east and west of Saffy Shaft have at least two deflections to three deflections at most per borehole, for the purpose of the analysis the deflection data is combined with the mother/main borehole and all interpreted as a borehole composite. The total number of surface boreholes analysed for this study is 19 boreholes with 10 boreholes are from the west side of Saffy Shaft and 9 boreholes are from the east side of Saffy Shaft lease area (Fig.16). The surface boreholes from the east side of the shaft are in between sub vertical major faults.

The surface boreholes were drilled at an inclination of -90^{o} from surface to hangingwall units through UG2 chromitite layer to the footwall units under the ground, the average thickness of the UG2 chromitite layer is approximately 1.2 m from both east and west sides of Saffy Shaft. Boreholes drilled from the east side of the shaft in the vicinity of sub vertical faults show structural complexity throughout the borehole core; where intense jointing, thrust planes and pegmatite veins were observed compared to the less geologically structured boreholes drilled from the west side of the shaft. The UG2 underlying pegmatitic pyroxenite from both east and west of the shaft is showing no visual difference in the modal mineralogy, colour and texture, whereas the overlying hangingwall pyroxenite (UHW1b) immediately above the UG2 chromitite package shows a greenish discolouration at Saffy East, Fig.17 (a) and Fig.17 (b).

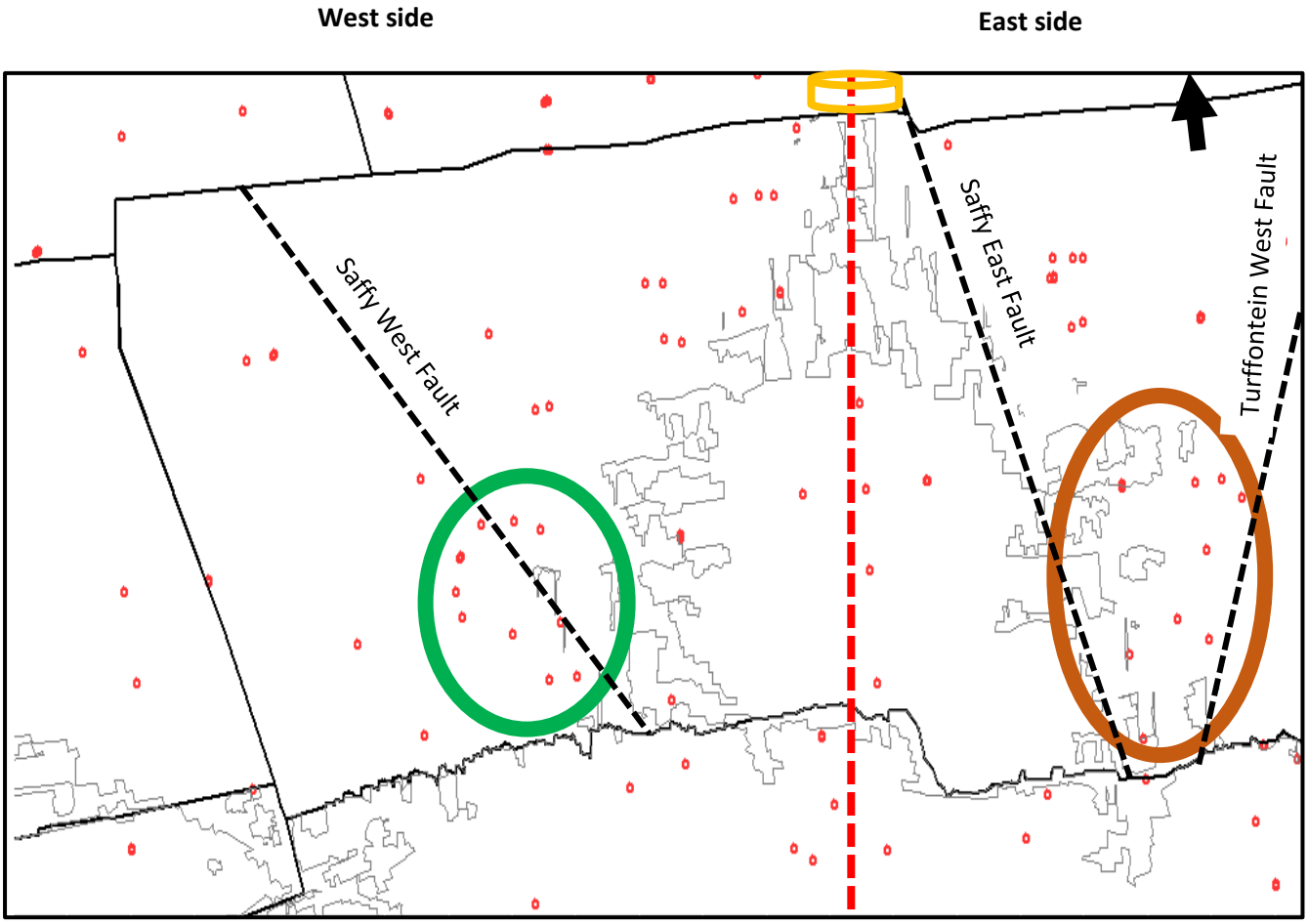


Fig 16: Plan view showing the surface boreholes drilled at Saffy Shaft, with green circle showing analysed surface boreholes drilled from Saffy West, while the brown circle indicates the analysed surface boreholes drilled from Saffy East lease area; the dashed black lines shows the sub-vertical major faults, while the north-south red dashed line is the boundary between Saffy East and West and the orange ring on top is the shaft with black north arrow indicated (Lonmin Saffy Shaft database).

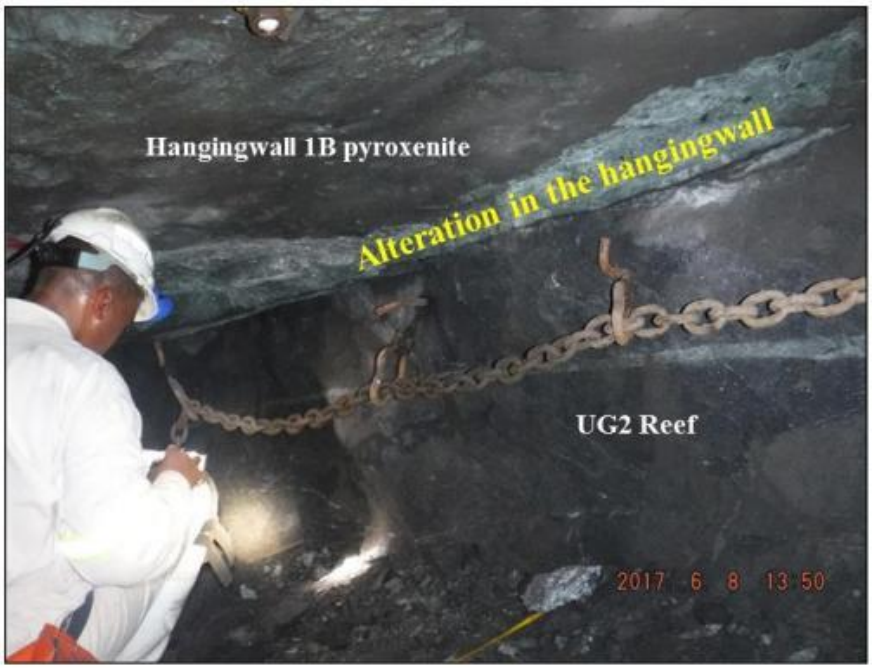


Fig 17 (a): Typical east of Saffy Shaft stope panel photo, showing the hydrothermal alteration above the UG2 reef horizon (Hartzenberg, 2019).

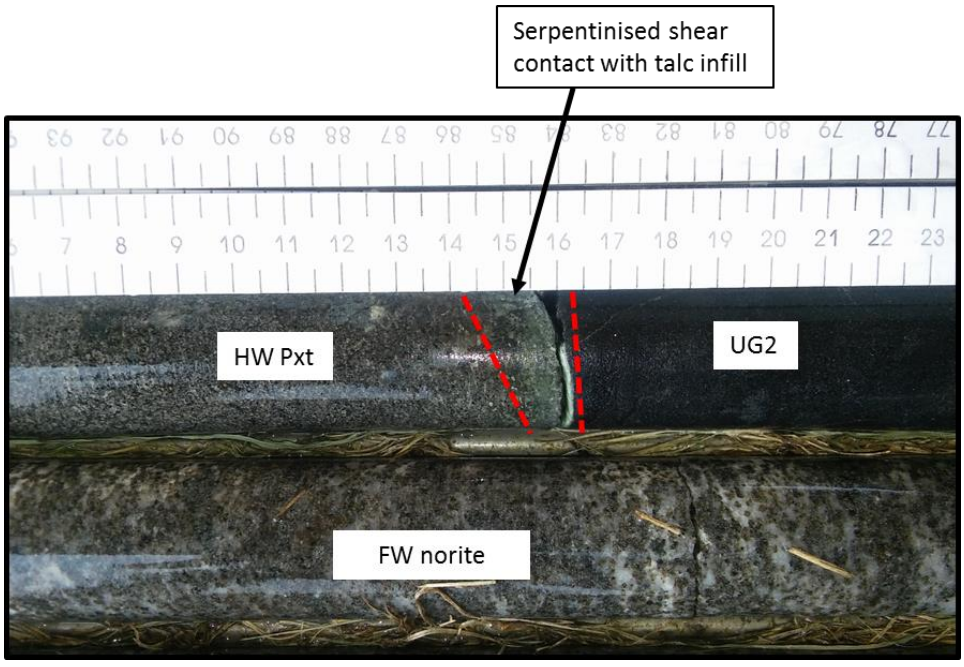


Fig 17(b): Photo grab of borehole core showing the UG2 chromitite (UG2) with the sheared upper contact, the immediate hangingwall pyroxenite (HW Pxt) has the greenish colour and infill minerals, while footwall norite (FW norite) shows no visual difference in the modal mineralogy, colour and texture (Lonmin Saffy Shaft database).

Historical surface borehole data plotted in Fig.18 and Fig.19 shows a similar trend of grade distribution from both east and west of Saffy UG2 chromitite analysed samples, where PGE grade peaks are observed in the middle and at the bottom contact (basal peak) of the UG2 chromitite horizon. The surface borehole samples also have similar average PGE grade (6E) compared to channel samples from the east and west UG2 chromitite layer.

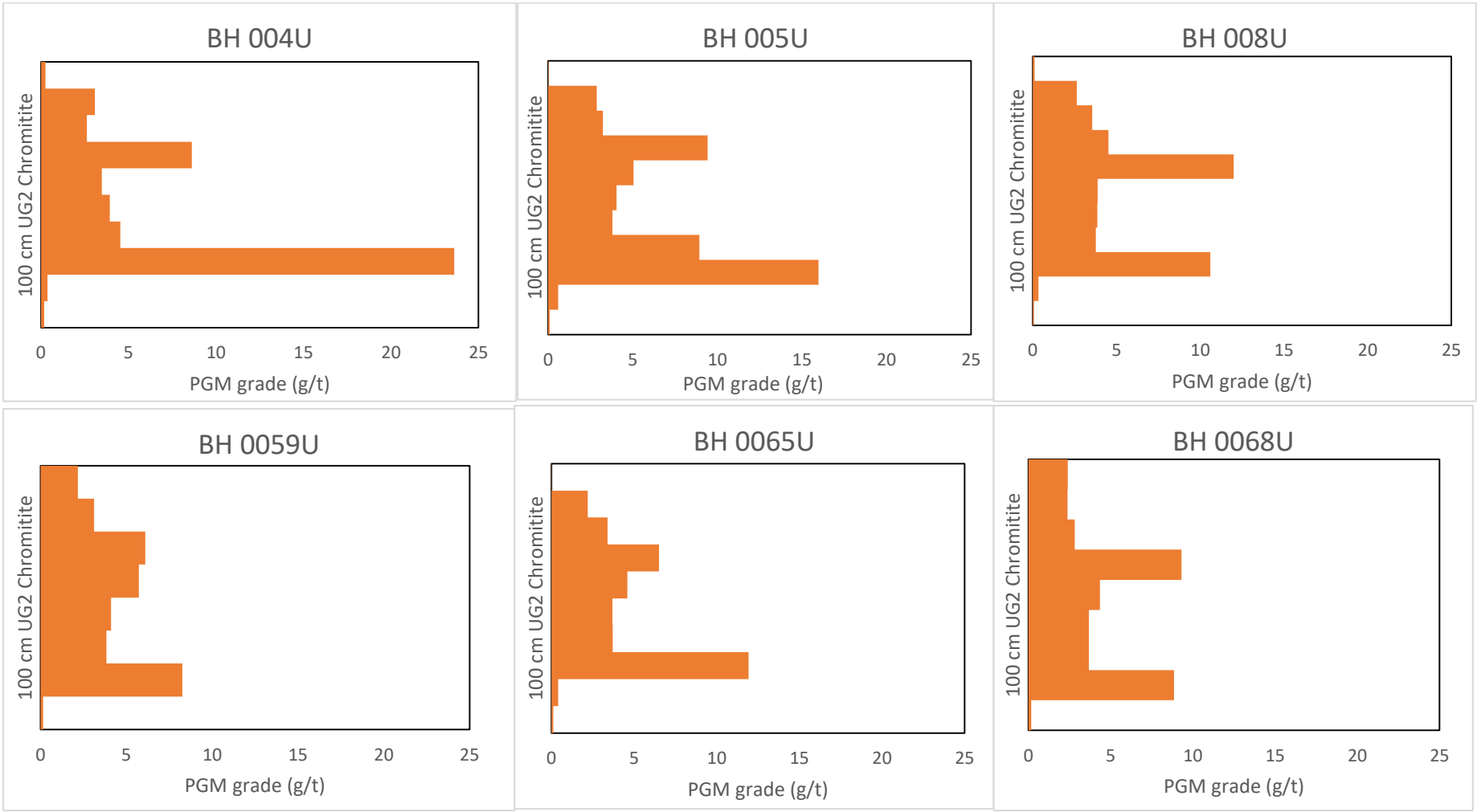


Fig 18: Surface borehole histograms showing PGE grade and grade distribution of UG2 chromitite layer from Saffy West.

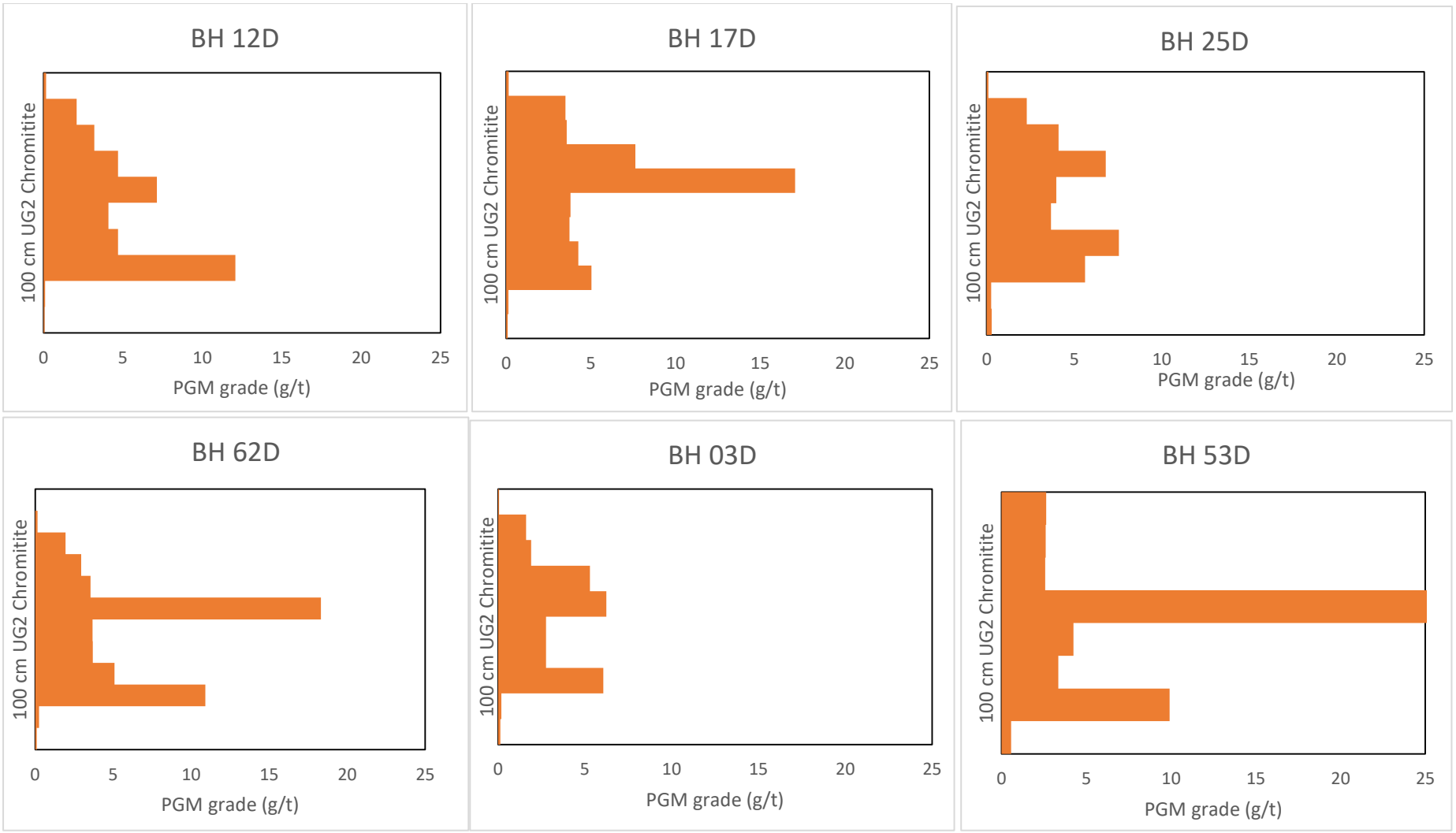


Fig 19: Surface borehole histograms showing PGE grade and grade distribution of UG2 chromitite layer from Saffy East.

Chapter 3

3. Petrography and chromite mineral chemistry from Saffy Block

3.1 The formation of chromitite layers

The UG2 chromitite is an important economic horizon and is defined as a massive chromitite unit with a chromite content of about 60 to 90% and between 1.2 to 1.4 m in thickness with approximately 43.5% Cr_2O_3 (Lee, 1996). Brough *et al.*, 2015 suggested that chromitite is derived from a variety of mantle melts with variable composition. It is suggested that the chromitites tend to be PGE enriched and they either concentrate PPGE (Pt, Pd and Rh) or IPGE (Ir, Ru and Os).

3.1.1 The UG2 chromitite layer at Lonmin lease area

The Lonmin UG2 chromitite is known to be a stratiform chromitite, which is fine-grained, consisting mainly of cumulus chromite, intercumulus orthopyroxene and plagioclase. A number of models have been suggested regarding the formation of the UG2 chromitite layers and they include; magma mixing, pressure changes, magma contamination with silica, addition of water and injection of a chromite slurry (Kinnaird *et al*., 2002). Whereas Latypov *et al*.2017, suggest that Bushveld Complex chromitites formed from magma emplaced along the floor of the chamber, from which crystallization took place essentially in situ, on the magma cumulate interface. The UG2 chromitite varies from 1- 1.2 m thick in the Marikana Operations lease area and the immediate footwall to the UG2 is mostly medium-grained mottled anorthosite in the western side of Lonmin lease area and a coarse grained pegmatitic pyroxenite in the eastern side of Lonmin lease area; while the immediate hangingwall to the UG2 horizon is a barren brownish medium-grained pyroxenite.

3.2 Chromitite petrography

A total of 22 polished thin sections of chromitite were studied to assess the morphology of the chromite, mineral matrix, the mineral association of the chromite, the primary silicates and possible secondary minerals and textures. Due to limited Lonmin departmental sampling resources the polished thin sections were prepared from the underground UG2 channel samples from Saffy East, whereas the samples from Saffy West were taken from the existing UG2 underground drilled boreholes. The total of 15 samples were prepared from Saffy East which is perceived as hydrothermally altered, these samples were prepared through the mineral resource departmental channel sampling system. The 7 samples were prepared from Saffy West, which is perceived as not affected by hydrothermal alteration. The UG2 chromitite samples from both east and west of the shaft do not show any visual discolouring, however some samples from Saffy East chromitites show a

crumbling behaviour compared to samples from Saffy West, which seemed normal with no crumbling behaviour.

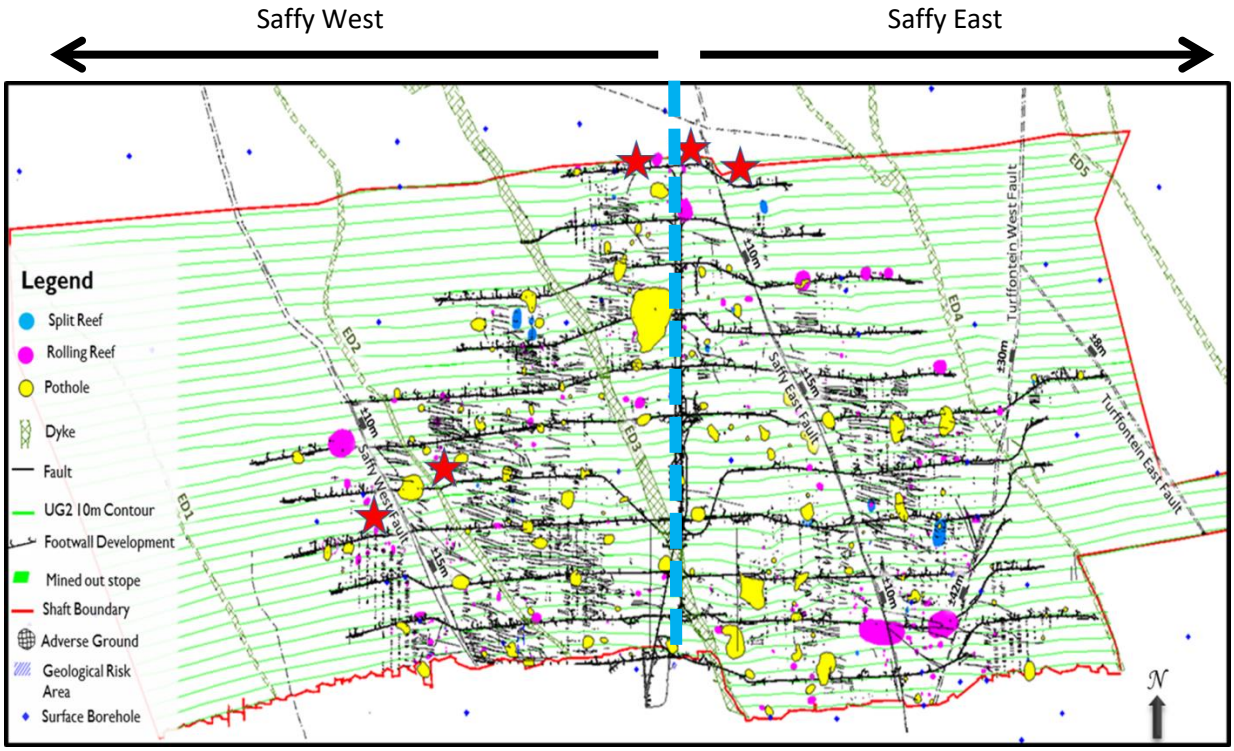


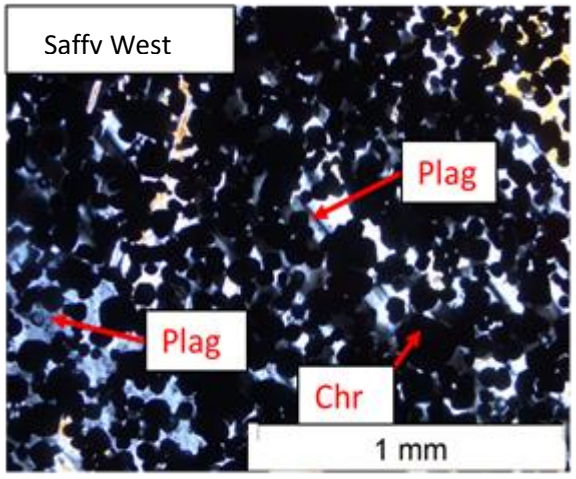
Fig 20: Plan showing the spatial distribution of the prepared thin sections from underground channel sampling at Saffy East and cover drilled boreholes at Saffy West (Lonmin Saffy Shaft database). The red stars indicates the location of the prepared samples, the blue dashed line indicates the east and west boundary of Saffy Shaft.

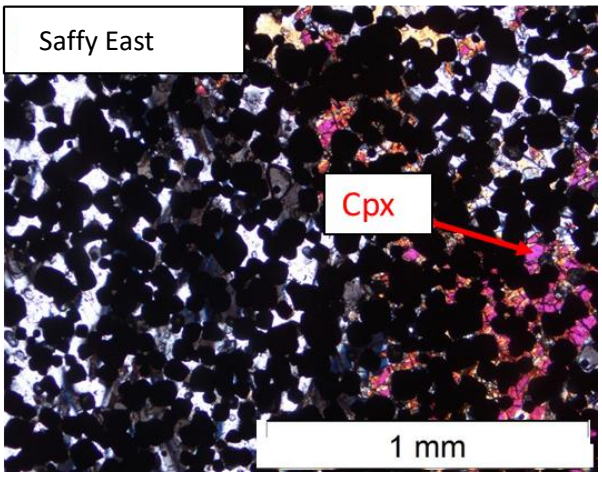
3.2.1 Similarities and the differences from Saffy East and West samples

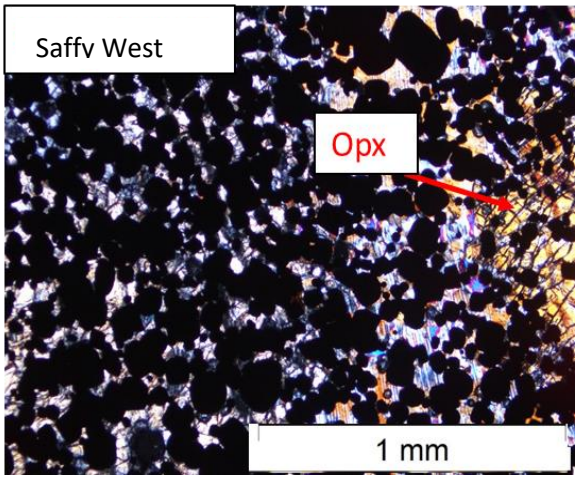
The UG2 samples from east of Saffy Shaft and samples from west of Saffy Shaft show a significant difference as the samples from east of the shaft they tend to possess a coarser grains (“sugar like”), hence some are crumbling; and they seem to be brittle compared to samples from Saffy West. The visible alteration or discolouring is not seen on the UG2 itself in both east and west samples. However, the underlying footwall norite and the overlying hangingwall pyroxenite tend to be greenish in colour from the areas perceived to be affected by hydrothermal alteration at Saffy East.

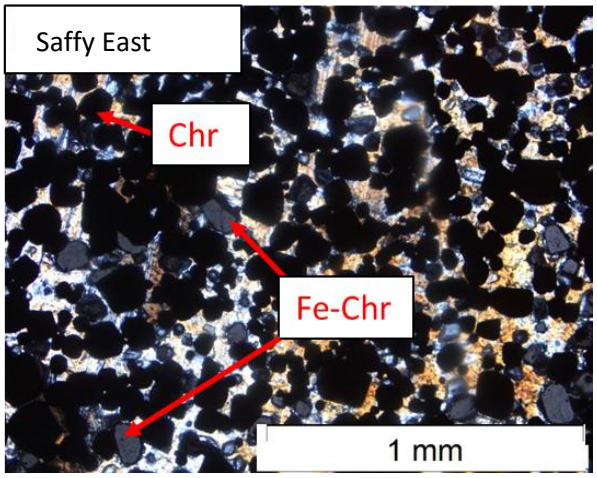
The comparative description of chromite from the eastern and western sides of Saffy Shaft shows no significant morphological differences. The shape of the chromite grains from both east and west of the shaft within the UG2 chromitite layer is mostly euhedral and is dominantly interlocked to each

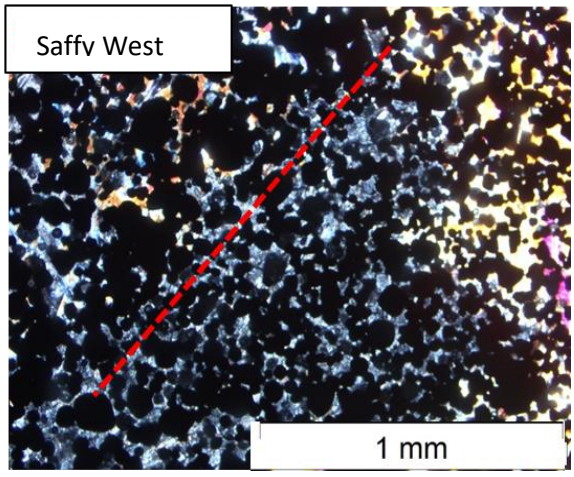
other with grain size ranging between 0.05 mm to 0.5 mm. The chromite grains form up to 85% of the chromitite layer, and are hosted in an orthopyroxene and plagioclase groundmass which constitute approximately 15% of chromitite layer studied. However a localised clinopyroxene matrix is observed in some thin sections from east of the shaft.

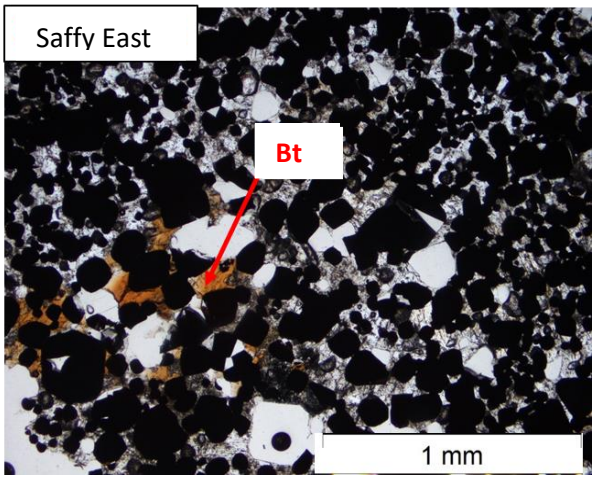












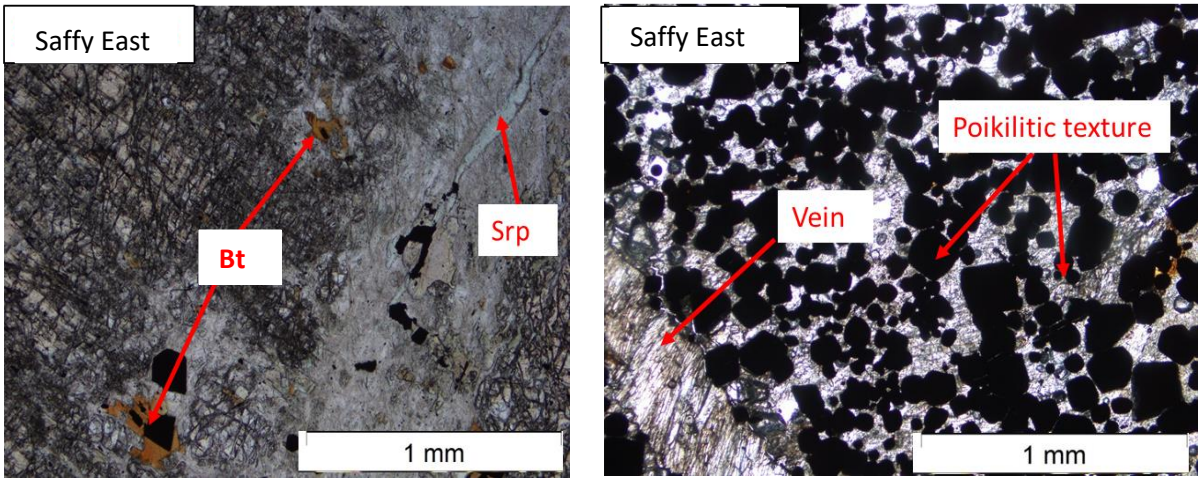


Fig 21: Photomicrographs illustrating polished thin sections from Saffy West and East samples of chromitite layer of Saffy Shaft; where "Plag" is Plagioclase, "Chr" is Chromite,"Cpx" is Clinopyroxene,"Opx" is Orthopyroxene,"Fe-Chr" is Ferrichromite,"Srp" is Serpentine and "Bt" is Biotite.

Saffy East and West show a plagioclase (Plag) matrix with cumulus chromite grains, some samples from Saffy West indicate the segregation of small and large chromite grains. On both the east and west side of Saffy Shaft a matrix of orthopyroxene (Opx) is identified, while some Saffy East samples show the localised matrix of clinopyroxene (Cpx).

Saffy East samples also shows biotite (Bt) surrounding chromite grains, while some samples from the east side of Saffy show ferrichromite (Fe-chr) grains together with normal chromite grains (Chr), pyroxenite lenses separating chromitite layer into two bands with serpentine filling (Srp) in a microfracture and biotite (Bt) surrounding chromite grains is identified at Saffy East. The distinctive veinlets with talc and a poikilitic texture also identified on the east side of Saffy Shaft.

	Chromite % (Chr)	**Plagioclase % (Plag)**	**Orthopyroxene % (Opx)**	**Clinopyroxene % (Cpx)**	**Average grain size (mm)**	**Comments**
Samples from Saffy West	85%	11%	4%	none	0.05-0.5mm	Segregation of chromite grains is identified.
Samples from Saffy East	85%	11%	3%	1%	0.05-0.5mm	Clinopyroxene,Fe-Chromite, Biotite, veinlets and serpentines are identified. Poikilitic texture is identified

Table 2: Typical mineral composition of the samples from Saffy East and West

3.3 Chromite mineral chemistry analysis using Electron Microprobe

For the purpose of this study, chromite grains from eight polished thin sections were analysed; where four thin sections were from Saffy Shaft East, which is perceived to be hydrothermally altered, while another 4 thin sections were from Saffy Shaft West, which is perceived not to be hydrothermally altered. A total of five chromite grains from each thin section were analysed for their rim and core chemical composition variation, however for one thin section instead of analysing five chromite grains, only two chromite grains were successfully analysed due to a technical error with the electron microscope.

The electron microprobe analysis (EMPA) of chemical composition of chromite was carried out using Cameca FE- SX5 at the University of the Witwatersrand. The major element oxides of MgO, Al_2O_3, SiO_2, TiO_2, V_2O_3, Cr_2O_3, MnO, FeO, NiO, and ZnO were analysed. This analysis was conducted in order to determine any compositional differences between chromite grains from the different localities of Saffy Shaft. The chromite grains that were analysed are hosted in both intercumulus plagioclase and orthopyroxene while some samples from Saffy East contained clinopyroxene matrix.

The morphology of the chromite grains seem to differ as some chromite grains from the east show a more interlocking texture to each other compared to those from the west. Some chromite grains from Saffy East shows irregular edges with random fractures. The overall Fe_3 content from both east and west is high in the chromite grains (ranging between 27% to 31%). The samples from both Saffy East and Saffy West chromitite do not show any appreciable MnO content, however Cr_2O_3, FeO, Al_2O_3, MgO, TiO_2, V_2O_3, NiO and ZnO are present in both Saffy West and Saffy East.

Sample	MgO	Al2O3	SiO2	TiO2	V2O3	Cr2O3	MnO	FeO	NiO	ZnO	Total
407	8.38	14.61	0	1.16	0.35	44.79	0	31.42	0.1	0.12	100.93
407	8.56	15.09	0.03	1.07	0.32	45.73	0	28.73	0.11	0.14	99.77
407	8.56	14.46	0.01	1.24	0.35	44.57	0	31.44	0.15	0.03	100.81
407	7.9	13.7	0.02	1.22	0.29	44.76	0	30.97	0.17	0.14	99.18
407	8.4	14.76	0.03	1.25	0.37	45.97	0	29.77	0.12	0.1	100.77
407	7.87	13.92	0.03	1.16	0.35	44.36	0	31,0	0.14	0.12	98.96
407	8.51	14.57	0.01	1.18	0.35	45.3	0	29.35	0.13	0.08	99.49
407	8.33	14.66	0.05	1.19	0.39	46.45	0	29.21	0.15	0.16	100.59
407	8.24	14.7	0	1.27	0.29	44.1	0	31.3	0.13	0.16	100.18
407	8.07	13.95	0.02	1.1	0.34	45.35	0	31.78	0.13	0.12	100.87
404	9.2	17.26	0.01	0.95	0.33	43.92	0	28.83	0.23	0.12	100.86
404	9.38	17.69	0.03	0.95	0.32	44.63	0	26.37	0.13	0.17	99.66
404	9.12	17.26	0.01	0.99	0.27	43.27	0	28.34	0.2	0.12	99.56
404	9.06	16.9	0.03	0.22	0.23	43.42	0	28.8	0.19	0.07	99.6
404	9.18	17.08	0.01	1.05	0.29	45.04	0	28.83	0.17	0.15	101.81
404	9.03	16.71	0.05	0.79	0.31	43.62	0	28.42	0.18	0.06	99.17
404	9.17	16.66	0.02	0.97	0.27	45,0	0	28.19	0.19	0.07	100.53
404	9.38	17.2	0.03	0.95	0.25	44.44	0	27.74	0.16	0.11	100.28
404	9.13	17.24	0	0.95	0.24	43.81	0	28.64	0.19	0.11	100.3
404	9.15	17.36	0.02	0.94	0.24	43.36	0	28.53	0.21	0.12	99.92
400	9.07	16.59	0.03	1.13	0.18	44.48	0	27.05	0.16	0.17	98.86
400	9.23	16.84	0.04	1,0	0.17	44.68	0	26.8	0.15	0.11	99.04
400	8.88	16.86	0	1.11	0.2	44.92	0	27.69	0.15	0.16	99.96
400	8.78	16.5	0.03	0.97	0.18	44.94	0	26.69	0.14	0.05	98.28
400	9.06	17.02	0	1.04	0.25	45.06	0	26.89	0.19	0	99.51
400	9.29	17.08	0.04	0.93	0.14	45.05	0	26.29	0.18	0.09	99.09
400	9.11	17.7	0.03	0.81	0.25	44.93	0	26.31	0.19	0.06	99.38
400	9.13	17.15	0.03	0.87	0.26	45.72	0	26.6	0.14	0.15	100.05
400	8.77	17.16	0	0.9	0.2	45.8	0	27.4	0.22	0.01	100.47
400	9.18	17.5	0.06	0.94	0.27	44.4	0	26.18	0.14	0.07	98.73
412	8.9	15.37	0.03	0.94	0.37	45.02	0	27.65	0.11	0.04	98.41
412	8.95	15.67	0.03	1.19	0.36	45.9	0	27.57	0.18	0.06	99.92
412	8.78	15.67	0.01	1.22	0.36	45.43	0	28.06	0.14	0.13	99.79
412	8.57	15.67	0	1.13	0.32	45.58	0	27.9	0.16	0.11	99.44
412	8.95	15.16	0	1.1	0.37	45.77	0	27.48	0.1	0.11	99.06
412	8.72	14.93	0.04	1.06	0.38	45.94	0	27.42	0.15	0.24	98.87
412	8.79	15.47	0	1.04	0.39	46.99	0	27.63	0.13	0.1	100.54
412	8.85	15.88	0.01	0.99	0.36	45.76	0	27.17	0.11	0.04	99.16
412	8.91	15.47	0.02	1.14	0.33	45.9	0	27.19	0.12	0.11	99.2
412	8.73	15.49	0.01	1.2	0.41	47.05	0	27.27	0.09	0.09	100.35

Table 3: Saffy East average compositions of the chromite grains from the UG2 chromitite.

Sample	MgO	Al2O3	SiO2	TiO2	V2O3	Cr2O3	MnO	FeO	NiO	ZnO	Total
416	8.87	16.24	0.04	0.84	0.29	44.87	0	29.44	0.15	0.1	100.85
416	8.63	16	0.01	0.93	0.28	45.77	0	27.95	0.16	0.12	99.84
416	8.47	16.28	0.02	0.95	0.21	46.41	0	27.85	0.19	0.08	100.46
416	8.35	16.24	0.03	1,0	0.25	46.54	0	28.06	0.14	0.19	100.8
416	8.51	15.95	0.01	0.87	0.25	45.5	0	29.21	0.18	0.04	100.52
416	7.95	14.97	0	0.93	0.28	44.55	0	28.49	0.13	0.05	97.36
416	8.49	16.18	0.02	0.89	0.28	46.03	0	27.63	0.14	0.16	99.82
416	8.45	15.34	0.02	0.87	0.24	44.83	0	28.53	0.15	0.06	98.49
416	8.64	16.1	0.02	0.96	0.28	44.63	0	29.07	0.13	0.09	99.91
416	8.52	15.83	0	0.87	0.26	45.72	0	29.37	0.15	0.13	100.84
415	8.8	15.6	0	1.1	0.3	45.26	0	28.07	0.14	0.08	99.36
415	8.72	15.53	0	1.08	0.37	46.06	0	27.95	0.15	0.1	99.95
415	8.61	15.62	0	1.13	0.34	45.12	0	27.56	0.12	0.02	98.52
415	8.95	15.62	0	1.07	0.35	45.35	0	27.73	0.16	0.08	99.32
419	8.41	15.58	0.19	0.93	0.4	45.66	0	28.44	0.11	0.09	99.81
419	8.61	15.05	0.01	0.89	0.29	44.92	0	28.81	0.16	0.15	98.88
419	8.88	15.52	0.04	0.95	0.37	46.72	0	28.13	0.14	0.15	100.91
419	8.4	14.3	0.02	0.99	0.3	46.39	0	28.28	0.12	0.18	98.97
419	8.5	15.02	0.01	1.01	0.25	45.99	0	28.02	0.08	0.16	99.05
419	8.53	14.84	0.01	0.91	0.4	46.78	0	27.99	0.08	0.16	99.69
419	8.59	14.87	0	1.07	0.34	47.02	0	28	0.13	0.21	100.22
419	8.63	14.97	0.03	0.9	0.33	45.27	0	28.24	0.09	0.02	98.5
419	8.56	15.05	0.02	1.06	0.3	46.08	0	27.84	0.1	0.1	99.11
419	8.79	15.29	0.03	1	0.3	46.09	0	28.43	0.12	0.22	100.27
418	8.11	14.1	0.03	1.35	0.37	44.75	0	29.48	0.13	0.1	98.43
418	7.86	13.58	0.03	1.09	0.33	45.82	0	29.32	0.13	0.04	98.2
418	8.43	14.49	0.01	1.25	0.31	45.65	0	29.27	0.1	0.18	99.7
418	8.15	14.21	0.01	1.25	0.32	45.98	0	29.34	0.12	0.11	99.49
418	8.51	14.65	0	1.22	0.31	46.01	0	29.55	0.11	0.13	100.5
418	8.17	13.85	0.03	1.25	0.34	45.54	0	29.47	0.17	0.17	99
418	8.45	14.68	0	1.18	0.31	45.42	0	29.45	0.1	0.12	99.71
418	8.35	13.88	0.02	1.35	0.32	45.71	0	28.82	0.11	0.08	98.64
418	8.52	14.35	0.03	1.24	0.37	45.31	0	28.97	0.13	0.14	99.06
418	8.59	14.76	0.02	1.39	0.41	45.15	0	29.15	0.12	0.11	99.69

Table 4: Saffy West average compositions of the chromite grains from the UG2 chromitite.

At Saffy West the aluminium oxide content (Al_2O_3) is about 14% to 16%, while the magnesium oxide (MgO) is about 8% to 9% and titanium oxide (TiO_2) is approximately 1% (Fig.22a). At Saffy East the values are similar with aluminium oxide (Al_2O_3) about 14% to 18%, magnesium oxide (MgO) is 8% to 10% and titanium oxide (TiO_2) is approximately 1% (Fig.22a and Fig.22b).

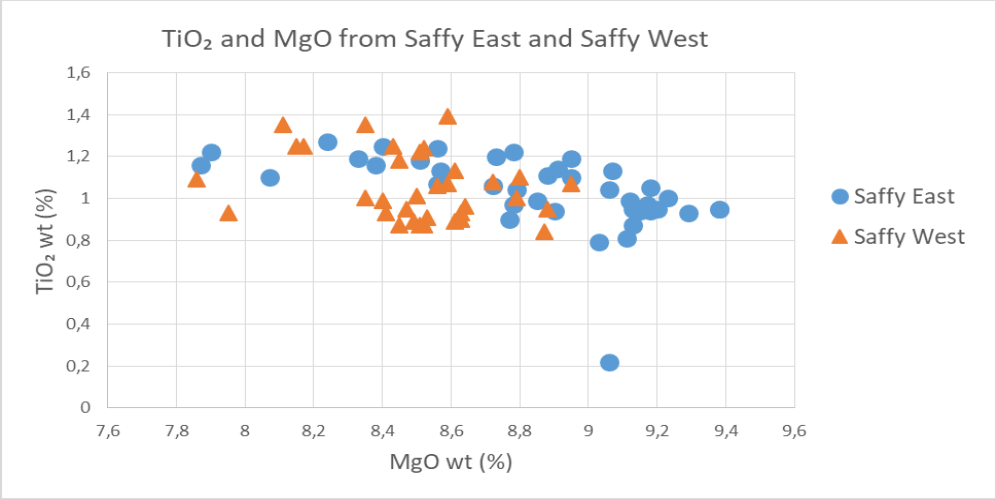


Fig 22 (a): Graph showing the concentration of Ti_2O vs MgO from Saffy East and Saffy West chromite grains.

The TiO_2 content from both Saffy East and West has similar values ranging between 0.8 % and 1.4% with outlier of approximately 0.2% at Saffy East (Fig.22a and Fig.22b). Whereas the MgO is higher at Saffy East, ranging between 7.9% to approximately 9.4%. There is an overlap between data from Saffy East and Saffy West chromites.

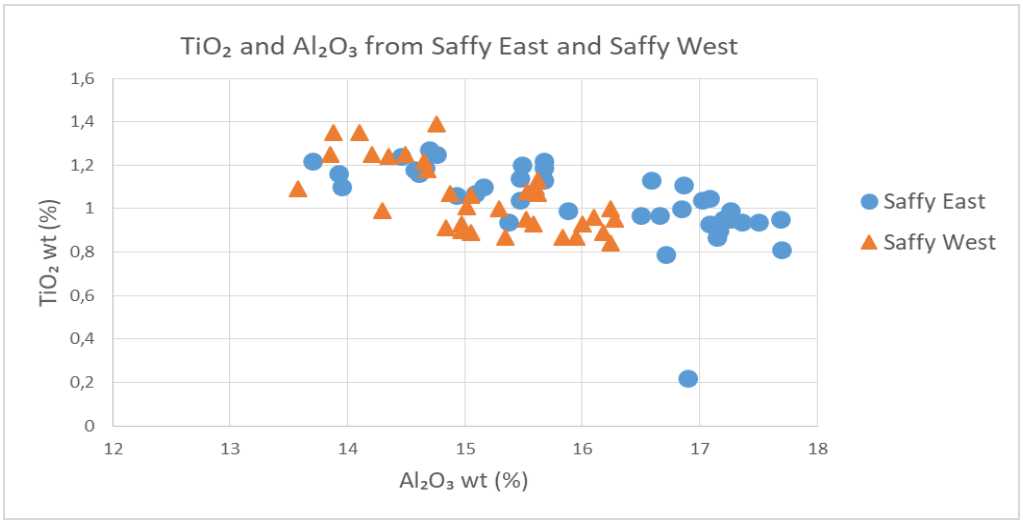


Fig 22 (b): Graph showing the concentration of Ti_2O vs Al_2O_3 from Saffy East and Saffy West chromite grains.

The Al_2O_3 is higher at Saffy East, ranging between 14% to approximately 18%, whereas at Saffy West the Al_2O_3 is lower, ranging between 13.5% to about 16.5%. There is an overlap between data from Saffy East and Saffy West chromites, the TiO_2 and MgO trend in Fig.22a is the similar to TiO_2 and Al_2O_3 trend in Fig.22b.

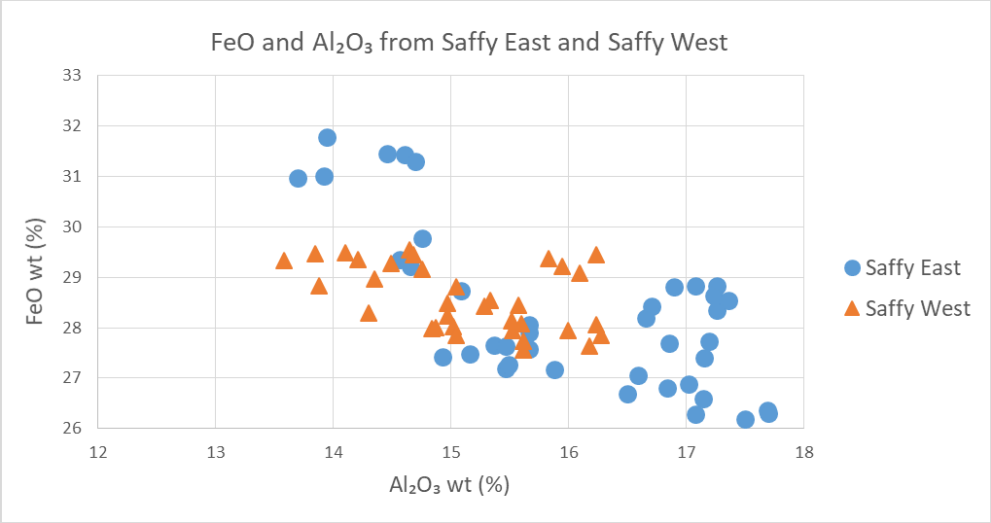


Fig 22 (c): Graph showing the concentration of FeO vs Al_2O_3 from Saffy East and Saffy West chromite grains (FeO, is total Fe recalculated as divalent FeO).

Saffy East chromite data shows that the lower the FeO then the higher the Al_2O_3, whereas Saffy West chromite shows lower values of FeO and Al_2O_3 compared to Saffy East chromite, (Fig.22c).

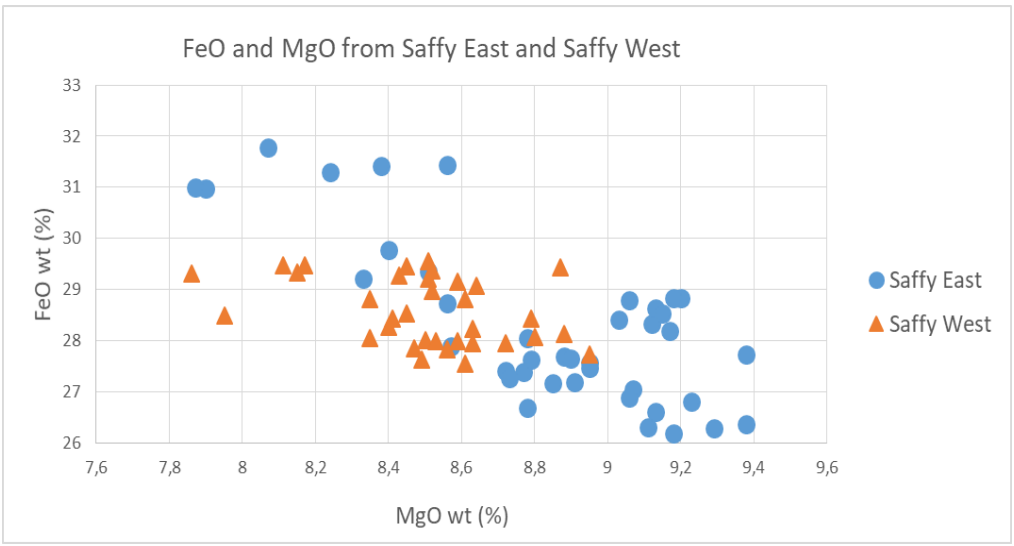


Fig 22 (d): Graph showing the concentration of FeO vs MgO from Saffy East and Saffy West chromite grains (FeO, is total Fe recalculated as divalent FeO).

Saffy East chromite data shows that the lower the FeO content then the higher the MgO, whereas Saffy West shows lower values of FeO and MgO contents compared to Saffy East chromite data, (Fig.22d). The FeO and Al_2O_3 trend in Fig.22c is similar to FeO and MgO trend in Fig.22d.

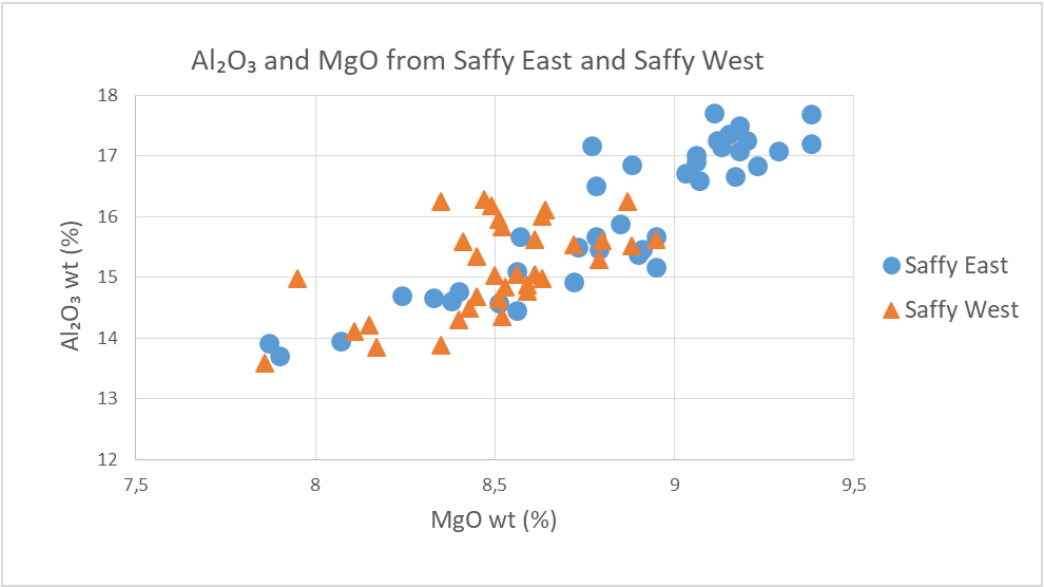


Fig 22 (e): Graph showing the concentration of Al_2O_3 vs MgO from Saffy East and Saffy West chromite grains.

The Al_2O_3 is increasing with MgO for both Saffy East and Saffy West chromite grains Fig.22(e), however Saffy East tend to have higher Al_2O_3 vs MgO compared to Saffy West. There is an overlap between data from the Saffy East and Saffy West chromites, Fig.22 (e).

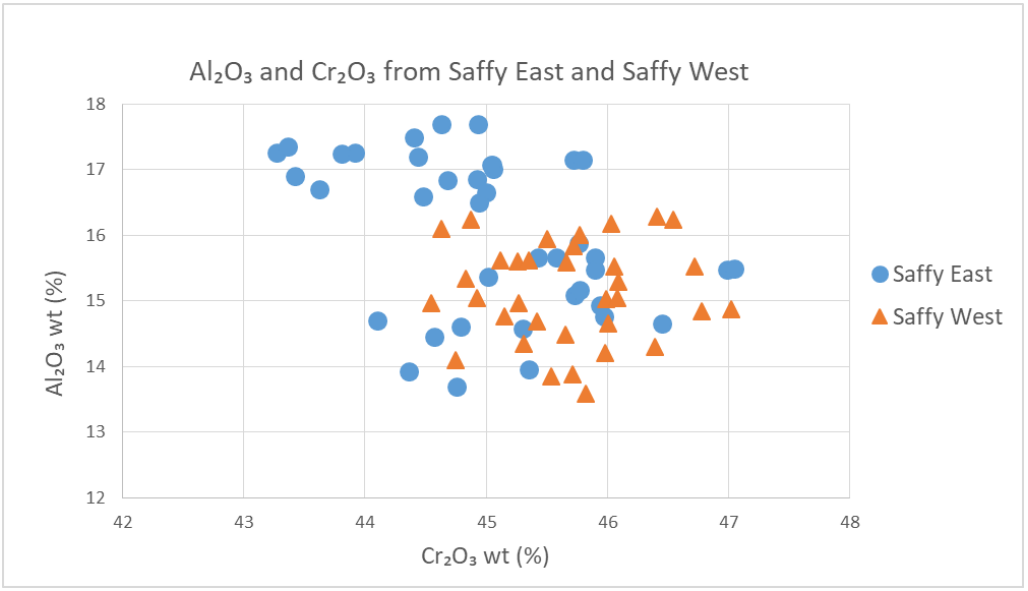


Fig 22 (f): Graph showing the concentration of Al_2O_3 vs Cr_2O_3 from Saffy East and Saffy West chromite grains.

The Al_2O_3 is higher at Saffy East while the Cr_2O_3 ranges between 43% and 47%. The Saffy West chromite grains tend to have similar Al_2O_3 vs MgO values. There is an overlap between data from the Saffy East and Saffy West chromites, Fig.22 (f).

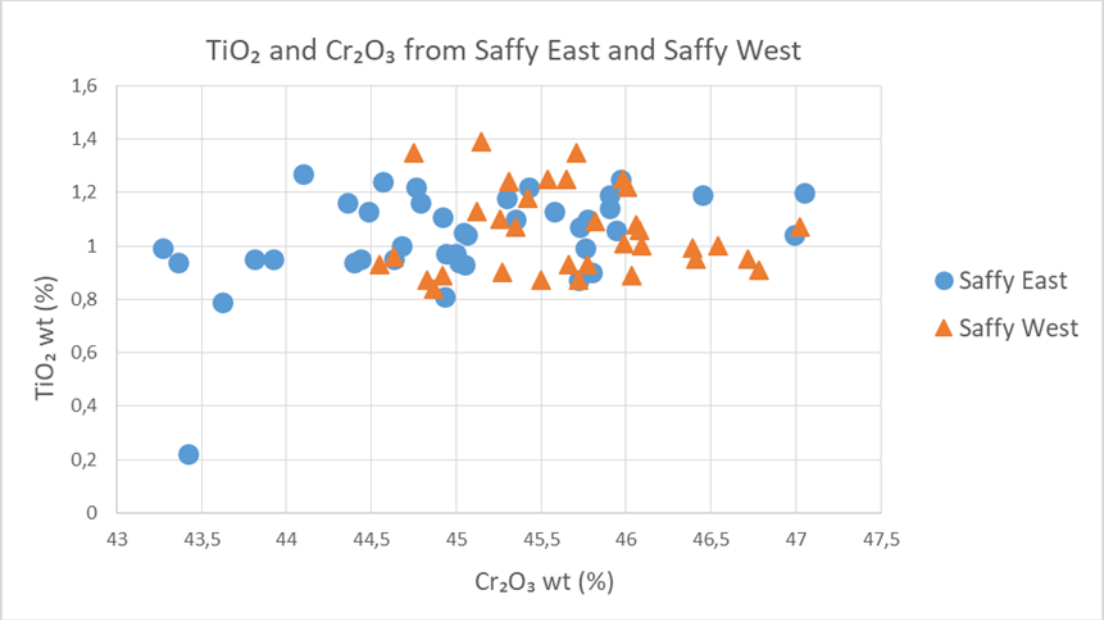


Fig 22 (g): Graph showing the concentration of TiO_2 vs Cr_2O_3 from Saffy East and Saffy West chromite grains.

At Saffy East shows scattered values of the Cr_2O_3 and TiO_2, with Cr_2O_3 ranging at about 43% to 47%, while TiO_2 show values of approximately 1%, with outlier of about 0.2% (Fig.22g). Whereas at Saffy West Cr_2O_3 shows values of about 44% to 47%, while the TiO_2 show similar values of approximately 1% (Fig.22g).

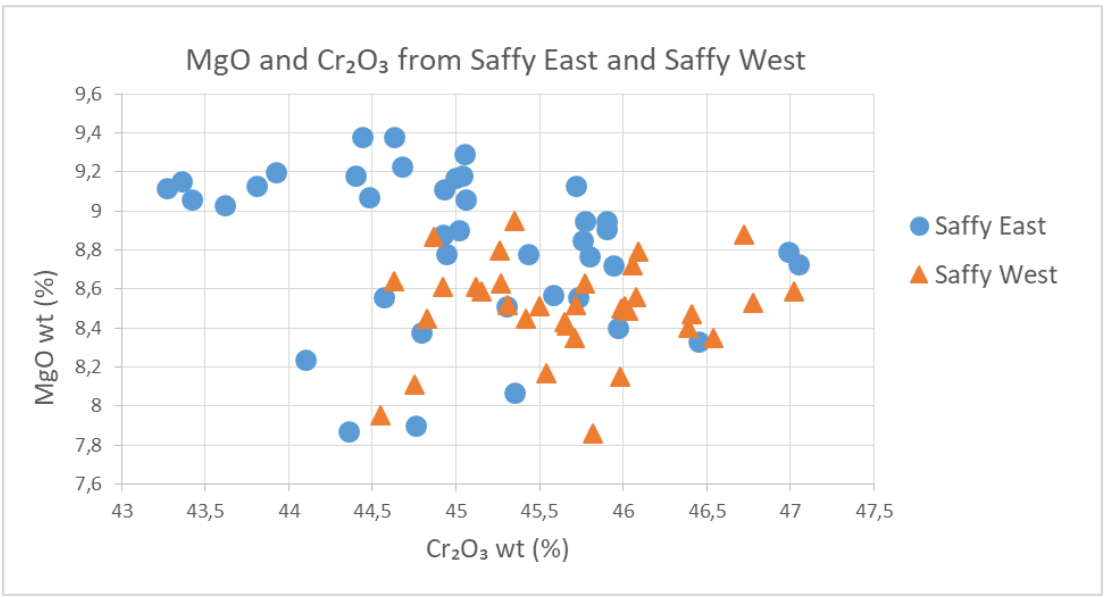


Fig 22 (h): Graph showing the concentration of MgO vs Cr_2O_3 from Saffy East and Saffy West chromite grains. (Saffy East shows higher MgO than Saffy West, the Cr_2O_3 at Saffy East is about 43% to 47%, whereas at Saffy West Cr_2O_3 is about 44.5% to 47%, Fig.22h).

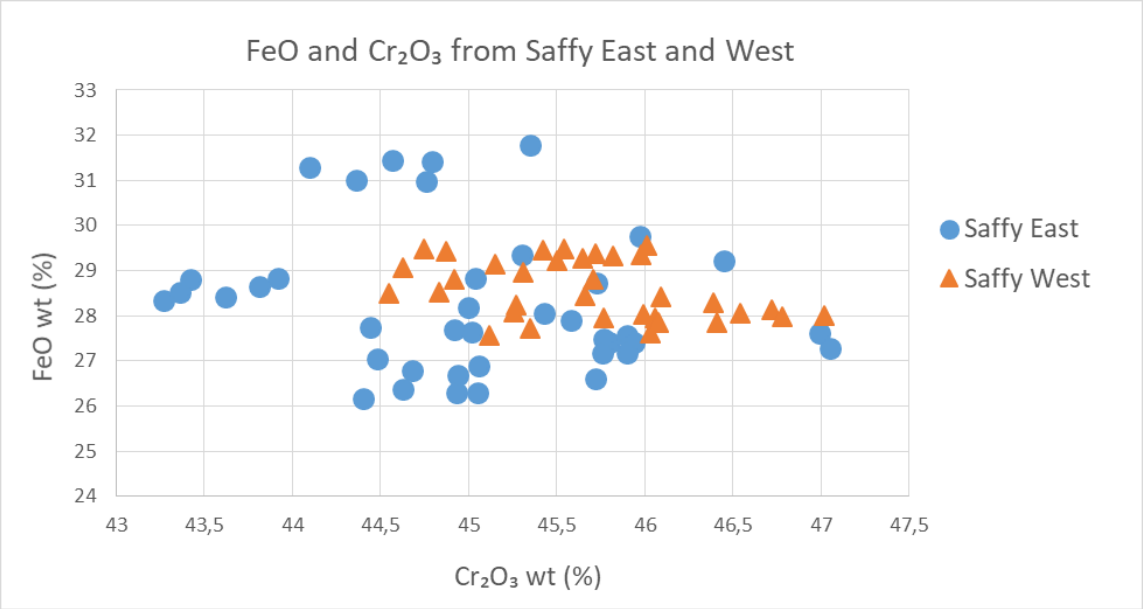


Fig 22 (i): Graph showing the concentration of Fe0 vs Cr_2O_3 from Saffy East chromite grains (FeO, is total Fe recalculated as divalent FeO).

The FeO and Cr_2O_3 at Saffy East demonstrates scattered distribution, whereas at Saffy West both FeO and Cr_2O_3 values tend to be similar to each other with closely spaced distribution. The FeO at Saffy East is higher, whereas the Cr_2O_3 is lower compared to Saffy West.

3.3.1 Chromium and Magnesium number

The chromium and magnesium ratios (Cr# and Mg#) are used to compare any possible variation in the chromites from Saffy East and Saffy West. The Mg# and Cr# are calculated as cations, 100 x Mg/ (Mg + Fe^{2+}) and 100 x Cr/ (Cr + Al). The Cr# and Mg# between Saffy East and Saffy West chromite shows variations in chemical compositions, as the Saffy East chromite grains show lower Cr# and a higher Mg#; while Saffy West chromite grains shows higher Cr# and lower Mg# (Fig.22j and Fig.22k).

The Cr# and Mg# from east of Saffy Shaft chromite grains are sub-divided into clusters based on the Cr# and Mg#. Three different clusters for east chromite grains are identified (Fig.22j), where only few samples fall under cluster 1 with Cr# (68.1 – 68.6) and Mg# (38.0 – 38.3). Cluster 2 of east of Saffy chromite grains contains Cr# (65.9 – 68.0) and Mg# (39.0 – 42.8), whereas cluster 3 has Cr# (62.7 – 64.6) and Mg# (41.2 – 44.1). The east of Saffy Shaft chromite grains in Fig.22 (j) present scattered distribution from cluster 1 to cluster 3.

Saffy West chromite grains are categorised into a two clusters based on Cr# and Mg# (Fig.22k). Cluster 1 of west of Saffy Shaft chromite grains has Cr# (66.6 – 69.9) and Mg# (38.3 – 41.0), whereas cluster 2 has Cr# (64.9 – 66.9) and Mg# (39.7 – 42.6). The Saffy West chromite grains within cluster 2 are

presenting closely spaced distribution and it is observed that both cluster 1 and cluster 2 at Fig.22 (k) and correlates with cluster 2 in Fig.22 (j).

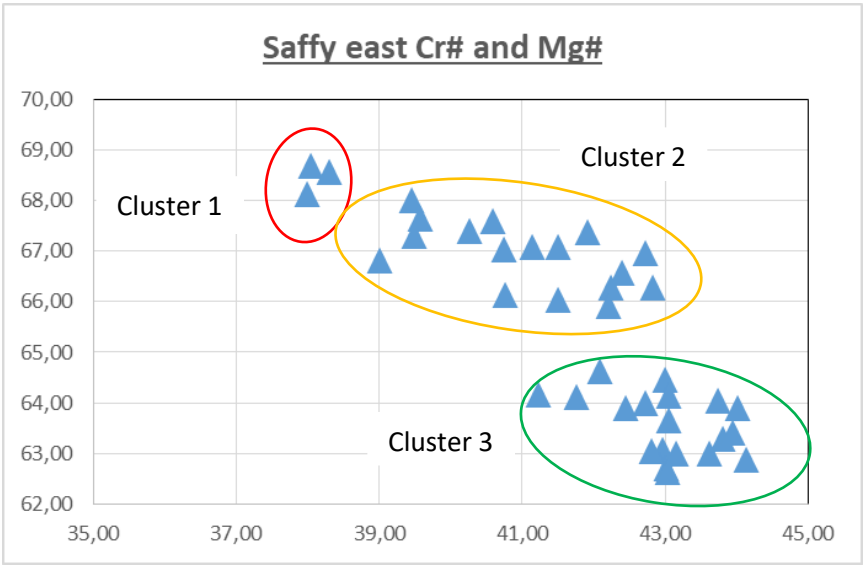


Fig 22 (j): Graph showing the Cr# versus Mg# of chromite grains from the east side of Saffy Shaft.

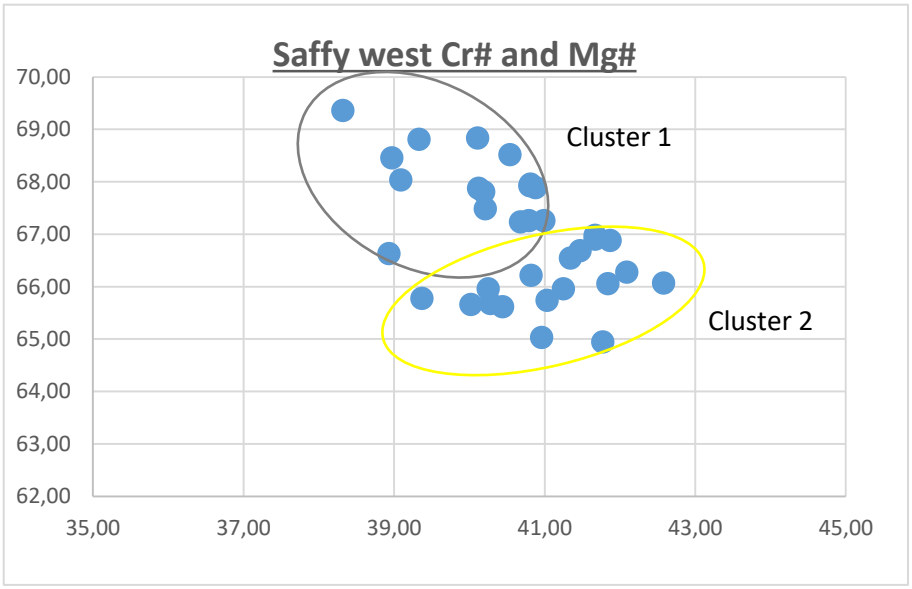


Fig 22 (k): Graph showing the Cr# versus Mg# of chromite grains from the west side of Saffy Shaft.

3.4 Bright Phase Scanning Electron Microscopy (SEM)

The Scanning Electron Microscope (SEM) using TIMA3 LMH microscope with serial number 118-0118, detector model EDAX Element 30, was utilised to identify and analyse mineral grains with a high average atomic number through a Bright Phase Search (BPS). The BPS is a method of identifying mineral grains in a rock thin section, using back-scattered electron images. The brighter the mineral grain appears, the easier the BPS identify and analyse such minerals for their chemical composition.

For the purpose of this study, six polished thin sections were scanned, three thin sections were from the east of Saffy Shaft areas, while another three thin sections were from west of Saffy Shaft areas. A total of ten bright particles from four analysed thin sections were identified. Out of ten bright particles identified, seven bright particles are identified from Saffy West two thin sections, where six bright particles are identified from the same thin section. Only three bright particles were identified from Saffy East thin sections, two particles from the same thin section, whereas one particle is from a different Saffy East thin section.

Due to the limited resources and that most bright particles from both east and west of Saffy Shaft yields similar characteristics and similar chemical composition, only two bright particles showed a slight difference in chemical composition, of which one is from Saffy East thin section (Fig.23a and Fig.23b) and while other one is from Saffy West thin section (Fig.26).

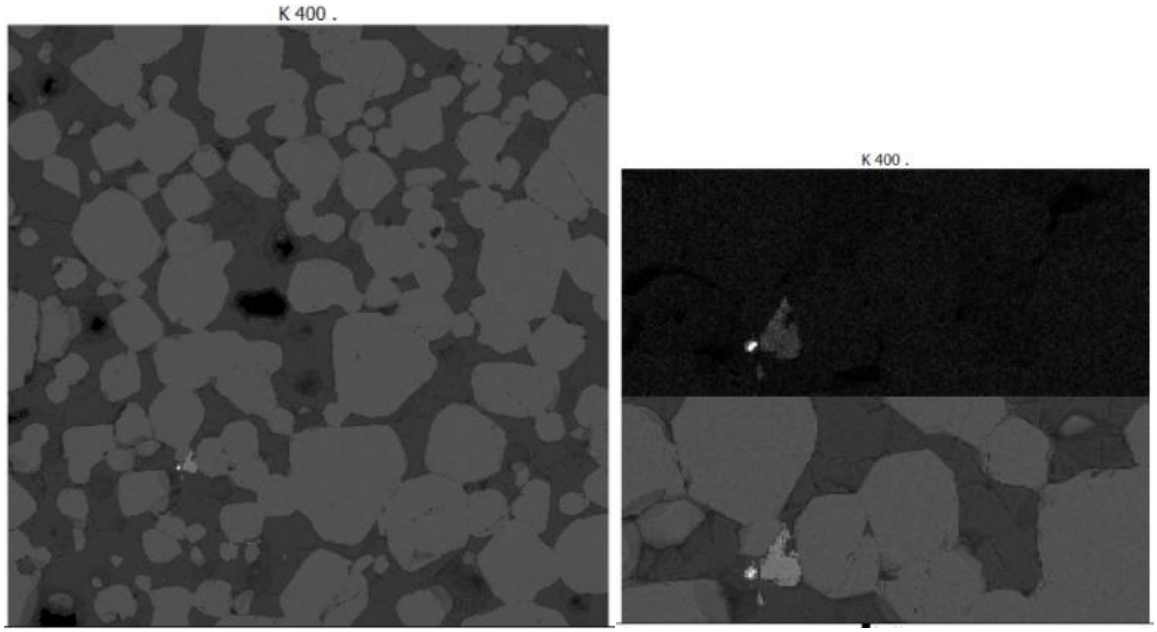


Fig 23 (a): Photomicrographs showing bright particle 1 from Saffy East thin section, with a zoomed-in view of the same particle on the right; bright white particle are platinum-group minerals, whereas the moderately bright are sulphides, light grey particles are chromite grains and dark grey areas is the plagioclase and orthopyroxene ground mass.

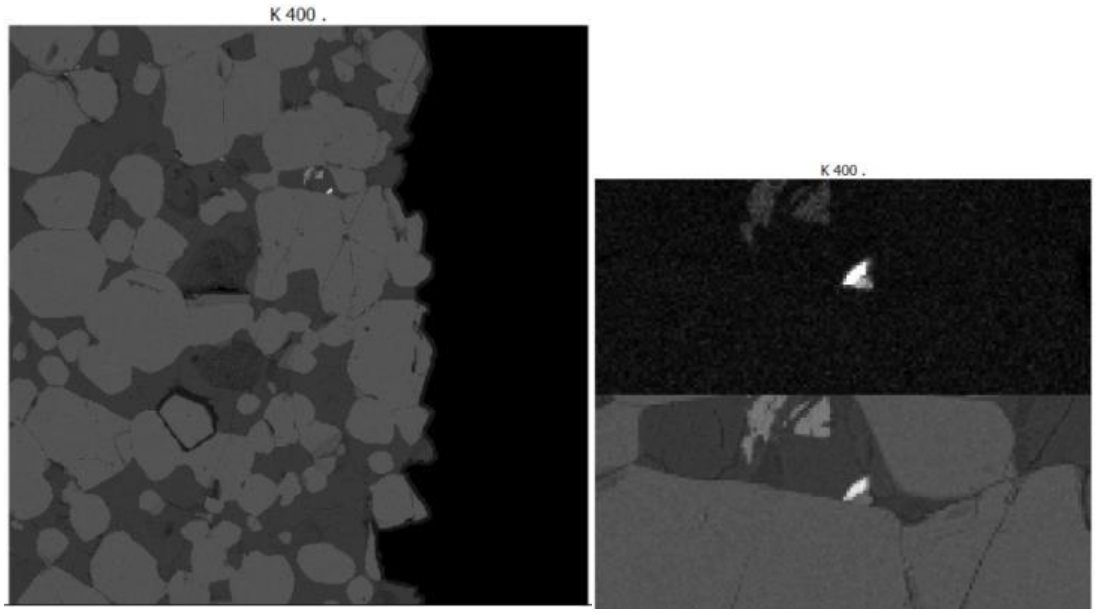


Fig 23 (b): Photomicrographs showing bright particle 2 from Saffy East thin section with a zoomed-in view of the same particle on the right; bright white particle are platinum-group minerals, whereas the moderately bright are sulphides, light grey particles are chromite grains and dark grey areas is the plagioclase and orthopyroxene ground mass.

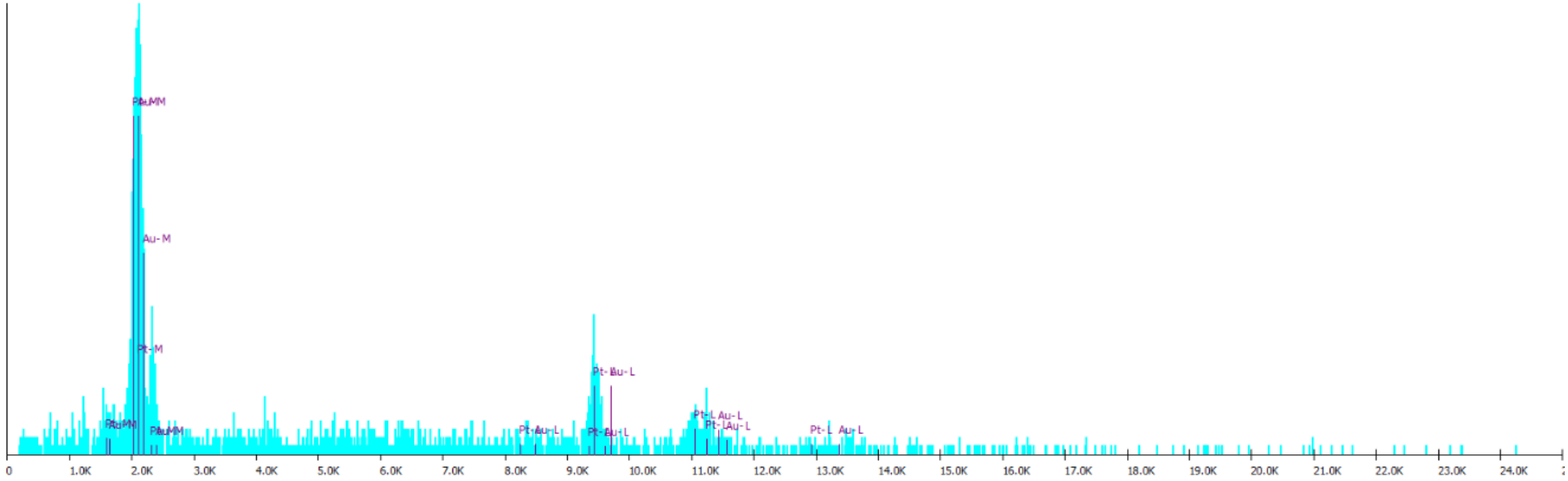


Fig 24: Typical mineral spectra for Saffy East bright particle 1, indicating the dominating elements; where platinum (Pt) and gold (Au) show significant peaks.

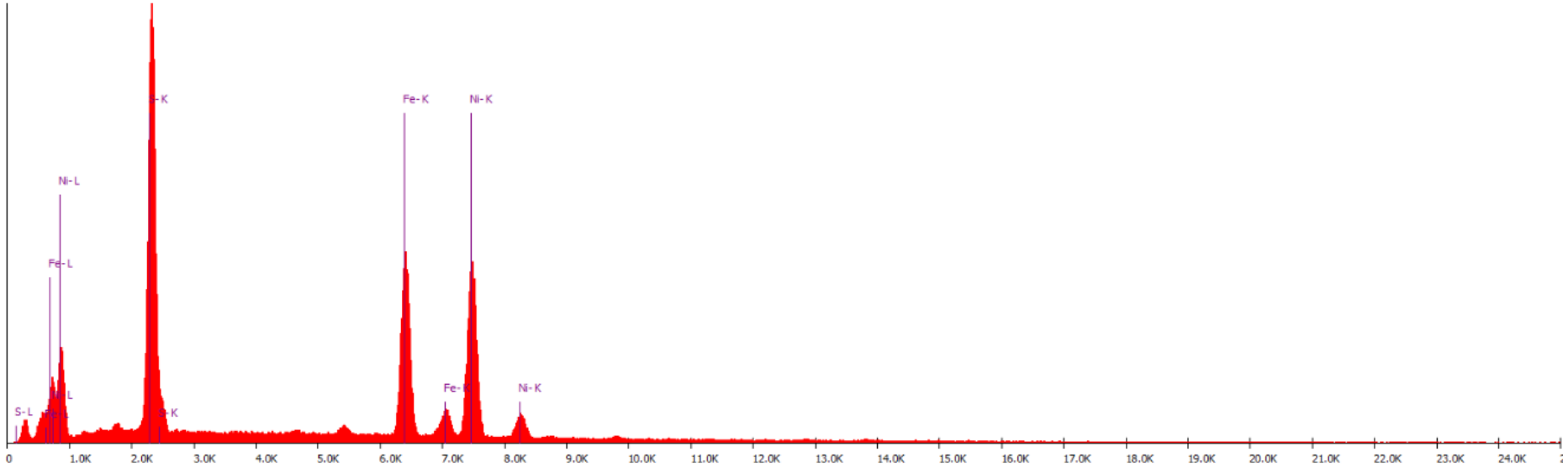


Fig 25: Spectra for particle 1, indicating the dominating elements within the bright particle of Saffy East, where iron (Fe), potassium (K), nickel (Ni) and sulphur (S) are present.



Fig 26: Photomicrographs showing the identified six particles from Saffy West thin section; bright white particle are platinum-group minerals, whereas the moderately bright are sulphides, light grey particles are chromite grains and dark grey areas is the plagioclase and orthopyroxene ground mass.

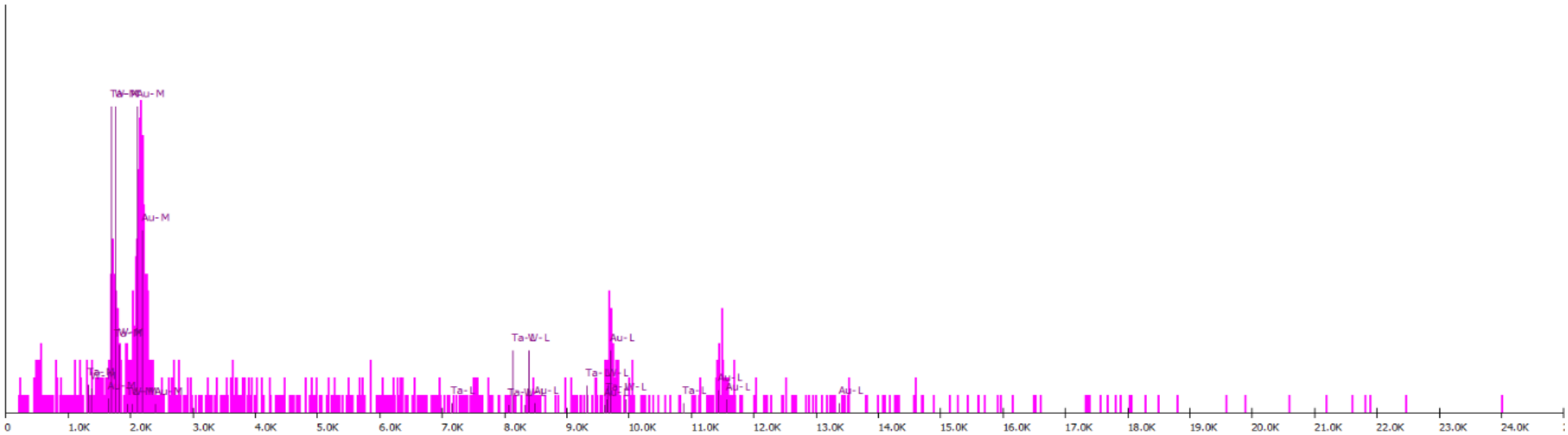


Fig 27: Spectra for particle 3, indicating the dominating elements within the bright particle of Saffy West, where tantalum (Ta), tungsten (W) and gold (Au) are present.

The Saffy East bright particle spectra Fig. 25 shows the typical presence of elements from the analysed thin sections from east chromitite, whereas Fig.24 shows a number of peaks indicating the presence of platinum (Pt) and gold (Au). Saffy East bright particles shows that iron (Fe), potassium (K), nickel (Ni) and sulphur (S) are present as they show a number of peaks. On the west of Saffy Shaft the tantalum (Ta), tungsten (W) and gold (Au) are present (Fig.27.)

Chapter 4

4. Discussion

The hydrothermal alteration has affected the UG2 chromitites in several eastern areas of Lonmin proprietary, which include Newman Shaft, however at Saffy Shaft the hydrothermal alteration has shown more prominence. Skinner (1995), suggests that the hydrothermal alteration is primarily associated with geological processes such as tectonics, heated water and volcanic processes. The sub-vertical major faults at Saffy East might have been the conduits to the hydrothermal fluids that resulted to the occurrence hydrothermal alteration. The major faults at Saffy Shaft are associated with water pockets, which percolates through these major geological structures, forcing the service departments to drain the water prior continuing with mining activities; it has been observed that these water pockets contain water with foul smell. Work by Skinner (1995), Jones *et al.* (2000) and Lagat (2009) suggests that hydrothermal fluids percolate through rock fractures or cracks, where the high saline content of the aqueous solution causes the change in composition and in characteristics of the country rock. Skinner, (1995) further suggests that the sources of water includes either meteoric waters; sea water; formation water; metamorphic water and magmatic water.

4.1 The effect of hydrothermal alteration and grade distribution

Hydrothermal alteration is a change in the mineralogy as a result of interaction of the rock with hydrothermal fluids; where the fluids carry metals in solution, either from a nearby igneous source, or from leaching out of some nearby rocks changing their composition by adding or removing or redistributing components (Shacks 2012). The underground mappings and observations have shown decrease of visual alteration intensity away from the major faults, Lagat (2009) suggests that the faults are the conduits to the hydrothermal fluids, which influences the alteration on host rocks, hence the closer the area to the major faults, the severe is the hydrothermal alteration.

It is of utmost importance that for mine planning purposes mining geology personnel should be proactive and study variations in grade and grade distributions for the affected hydrothermal altered areas, the variations in mineralogy as well as the presence of secondary minerals in the UG2 chromitite as they could potentially impact mining activities and mineral processing, Hartzenberg (2019) suggests that the alteration zones have not been identified by geologists and rock engineers during the borehole core logging at Lonmin Platinum, and further suggests that this is due to a lack of knowledge and experience, hence they identify the hydrothermal alteration zones as ‘core loss’.

There is little information documented on UG2 chromitite hydrothermal alteration in the Bushveld Complex, hence the specific locality with proved hydrothermal alteration affected the immediate hangingwall is ideal to study the possible effect of the hydrothermal alteration on the UG2 chromitite horizon, as the hydrothermal alteration is quite difficult to be identified on the UG2 horizon with the naked eye, hence the analysed Saffy UG2 chromitite layer has shown no discolouration but remained with its fine grained and grey to black in colour, this is due to less permeability or resistance to fluid of chromitite rock type (Fig.17a and Fig.17b).

Shacks (2012) confirms that permeability of the rocks controls the access of thermal fluids as it controls the hydrothermal alteration of the rocks and precipitation of secondary minerals in open spaces or pores, as the impermeable rocks tend to be slightly altered when affected by alteration. Furthermore Zhu (2012) confirms that spinel and chromite are relatively resistant to fluid-driven alteration relative to the associated silicate minerals, thus they tend to preserve original magmatic features.

However the immediate hangingwall of UG2 chromitite layer assumes a greenish colour with compromised rock strength (Fig.17a and Fig.17b), possibly due to the effect of hydrothermal alteration, this is confirmed by Lagat (2009) stating that the serpentine and talc hydrothermal alteration causes permeable rocks to assume softness, waxy and greenish appearance. The presence of talc and serpentine in the hydrothermal altered areas at Lonmin Shafts has also been analysed and confirmed by Hartzenberg (2019), Fig.28.

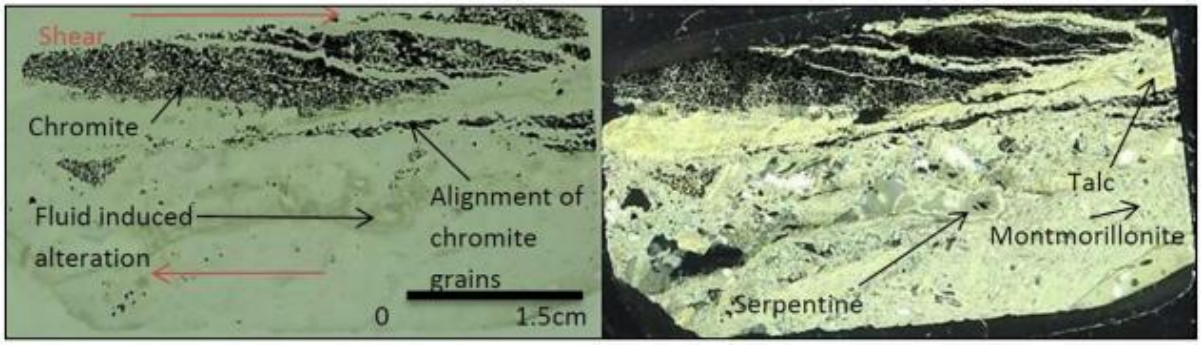


Fig 28: The presence of talc, serpentine and shearing in chromitite layers at Lonmin Platinum (Hartzenberg, 2019)

Talc and serpentine are known to be the low temperature minerals and talc indicates that a significant content of magnesium was present during the crystallisation process. Serpentine and talc alteration is only known when the host rocks are either mafic or ultramafic in composition with relatively higher iron and magnesium contents (Lagat 2009).

The UG2 chromitite of the Bushveld Complex is broadly studied, hence various models are proposed regarding the high concentrations of PGE's in UG2 chromitite layers, which are hosted by platinum group metals (Hiemstra, 1985). PGE enriched seams are generally poor is sulphur (Scoon and Teigler, 1994). The UG2 chromitite PGE grade distribution is highly concentrated in the middle of UG2 package and also at the bottom contact of chromitite package as modelled from the surface boreholes interpreted for this study (Fig.18, Fig.19). The general trend in the vertical distribution of the PGE concentration of UG2 chromitite at Lonmin shows high Pt and Pd concentration at the base and in the middle of UG2 chromitite layer (Campbell *et al*., 1983; Hiemstra, 1985 and Junge, 2014, Fig.29). This analysis corresponds to the Lonmin Platinum mineral resource modelling information (Fig.30). However the channel sampling histograms analysed for this study are showing slight different grade distribution as they show PGE grade distribution in the middle and at the top of the UG2 horizon; this might be influenced by the effect of hydrothermal alteration at Saffy Shaft (Fig.13, Fig.14 and Fig.15).

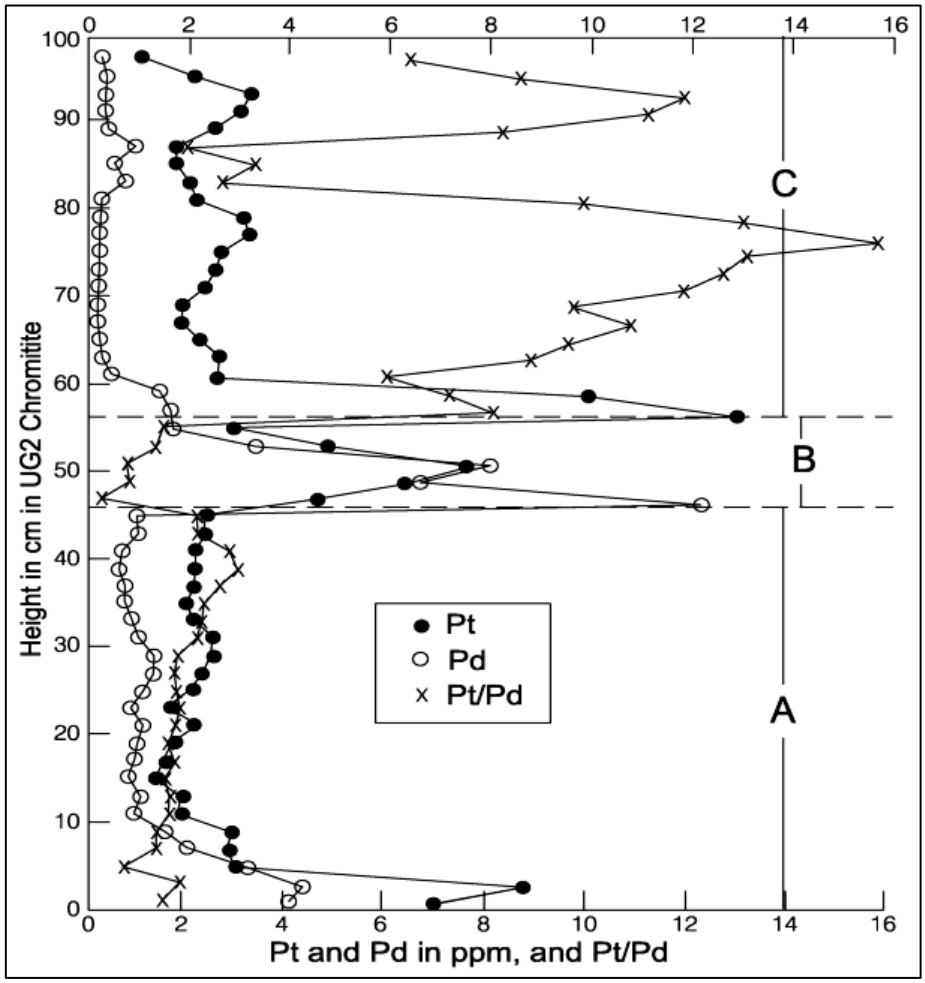


Fig 29: Plot of Pt, Pd and Pt/Pd ratio in 2cm thick samples of the UG2 chromitite from Lonplats Mines (Hiemstra, 1985).

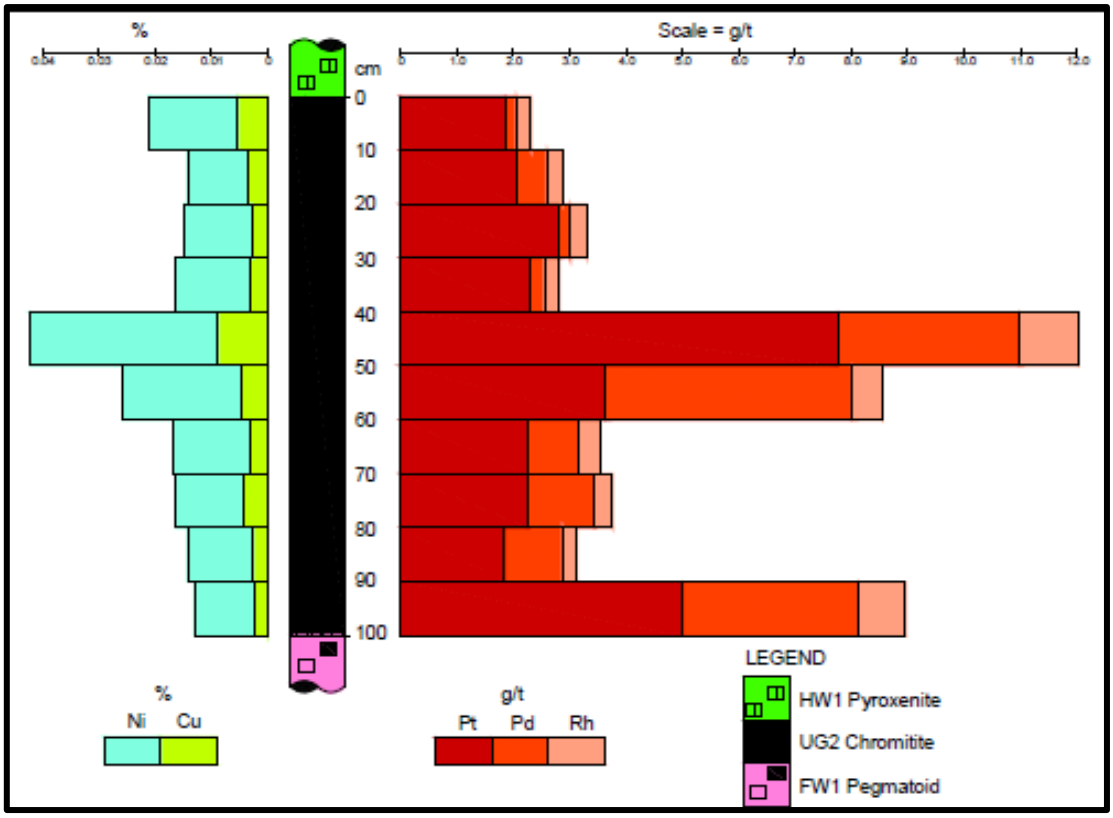


Fig 30: Vertical distribution of the PGE concentration, nickel and copper in the UG2 chromitite layer at Lonmin (Lonmin pub, 2009).

Saffy West channel sampled chromitite layer shows the better 4E grade concentration (Pt, Pd, Rh and Au) with a significant peak in the middle and on top contact of the UG2 chromitite horizon (Fig.13), indicating a grade of between 9 and 12 g/ton, while Saffy East 4E (Fig.14) shows a grade of between 7 and 9g/ton. However the grade distribution of Saffy West and Saffy East (Fig.15) is similar with peaks on top and in the middle of the UG2 horizon, this grade distribution contradicts the literature by Hiemstra (1985). Cawthorn (2011) and Lonmin pub (2009) suggests that the UG2 has distinctive upward depletion cycle of economic content. The difference of Saffy Shaft PGE grade and distribution of UG2 chromitite horizon is of a major concern, hence it cannot be ignored that Saffy Shaft grade redistribution might have been influenced by the hydrothermal fluid migration direction within the stratigraphy.

Shanks (2012), suggests that circulation of fluid in hydrothermal alteration zones disturbs both PGE chemical and mineral distribution. This means that the basal grade peak of UG2 chromitite layer from Saffy East and West, might have been migrated to the middle of UG2 chromitite, while the middle peak redirected to the top contact of the UG2 chromitite layer (Fig.15). The 4E grade of Saffy East channel sampling data shows less 4E grade as it varies between 7 g/ton and 9 g/ton; this is approximately 2% lower than Saffy West which is between 9 and 12 g/ton.

It is of utmost importance to note that the average grade from Saffy West chromitite has been affected by waste mining of approximately 1.5m in the development areas, whereas average waste mining from Saffy East areas is only 78cm (Table:1). The total waste mining in Saffy West and Saffy East chromitite includes both waste mining from the underlying footwall and from the overlying hangingwall. It is therefore clear that the average waste mining from Saffy West is almost twice as much the average waste mining from Saffy East, nevertheless the PGE grade at Saffy West remains 2% higher than Saffy East. Grieco and Merlini (2011) suggests that the post-magmatic changes in chromite can have an impact on chemical and textural characteristics of chromitite ore bodies with direct consequences on economic value of the rock.

Saffy Shaft hydrothermal alteration is an epigenetic and metasomatic alteration as it involves fluid-induced redeposition, whereby there are minerals that are being replaced by others. The geological structures such as joints, minor faults, thrust planes and veinlets witnessed from underground observations are due to the change in composition as well as the introduction of secondary minerals in a UG2 chromitite layer which have compromised the rock strength and hardness of lithologies affected by alteration. Lagat (2009) confirms that the rocks affected by hydrothermal alteration change the strength and hardness. The identified hangingwall hydrothermal alteration areas between Saffy East and Turffontein major faults are identified as geological risk areas, this is due to the unstable and crumbling ground condition they possess. During underground mapping of the underground areas the veinlets were identified and Lagat (2009) suggests that a formation which has a well-developed fracture system serve as an excellent host rock where the veins form due to fluid flow through cracks and fractures precipitating mineralisation along the walls of the fracture, ultimately filling it to form the veins and veinlets. The size and orientation of the veins and veinlets will then depend on the size and orientation of the crack or fractures.

It is noted that the average thickness of the UG2 chromitite layer from both Saffy East and West is not affected by the hydrothermal alteration as it remain approximately 1.02 m; more importantly it should be taken into consideration that alteration is a post magmatic process which, occurs at relatively low temperatures, whereas extreme high temperatures are required to deform chromitite. The identified thin pyroxenite lenses, which assumed the greenish colour splits the UG2 chromitite into at least two bands, with top band becomes thinner than the bottom band (Fig.9). These pyroxenite lenses are not influenced by the hydrothermal alteration, they essentially formed with UG2 chromitite layer. Voordouw *et al*. (2009), Cawthorn (2011) and Junge (2014) confirms that the pyroxenite lenses are due to a time break during the formation of the UG2 chromitite layer. Latypov *et al*.2017, confirms that most main chromitite layers are not single layers, but are composed of at least two to three thinner

sublayers that are locally separated by a discontinuous orthopyroxenite or sometimes anorthosite, which is up to a few centimetres to decimetres thick, he further suggests that main chromitite layers and sublayers may laterally merge or split, of which the splitting of chromitite layers occurs when chromitite sublayers start draping over the hill-like silicate rocks of antipotholes.

4.2 Chromite petrography interpretation

Both Saffy East and Saffy West polished thin sections are showing euhedral shape chromite grains with poikilitic texture and they dominantly interlocked to each other with grain size between 0.05 mm to 1 mm. Grieco and Merlini (2012) confirms that chromitite bodies consists of euhedral to subeuhedral chromite crystals with grain sizes varying between 0.1 and 2 mm, with some rare nodular textures showing crystals of up to 5 mm in size. The groundmass from Saffy West chromite grains seem to be slightly different with dominantly showing plagioclase and orthopyroxene, whereas Saffy East sample groundmass has a localised clinopyroxene (Fig.21). Saffy East and Saffy West chromite grains are interlocked to each other, Junge (2014) confirms that chromite grains are annealed in more compact accumulations, often showing triple junctions, whereas Vukmanovic *et al.*2013 suggests that chromite grains can show a range of orientations with no consistent orientation. The chromite grains are dominantly forming up to 85% of the chromitite layer, these chromite grains are hosted in orthopyroxene and plagioclase groundmass which constitute approximately 15% of chromitite layer studied, Naldrett *et al.*2012 suggests that UG2 modal abundance of chromite is between 60-90%, while the plagioclase and orthopyroxenes constitutes approximately 10%.

Secondary minerals such as serpentine, talc and biotite are present in Saffy East chromite samples (Fig.21 and Fig.28), Vukmanovic *et al*.2013, suggest that deformed chromites bear inclusions composed mainly of polymineralic aggregates of orthopyroxene, clinopyroxene, biotite, phlogopite, apatite and rutile. Whereas Lagat (2009) confirms that talc indicates that there was a significant content of magnesium during the crystallisation process, he further suggests that serpentine and talc alteration occurs merely when the host rocks are either mafic or ultramafic in composition which are relatively higher iron and magnesium contents. Some chromite grains at Saffy East samples have shown presence of iron concentration (Fig.21), Ulmer (1974) suggests that the outer chromite rim is low in magnesium, aluminium and close to ferrichromite by composition unlike the chromite core. He further stated that the abundance and distribution of Fe-chromite is strictly associated with serpentinisation not necessarily influenced by the presence of magnetite, as the Fe-chromite is rare in mafic rocks but mostly occurs as a substitution for chromite at the rim of original chromite grains. Ulmer, 1974 further suggests that the non-pervasive alteration of Cr-spinel into Fe-chromite, mighty be strongly affected by local conditions of fluid flow, suggesting a relatively shallow environment

associated with temperatures in excess of 200–300°C or even at ambient conditions. Saffy East chromitite samples are showing presence of serpentine and talc dominantly in linear structures, fractures and shear zones, whereas biotite encloses some chromite grains (Fig.21); literature by Junge (2014) suggests that at high alteration intensity, rocks may be pervasively altered where all primary minerals in a rock are altered to new hydrothermal minerals.

4.3 Electron Microprobe analysis interpretation

Electron Microprobe analysis has been used to analyse compositional difference between chromite grains from Saffy West and Saffy East adjacent to Saffy East Fault, presence of secondary and primary minerals (e.g. orthopyroxene being replaced by minerals such as serpentine, amphibole or talc, also analysing plagioclase as it might be replaced by mineralisation such as saussurite alteration). The analysed Saffy West chromite grains seem to be more consistent and homogeneous as compared to the less consistent Saffy East chromite grains under microprobe analysis Vukmanovic *et al.*2013 suggests that chromite crystal morphology is defined by its size and its solidity. The chromite grains that were analysed are hosted in both intercumulus plagioclase and orthopyroxene while some samples from Saffy East contained clinopyroxene. Kaufmann *et al*.2019 confirms that chromitites are composed of chromites, which are cemented by intercumulus plagioclase and orthopyroxene. This means the presence of localised of clinopyroxene at Saffy East might have been influenced by the effect of the hydrothermal alteration.

The texture of chromite grains slightly differ between Saffy East and West as some chromite grains, from east are more interlocked to each other compared to west. It is also noted that Saffy East samples shows irregular edges with random fractures. Vukmanovic *et al*.2013 suggests that the chromite grain boundaries are construed as early magmatic deformation microstructures and are possibly due to the compaction and cooling of the magmatic column above the solidus temperature, hence the deformation microstructures with chromite grain morphology is an evidence that chromites attained their irregular morphologies at the cumulus stage. These chromite characteristics identified under electron microscope from both Saffy West and Saffy East, indicates the possibility of hydrothermal alteration from both east and west of Saffy Shaft.

For the purpose and comparison of the study, Saffy East and West chemical composition (Table 3 and Table 4) are compared with data from Vukmanovic *et al* 2013 (Table 5), where they compare lower and upper chromitite thin layers of the Merensky reef in Bushveld Complex. It is not ignored that the similarities and the differences between UG2 chromitite and Merensky chromite composition might also be prone by their different stratigraphic positions and distinct composition of their parental

magmas. This means the deformation or alteration that might have observed on these ore bodies might not be the primary reason for the similarities and differences between UG2 and Merensky chromite composition. Nevertheless in Vukmanovic *et al* 2013, the lower chromitite thin layer is considered as the deformed chromitite due to the presence of inclusion in chromite grains, whereas the upper chromitite thin layer is considered as the normal or ideal chromitite as it does not have any deformation characteristics. The contents of Al_2O_3, MgO, TiO_2 in Saffy East chromite (Fig.22(a), Fig.22(b), Fig.22(c), Fig.22(d), Fig.22(e), Fig.22(f), Fig.22(g), Fig.22(h) and Fig.22(i) are similar to those reported by Vukmanovic *et al* 2013 (lower chromitite thin layer of Merensky data, Table 5), where the composition of deformed chromite grains is characterised by slightly higher concentration of Al_2O_3 and MgO (Table 5), where the average concertation of Al_2O_3 is 16%, average concertation of MgO is approximately 8%, while TiO_2 is approximately 1%. The Al_2O_3 is increasing with MgO for both Saffy East and Saffy West chromite grains, however Saffy East tend to have higher Al_2O_3 vs MgO compared to Saffy West, (Fig.22e). Saffy East chromite data shows that the lower the FeO total content then the higher the MgO, whereas Saffy West shows lower values of FeO and MgO contents compared to Saffy East chromite data, (Fig.22d).

Saffy West chromite composition is also similar to Vukmanovic *et al* 2013 (upper chromitite thin layer of Merensky data, Table 5), where the composition of undeformed/normal chromite grains is presented with average Al_2O_3 of approximately 13%, MgO to be about 8%,while TiO_2 is also approximately 1%. It is of utmost importance to note that the deformed chromite thin layer composition from Vukmanovic *et al* 2013 are similar to Saffy East chromite composition, this suggests that there was chromite deformation secondary process that took place at Saffy East, hence the hydrothermal alteration is suggested to be the possible process that has led to Saffy East current chemical composition. It is also noted that Cr_2O_3 composition from both Saffy East and West is slightly different from Vukmanovic *et al* 2013,Table 5; however they suggests that the deformed chromitite grains show lower values of Cr number, Ti and Fe than the grains from the undeformed chromitite layer.

	Lower chromitite								Upper chromitite			
	Idiomorphic grain				Ameboidal grain				Idiomorphic grain			
	Core		Rim		Core		Rim		Core		Rim	
	Av	Sdev	Av	Sdev	Av	Sdev	Av	Sdev	Av	Sdev	Av	Sdev
n	11		12		24		25		26		22	
TiO_2	1.07	0.02	1.18	0.02	1.05	0.02	1.32	0.03	2.17	0.03	2	0.03
Al_2O_3	16.51	0.03	16.35	0.03	16.47	0.03	16.85	0.03	12.23	0.02	12.36	0.02
V_2O_3	0.33	0.01	0.33	0.01	0.34	0.01	0.34	0.01	0.5	0.01	0.5	0.01
Cr_2O_3	40.03	0.12	40.15	0.12	40.17	0.12	40.83	0.12	39.83	0.12	40.07	0.12
NiO	0.26	0.02	0.25	0.02	0.25	0.02	0.25	0.02	0.31	0.02	0.29	0.02
FeO	23.06	0.6	23.33	0.62	23.38	0.52	23.98	1.46	25.31	0.18	25.15	0.26
Fe_2O_3	11.4	0.71	10.91	0.55	11.15	0.42	10.87	0.87	12.87	0.59	12.8	0.64
MnO	0.16	0.01	0.17	0.01	0.16	0.01	0.16	0.01	0.19	0.01	0.18	0.01
MgO	7.87	0.02	7.8	0.02	7.83	0.02	7.95	0.02	6.75	0.02	6.77	0.02
Total	99.56		99.38		99.66		101.47		98.86		98.84	
Ti	0.026		0.029		0.026		0.031		0.055		0.05	
Al	0.634		0.629		0.632		0.631		0.484		0.489	
V	0.007		0.007		0.007		0.007		0.011		0.011	
Cr	1.03		1.036		1.032		1.037		1.058		1.063	
Ni	0.007		0.007		0.007		0.006		0.008		0.008	
Fe^{2+}	0.638		0.643		0.64		0.646		0.711		0.706	
Fe^{3+}	0.269		0.262		0.269		0.255		0.325		0.323	
Mn	0.005		0.005		0.004		0.004		0.005		0.005	
Mg	0.382		0.379		0.38		0.379		0.338		0.339	
Mg#	37.82		37.33		37.33		37.13		32.21		32.42	
Cr#	61.92		62.23		62.06		61.92		68.6		68.5	
Fe^{3+}/R	0.308		0.296		0.3		0.289		0.17		0.17	

Table 5: Average compositions of the chromite crystals from the lower and upper chromitite layer from the Merensky Reef, (Vukmanovic *et al*.2013).

4.3.1 Cr# and Mg# interpretation

The chromite grains analysed for Cr# and Mg# have revealed chemical variations, where the Cr# from Saffy West chromite seem to be higher whereas the Mg# is showing lower values, while the analysed Saffy East chromite grains reveals slightly lower Cr# with higher Mg#, this observation is confirmed by Eales and Reynolds (1986) and Junge *et al*. 2014, who suggest that the unaltered chromite samples shows chromium trends that has an upwards increasing Cr# and decrease in Mg# content and further states that chromite grains which are mainly surrounded by orthopyroxene, have generally lower Mg# and larger Cr# than chromite grains surrounded dominantly by plagioclase. Vukmanovic *et al.*2013, confirms that chromite crystals from the deformed chromitite layer shows significantly higher Mg# compared with chromite crystals from the undeformed chromitite layer. These authors suggest that deformed chromitite crystals show lower values of Cr#, Ti and Fe than the crystals from the undeformed chromitite layer.

Different clusters are shown in Fig.31 with cluster 1 indicating chromite grains with very low Mg# of 0-10 and extreme high Cr# (81-93). Junge *et al*.2014 suggests that this is due to the effect of hydrothermal alteration, with enrichment of Fe and Cr and depletion of Mg and Al. Clusters III, IV, V and VII of Fig.31 correlates with both Saffy East and West clusters analysed for this study Fig.22 (j) and Fig.22 (k). This might mean that Saffy East chromite, which was expected to show a significant difference from Saffy West, is not as severely altered as it was initially predicted, perhaps, it is

moderately affected by hydrothermal alteration, alternatively it might mean that both Saffy East and Saffy West chromitites are affected by hydrothermal alteration at different degrees of alteration, where the east side is relatively more affected by hydrothermal alteration compared to Saffy West.

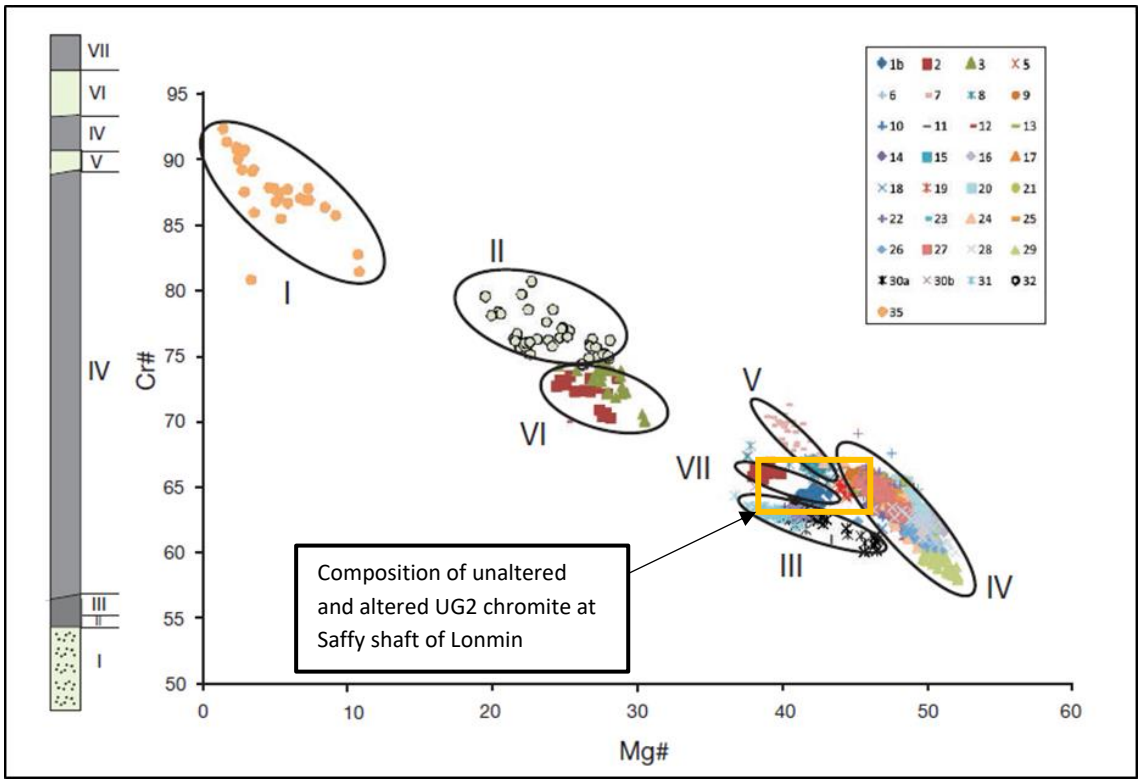


Fig 31: Analysis showing the Cr# and Mg# of seven chemical group layers, showing variation in host rock units (after Junge *et al.* 2014).

4.4 Scanning Electron Microscope (SEM) interpretation

SEM analysis has also confirmed the morphology and the matrix of the chromitite, with approximately 85% of euhedral chromite. UG2 chromitites from both Saffy East and West contain PGM (platinum group minerals), which are interlocked in the matrix not on the chromite grains (Fig.23a, Fig23b and Fig.26). The sulphides are the hosts of the PGM grains on the chromitite layers, Bamba (1974) confirms that chromitite bodies tend to be distinguished from the other chromitites based on the difference in PGE concentration. PGM's are identified using a Bright Phase Search of scanning electron microscope in most thin sections as they tend to be the brightest minerals compared to other surrounding minerals (Fig.23a, Fig23b). PGM's from Saffy East and West seem to be affected by the hydrothermal alteration as their occurrence is observed to be abundant at Saffy West than Saffy East. It has been observed that the PGM grains and intergrowths do not occur on the chromite grains but they are

interstitial to chromite grains (Fig.23a, Fig.23b and Fig.26), Vukmanovic *et al.*2013 confirms that the sulphides occur either as an interstitial phase between chromite and silicate grains or more rarely as inclusions within chromites or silicates.

The only sulphides observed and identified in this analysis is pentlandite for both Saffy East and Saffy West (Fig.24), Vukmanovic *et al.*2013 suggests that base-metal sulphides consists of intergrowths of pyrrhotite, pentlandite and chalcopyrite which are present as minor components in Merensky reef chromitite layers. At Saffy West some bright particles show a spectral peaks of tantalum (Ta), tungsten (W) and gold (Au); whereas Saffy East bright particles indicates the presence of iron (Fe), potassium (K), nickel (Ni) and sulphur (S), (Fig.25).

Chapter 5

5. Conclusion

Saffy East is affected by hydrothermal alteration, which is associated with the dominant sub-vertical fault on the eastern block of the shaft, whereas Saffy West is partially affected by the hydrothermal alteration as there are few major faults on the west block of the shaft. The sub-vertical faults at Saffy Shaft are the conduits of hydrothermal fluids, which have contributed to the hydrothermal alteration. The hydrothermal alteration at Saffy Shaft of Lonmin has dominantly affected the east side of the shaft, which is known to be mostly separated by major sub-vertical faults with throw ranging between 20 and 40 m. Some of these faults are associated with water pockets and areas affected by hydrothermal alteration have shown unstable ground conditions with geological structures such as joints, veinlets, minor faulting and deteriorating ground condition. Hydrothermal alteration intensity and severity of geological structures decreases away from the faults. In areas where the UG2 chromitite horizon is separated by the horizontal pyroxenite thin lenses, the pyroxenite lenses presents more hydrothermal alteration than the UG2 chromitite. The UG2 chromitite layer is relatively resistant to fluid-driven alteration relative to silicate minerals, hence it tend to preserve original magmatic features.

The PGE grade is slightly affected by the hydrothermal alteration on the east of Saffy Shaft, reducing the overall average grade by approximately 2%, whereas the waste mining at Saffy West seem to be possibly caused by incompetence amongst mining personnel. Hydrothermal alteration at Saffy East affects the grade distribution of the altered UG2 chromitite layer, as it possesses higher PGE grade in the middle and on top contact of chromitite package, contrary to the ideal grade modelling of the lease area. Channel sampling data indicates that the hydrothermal alteration is the possible contributing factor on reducing the overall 4E grade and changing the grade distribution. Historical data of the surface boreholes analysed does not show any indication of hydrothermal alteration.

It has been identified that the chromite grains are euhedral in shape and they are hosted in plagioclase and orthopyroxene groundmass, where clinopyroxene is present in some altered samples from Saffy East. The chromite grains averages 85% of the chromitite layer, while plagioclase and orthopyroxenes occupies 15%. The chromite grains range between 0.05 and 1 mm in size. Petrographic analysis also indicated that Saffy East and Saffy West chromite vary in mineralogy and texture depending on the severity and the effect of hydrothermal alteration, where at Saffy East chromitite the veins and micro fractures associated with secondary minerals such as serpentine, talc and biotite are present. It has been revealed that the chemical composition of chromite grains at Saffy West and Saffy East is

homogeneous, however at Saffy East UG2 Cr# of chromite is lower, while the Mg# of chromite is higher. The Al_2O_3 is increasing with MgO for both Saffy East and Saffy West chromite grains, however Saffy East has higher Al_2O_3 vs MgO compared to Saffy West. Saffy East chromite shows that the lower the FeO total content the higher the MgO, whereas Saffy West shows lower values of FeO and MgO contents compared to Saffy East chromite data.

Therefore, it is concluded that Saffy East of Lonmin Platinum is indeed affected by hydrothermal alteration, furthermore it is of utmost importance to note that Saffy UG2 altered chromitite is not as severely altered as it was initially predicted, as there is no anthophyllite alteration minerals observed. Saffy West seem to be also affected by hydrothermal alteration at lesser degree compared to Saffy East. The UG2 chromitite horizons from both Saffy East and West contain PGM grains which are interlocked in the matrix not on the chromite grains. The only observed PGM from Saffy East and West contain Pt and Au as major components. The effect hydrothermal alteration on UG2 chromitite horizon at Saffy Shaft has to be further investigated possibly at PhD level, where a significant number of samples from a bigger area will be analysed and studied in more detail, comparing it with other shafts of Lonmin Platinum, where there is less or no possibility of hydrothermal alteration, such as Western Platinum and Karee Mine.

References

Bamba T. (1978). The Alpine chrome ores from Japan, Department of Geology and Mineralogy, Faculty of Science, Hokkaido University,No.1533,18,pp.167-179.

Barnes I and O'Neil J.R. (1969). The relationship between fluids in some fresh Alpine-type ultramafic and possible modern seperntinization,Western United States,U.S Geological Survey, Menlo Park, California.

Beeson M.H and Jackson E.D. (1969). Chemical composition of altered chromites from Stillwater Complex, Montana, Mineralogical Society America

Brough C.P, Prichard H.M, Neary C.R, Fisher P.C & MacDonald I. (2015). Geochemical Variations within Podiform Chromitite Deposits in the Shetland Ophiolite: Implications for Petrogenesis and PGE Concentration, School of Earth and Ocean Sciences, Main College, Cardiff University, Park Place, United Kingdom.

Campbell, I.H., Naldrett, A.J., and Barnes, S.J. (1983). A model for the origin of the platinum-rich sulfide horizons in the Bushveld and Stillwater Complexes: Journal of Petrology, 24,133–165.

Cawthorn R.G. & Walraven F. (1998). Emplacement and Crystallization Time of the Bushveld. Journal of Petrology, 39, 1669-1687.

Cawthorn R.G. (1999). The platinum and palladium resources of the Bushveld Complex. South African Journal of Science, 95,481–489.

Cawthorn, R.G. (2011). Geological interpretations from the PGE distribution in the Bushveld Merensky and UG2 chromitite reef. The Southern African Journal of Mining & Metallurgy, 111, 67-79.

Davis A. (2013). Nature and origin of secondary alteration in hangingwall pyroxenite of the UG2 Chromitite at Saffy shaft, University of Cape Town, South Africa (MSc thesis).

Eales, H.V., and Reynolds, I. (1986). Cryptic variations within chromitites of the Upper Critical zone, Northwestern Bushveld Complex: Economic Geology, 81, 1056–1066.

Good N. and de Wit M.J. (1997). The Thabazimbi-Murchison Lineament of the Kaapvaal Craton, South Africa: 2700 Ma of episodic deformation, Journal of Geological Society, 154, 93-97.

Grieco G., Merlini A. (2011). Chromite alteration processes within Vourinos ophiolite, International Journal of Earth Sciences (Geologische Rundschau), 101, 1523–1533.

Hiemstra S.A. (1986). The distribution of some platinum group elements in the UG2 chromitite layer of the Bushveld Complex, Economic Geology, 80,944-957.

Kaufmann F. E. D., Hoffmann M. C., Bachmann K., Veksler I. V., Trumbull R. B., Hecht L. (2019): Mineral chemistry of chromite, orthopyroxene and plagioclase of chromitite layers in the Lower and Middle Group of the northwestern Bushveld Complex. GFZ Data Services.

Kinnaird J.A., Kruger F.J., Nex P.A.M & Cawthorn R.G. (2002). Chromite formation a key understanding processes of platinum enrichment. Transactions of the Institute of Mining and Metallurgy, 111, B23-B35.

Kruger F.J. (2005). Filling the Bushveld Complex magma chamber: lateral expansion, roof and floor interaction, magmatic unconformities, and the formation of giant chromitite, PGE and Ti-V-magnetite deposits, Mineralium Deposita, 40, 451–472.

Lagat J. (2009). Hydrothermal alteration mineralogy in geothermal fields with case examples from Olkaria domes geothermal field, Geothermal Development Company, Nairobi, Kenya.

Latypov R., Chistyakova S., Mukherjee R. (2017). A Novel Hypothesis for Origin of Massive Chromitites in the Bushveld Igneous Complex. Journal of Petrology, 58, 1899-1940.

Lee C.A. (1996). A review of mineralization in the Bushveld Complex and some other layered intrusions. In: Cawthorn R.G (ed) Layered intrusions. Elsevier, Amsterdam, 103–145

Lonmin Pub. (2009). Local Geology of Lonmin Marikana Operations.

Lonmin Pub (2014). Geological Overview of Lonmin Marikana Operations.

Maier, W.D., and Barnes, S.J., (2008), Platinum group elements in the UG1 and UG2 chromitites, and the Bastard reef, at Impala platinum mine, western Bushveld Complex, South Africa: Evidence of late magmatic cumulate instability and reef constitution: South African Journal of Geology, Vol. 111, pp. 159-176.

Maier W.D, Barnes S.J & Groves D.I. (2012). The Bushveld Complex, South Africa: formation of platinum– palladium, chrome- and vanadium-rich layers via hydrodynamic sorting of a mobilized cumulate slurry in a large, relatively slowly cooling, subsiding magma chamber: Mineralium Deposita, v. 48, pp. 1–56.

Maier W.D, Groves D.I. (2011). Temporal and spatial controls on the formation of magmatic PGE and Ni–Cu deposits. Mineralium Deposita, 46,841–85.

Mihalik P. and Saager R. (1968).Chromite grains showing altered borders from the basal reef, Witwatersrand system, National institute for metallurgy,Cottesloe,Transvaal and Economic geology research unit University of the Witwatersrand ,Republic of South Africa, 53, 1543-1550.

Naldrett A. J, Wilson .A, Kinnaird .J, Yudovskaya .M, Chunnett .G (2012).The origin of chromitites and related PGE mineralization in the Bushveld Complex: new mineralogical and petrographic constraints, Mineralium Deposita 47, 203-232.

Naldrett A. J, Kinnaird .J, Wilson A, Yudovskaya .M, McQuade .S, Chunnett .G, Stanley .C. (2009a). Chromite composition and PGE content of Bushveld chromitites: part 1—the lower and middle groups. Transactions of the Institution of Mining and Metallurgy B118:131–16.

Pat Shanks III W.C. (2012). Hydrothermal alteration in volcanogenic massive sulfide occurrence model: U.S. Geological Survey Scientific Investigations Report, chapter 11, 2010–5070.

Penberthy C. J., Merkle R.K. (1999). Lateral variation of PGM's and mineralogy of the UG2 chromitite layer. Journal of South African Geology, 102(3), 240-250.

Schweitzer J. (2009). Technical Report: Lebowa Platinum Mine Limpopo Province, South Africa.

Scoon, R. N and Teigler, B. (1994). Platinum group element mineralization in the Critical Zone of the Western Bushveld: 1. Sulfide-poor chromitites below the UG2. Economic Geology, 89, 1094-1121.

Ulmer G.C. (1974). Alteration of Chromite during serpentinization the Pennsylvania-Maryland district, Geology Department, Temple University Philadelphia, Pennsylvania 19122, 59, 1236-1241.

Van der Merwe J.J., Vermaak A.H., Slabbert M.J., Mauve A.C. (1998). An overview of the geology of the UG2 Chromitite Layer and its surrounding lithologies on Lonrho Platinum's lease area (unpubl).

Voordouw R, Gutzmer J, Beukes N.J. (2009). Intrusive origin for Upper Group (UG1, UG2) stratiform chromitite seams in the Dwars River area, Bushveld Complex, South Africa. Mineral and Petrology, 97, 75–94.

Vukmanovic Z., Barnes S.J., Reddy S.M., Godel B., Fiorentini M.L. (2013). Morphology and microstructure of chromite crystals in chromitites from the Merensky Reef (Bushveld Complex, South Africa), Contributions to Mineralogy and Petrology, 165, 1031-1050.

Walraven F., Armstrong R.A, Kruger F.J. (1990). A chronostratigraphic framework for the north-central Kaapvaal craton, the Bushveld Complex and the Vredefort structure, Isotope Division, Geological Survey of South Africa, Pretoria South Africa, 171, 23-48.

Wilson M.G.C, Anhaeusser C.R. (1998). The mineral resources of South Africa. Council for Geoscience, Handbook, 16,740.

Zeh A., Ovtcharova M., Wilson A. L, Schaltegger U.(2015).The Bushveld Complex was emplaced and cooled in less than one million years – results of zirconology, and geotectonic implications, Earth and Planetary Science Letters, 418, 103–114.

Zhu Y. (2012). Hydrothermal alteration recorded in chromite deposit: implication for mobility of platinum group elements, School of earth and space science, Perking University, Beijing 1008711, China.

APPENDICE A

Surface borehole showing PGE grade per ton

Saffy West UG2 grade

BH 004U	BH 005U	BH 008U	BH 0059U	BH 0065U	BH 0068U	BH 0087U	BH 0088U	BH 0055U
0.184	0.082	0.071	0.149	0.106	0.169	2.16	0.419	0.39
0.374	0.58	0.336	8.253	0.413	8.854	11.617	9.127	7.19
23.619	15.986	10.613	3.831	11.921	3.679	3.968	6.347	12.7
4.53	8.944	3.773	4.098	3.704	3.671	3.844	4.875	3.71
3.921	3.798	3.858	5.726	3.688	4.342	11.129	12.547	4.06
3.472	4.037	3.875	6.094	4.596	9.316	6.416	3.205	6.7
8.624	5.042	11.999	3.117	6.511	2.821	3.069	2.99	5.64
2.624	9.424	4.522	2.168	3.393	2.384	2.088	1.846	3.09
3.071	3.238	3.558		2.195	2.387			2.24
0.254	2.866	2.638		0.021				
	0.031	0.111						

Saffy East UG2 grade

BH 09D	BH 12D	BH 17D	BH 25D	BH 62D	BH 86D	BH 40D	BH 53D	BH 83D	BH 03D
0.07	0.061	0.085	0.279	0.097	0.161	0	0.57	0.355	0.141
0.243	0.102	0.128	0.255	0.25	9.88	6.4	9.92	8.892	0.196
12.797	12.08	5.027	5.627	10.899	4.353	17.6	3.36	3.854	6.07
3.559	4.696	4.251	7.551	5.083	4.492	6.73	4.25	3.586	2.764
3.939	4.084	3.732	3.678	3.688	9.938	3.85	35.86	12.601	2.765
5.751	7.141	3.797	3.97	3.682	3.417	10.8	2.58	5.927	6.245
6.778	4.681	17.062	6.801	18.32	3.652	2.92	2.61	3.207	5.296

2.689	3.193	7.633	4.101	3.545	2.44	2.81	2.64	2.214	1.916
2.927	2.086	3.566	2.286	2.95		1.66		0.08	1.627
2.085	0.151	3.502	0.093	1.943					0.066
0.149		0.149		0.154					

APPENDICE B

Microprobe analysis (wt. %) from Saffy West samples

Sample	MgO	Al2O3	SiO2	TiO2	V2O3	Cr2O3	MnO	FeO	NiO	ZnO	Total
416	8.87	16.24	0.04	0.84	0.29	44.87	0	29.44	0.15	0.1	100.85
416	8.63	16	0.01	0.93	0.28	45.77	0	27.95	0.16	0.12	99.84
416	8.47	16.28	0.02	0.95	0.21	46.41	0	27.85	0.19	0.08	100.46
416	8.35	16.24	0.03	1	0.25	46.54	0	28.06	0.14	0.19	100.8
416	8.51	15.95	0.01	0.87	0.25	45.5	0	29.21	0.18	0.04	100.52
416	7.95	14.97	0	0.93	0.28	44.55	0	28.49	0.13	0.05	97.36
416	8.49	16.18	0.02	0.89	0.28	46.03	0	27.63	0.14	0.16	99.82
416	8.45	15.34	0.02	0.87	0.24	44.83	0	28.53	0.15	0.06	98.49
416	8.64	16.1	0.02	0.96	0.28	44.63	0	29.07	0.13	0.09	99.91
416	8.52	15.83	0	0.87	0.26	45.72	0	29.37	0.15	0.13	100.84
Sample	**MgO**	**Al2O3**	**SiO2**	**TiO2**	**V2O3**	**Cr2O3**	**MnO**	**FeO**	**NiO**	**ZnO**	**Total**
415	8.8	15.6	0	1.1	0.3	45.26	0	28.07	0.14	0.08	99.36
415	8.72	15.53	0	1.08	0.37	46.06	0	27.95	0.15	0.1	99.95
415	8.61	15.62	0	1.13	0.34	45.12	0	27.56	0.12	0.02	98.52
415	8.95	15.62	0	1.07	0.35	45.35	0	27.73	0.16	0.08	99.32
Sample	**MgO**	**Al2O3**	**SiO2**	**TiO2**	**V2O3**	**Cr2O3**	**MnO**	**FeO**	**NiO**	**ZnO**	**Total**
419	8.41	15.58	0.19	0.93	0.4	45.66	0	28.44	0.11	0.09	99.81
419	8.61	15.05	0.01	0.89	0.29	44.92	0	28.81	0.16	0.15	98.88
419	8.88	15.52	0.04	0.95	0.37	46.72	0	28.13	0.14	0.15	100.91
419	8.4	14.3	0.02	0.99	0.3	46.39	0	28.28	0.12	0.18	98.97
419	8.5	15.02	0.01	1.01	0.25	45.99	0	28.02	0.08	0.16	99.05
419	8.53	14.84	0.01	0.91	0.4	46.78	0	27.99	0.08	0.16	99.69
419	8.59	14.87	0	1.07	0.34	47.02	0	28	0.13	0.21	100.22
419	8.63	14.97	0.03	0.9	0.33	45.27	0	28.24	0.09	0.02	98.5

419	8.56	15.05	0.02	1.06	0.3	46.08	0	27.84	0.1	0.1	99.11
419	8.79	15.29	0.03	1	0.3	46.09	0	28.43	0.12	0.22	100.27
Sample	**MgO**	**Al2O3**	**SiO2**	**TiO2**	**V2O3**	**Cr2O3**	**MnO**	**FeO**	**NiO**	**ZnO**	**Total**
418	8.11	14.1	0.03	1.35	0.37	44.75	0	29.48	0.13	0.1	98.43
418	7.86	13.58	0.03	1.09	0.33	45.82	0	29.32	0.13	0.04	98.2
418	8.43	14.49	0.01	1.25	0.31	45.65	0	29.27	0.1	0.18	99.7
418	8.15	14.21	0.01	1.25	0.32	45.98	0	29.34	0.12	0.11	99.49
418	8.51	14.65	0	1.22	0.31	46.01	0	29.55	0.11	0.13	100.5
418	8.17	13.85	0.03	1.25	0.34	45.54	0	29.47	0.17	0.17	99
418	8.45	14.68	0	1.18	0.31	45.42	0	29.45	0.1	0.12	99.71
418	8.35	13.88	0.02	1.35	0.32	45.71	0	28.82	0.11	0.08	98.64
418	8.52	14.35	0.03	1.24	0.37	45.31	0	28.97	0.13	0.14	99.06
418	8.59	14.76	0.02	1.39	0.41	45.15	0	29.15	0.12	0.11	99.69

APPENDICE C

Microprobe analysis (wt. %) from Saffy East samples

Sample	MgO	Al2O3	SiO2	TiO2	V2O3	Cr2O3	MnO	FeO	NiO	ZnO	Total
400	9.07	16.59	0.03	1.13	0.18	44.48	0	27.05	0.16	0.17	98.86
400	9.23	16.84	0.04	1	0.17	44.68	0	26.8	0.15	0.11	99.04
400	8.88	16.86	0	1.11	0.2	44.92	0	27.69	0.15	0.16	99.96
400	8.78	16.5	0.03	0.97	0.18	44.94	0	26.69	0.14	0.05	98.28
400	9.06	17.02	0	1.04	0.25	45.06	0	26.89	0.19	0	99.51
400	9.29	17.08	0.04	0.93	0.14	45.05	0	26.29	0.18	0.09	99.09
400	9.11	17.7	0.03	0.81	0.25	44.93	0	26.31	0.19	0.06	99.38
400	9.13	17.15	0.03	0.87	0.26	45.72	0	26.6	0.14	0.15	100.05
400	8.77	17.16	0	0.9	0.2	45.8	0	27.4	0.22	0.01	100.47
400	9.18	17.5	0.06	0.94	0.27	44.4	0	26.18	0.14	0.07	98.73

Sample	MgO	Al2O3	SiO2	TiO2	V2O3	Cr2O3	MnO	FeO	NiO	ZnO	Total
404	9.2	17.26	0.01	0.95	0.33	43.92	0	28.83	0.23	0.12	100.86
404	9.38	17.69	0.03	0.95	0.32	44.63	0	26.37	0.13	0.17	99.66
404	9.12	17.26	0.01	0.99	0.27	43.27	0	28.34	0.2	0.12	99.56
404	9.06	16.9	0.03	0.22	0.23	43.42	0	28.8	0.19	0.07	99.6
404	9.18	17.08	0.01	1.05	0.29	45.04	0	28.83	0.17	0.15	10.,81
404	9.03	16.71	0.05	0.79	0.31	43.62	0	28.42	0.18	0.06	99.17
404	9.17	16.66	0.02	0.97	0.27	45	0	28.19	0.19	0.07	100.53
404	9.38	17.2	0.03	0.95	0.25	44.44	0	27.74	0.16	0.11	100.28
404	9.13	17.24	0	0.95		43.81	0	28.64	0.19	0.11	100.3
404	9.15	17.36	0.02	0.94	0.24	43.36	0	28.53	0.21	0.12	99.92

Sample	MgO	Al2O3	SiO2	TiO2	V2O3	Cr2O3	MnO	FeO	NiO	ZnO	Total
407	8.38	14.61	0	1.16	0.35	44.79	0	31.42	0.1	0.12	100.93
407	8.56	15.09	0.03	1.07	0.32	45.73	0	28.73	0.11	0.14	99.77
407	8.56	14.46	0.01	1.24	0.35	44.57	0	31.44	0.15	0.03	100.81
407	7.9	13.7	0.02	1.22	0.29	44.76	0	30.97	0.17	0.14	99.18
407	8.4	14.76	0.03	1.25	0.37	45.97	0	29.77	0.12	0.1	100.77
407	7.87	13.92	0.03	1.16	0.35	44.36	0	31	0.14	0.12	98.96
407	8.51	14.57	0.01	1.18	0.35	45.3	0	29.35	0.13	0.08	99.49
407	8.33	14.66	0.05	1.19	0.39	46.45	0	29.21	0.15	0.16	100.59
407	8.24	14.7	0	1.27	0.29	44.1	0	31.3	0.13	0.16	100.18
407	8.07	13.95	0,02	1,1	0.34	45.35	0	31.78	0.13	0.12	100.87
Sample	**MgO**	**Al2O3**	**SiO2**	**TiO2**	**V2O3**	**Cr2O3**	**MnO**	**FeO**	**NiO**	**ZnO**	**Total**
412	8.9	15.37	0.03	0.94	0.37	45.02	0	27.65	0.11	0.04	98.41
412	8.95	15.67	0.03	1.19	0.36	45.9	0	27.57	0.18	0.06	99.92
412	8.78	15.67	0.01	1.22	0.36	45.43	0	28.06	0.14	0.13	99.79
412	8.57	15.67	0	1.13	0.32	45.58	0	27.9	0.16	0.11	99.44
412	8.95	15.16	0	1.1	0.37	45.77	0	27.48	0.1	0.11	99.06
412	8.72	14.93	0.04	1.06	0.38	45.94	0	27.42	0.15	0.24	98.87
412	8.79	15.47	0	1.04	0.39	46.99	0	27.63	0.13	0.1	100.54
412	8.85	15.88	0.01	0.99	0.36	45.76	0	27.17	0.11	0.04	99.16
412	8.91	15.47	0.02	1.14	0.33	45.9	0	27.19	0.12	0.11	99.2
412	8.73	15.49	0.01	1.2	0.41	47.05	0	27.27	0.09	0.09	100.35

APPENDICE D

Channel sampling PGE grade results

Saffy West chromitite channel samples

11W31Raise	11W31Raise	13W35Raise	13W35Raise	12W37Raise	12W37Raise	12W36Raise	12W36Raise	12W35Raise	12W34Raise	11W33Raise
PGM Grade	**PGM Grade**	**PGM Grade**	**PGM Grade**	**PGM Grade**	**PGM Grade**	**PGM Grade**	**PGM Grade**	**PGM Grade**	**PGM Grade**	**PGM Grade**
1.96	1.55	2.1	1.34	1.56	2.04	1.58	2.76	1.79	2.49	2.51
2.64	2.6	4.11	3.21	3.12	3.56	1.63	1.79	2.68	2.5	2.81
9.62	0.04	10.15	6.81	2.99	3.71	1.97	2.08	7.2	6.52	4.37
5.64	6.13	5.9	8.18	11.5	4.86	15.21	5.35	13.13	0.04	4.93
3.46	3.09	0.04	3.56	2.64	7.89	6.2	5.07	2.67	7.08	8.61
0.04	3.74	2.81	3.24	0.04	9.46	4.17	5.41	4.18	4.82	3.96
4.98	4	2.89	3.31	2.76	4.34	5.39	4.83	4.44	4.7	3.8
9.58	7.24	4.5	3.96	6.56	3.22	9.39	9.2	8.59	14.28	5.23
0.86	0.47	0.04	7.82	3.94	9.36	0.04	0.76	0.4	0.39	8.59
			0.04	0.04	0.97					0.04

Saffy East chromitite channel samples

10E19 Raise	10E19 Raise	10E24Raise	10E24Raise	11E24Raise	11E24Raise	12E22Raise	12E22Raise	12E23Raise	12E23Raise	12E24 Raise	15E16Raise
PGM Grade	PGM Grade	PGM Grade	PGM Grade	PGM Grade	PGM Grade	PGM Grade	PGM Grade	PGM Grade	PGM Grade	PGM Grade	PGM Grade
3	1.6	3.23	1.68	1.89	1.62	2.15	1.87	1.55	1.55	1.55	1.96
5.88	2.28	1.79	2.92	2.27	2.34	3.19	2.73	2.23	1.88	1.78	1.72
5.68	4.18	5.2	4.46	2.86	7.78	2.75	3.08	3.01	2.26	1.74	2.46
4.96	5.72	6.09	2.8	9.04	3.89	9.19	5.1	5.11	9.01	2.4	12.72
3.4	3.8	3.85	6.91	4.6	15.75	5.09	14.01	3.95	3.41	4.57	4.12
10.2	5.92	5.42	1.08	3.23	9.79	3.91	3.44	4.43	2.61	3.53	5.16
11.04	3.96	0.04	4.23	0.04	4.56	12.55	8.28	2.8	4.31	4.85	0.8
0.04	7.48	0	5.22	7.04	5.69	0.04	0.04	11.49	4.11	7.58	0
		0.24	0.04	0.04	6.16		0	0.04	9.97	0.04	0.04
					7.63		0.04		0.04		
					0.04						

APPENDICE E

Cr# and Mg#

SaffyEast chromitite Mg# and Cr#

	Sample no	**407**	**407**	**407**	**407**	**407**	**407**	**407**	**407**	**407**	**407**
Mg#	**Mg/Mg+Fe2**	39.5	40.75	40.27	38.04	39.58	38	40.59	39.46	39.01	38.31
Cr#	**Cr/Cr+Al**	67.29	67.03	67.4	68.67	67.63	68.13	67.59	68.01	66.8	68.56
	Sample no	**404**	**404**	**404**	**404**	**404**	**404**	**404**	**404**	**404**	**404**
Mg#	**Mg/Mg+Fe2**	42.98	44.15	43.02	43.81	42.46	43.06	43	43.96	42.82	43.05
Cr#	**Cr/Cr+Al**	63.06	62.86	62.71	63.28	63.89	63.65	64.44	63.41	63.03	62.62
	Sample no	**400**	**400**	**400**	**400**	**400**	**400**	**400**	**400**	**400**	**400**
Mg#	**Mg/Mg+Fe2**	16.26	43.75	41.76	42.09	42.74	44.03	43.16	43.06	41.23	43.62
Cr#	**Cr/Cr+Al**	64.27	64.03	64.12	64.63	63.98	63.89	63	64.14	64.16	62.99
	Sample no	**412**	**412**	**412**	**412**	**412**	**412**	**412**	**412**	**412**	**412**
Mg#	**Mg/Mg+Fe2**	42.84	42.25	41.51	40.77	42.73	41.92	41.51	42.21	42.41	41.15
Cr#	**Cr/Cr+Al**	66.27	66.27	66.04	66.12	66.95	67.36	67.08	65.91	66.56	67.08

Saffy West chromite Mg# and Cr#

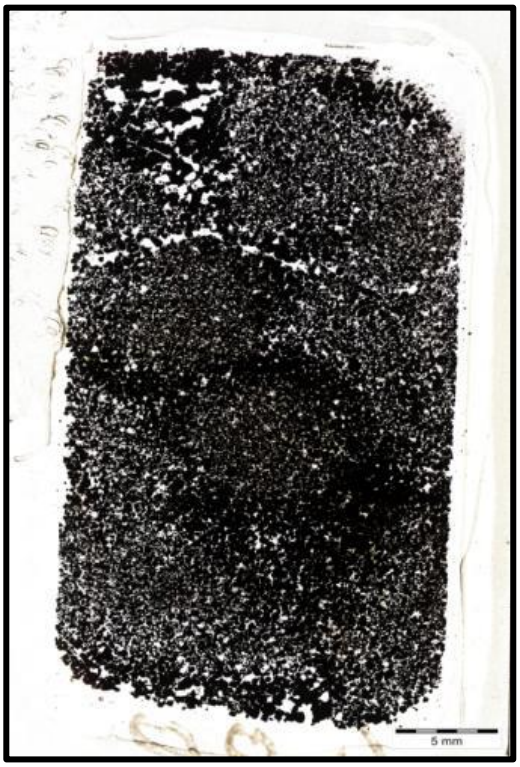
	Sample no	**416**	**416**	**416**	**416**	**416**	**416**	**416**	**416**	**416**	**416**
Mg#	**Mg/Mg+Fe2**	41.77	41.03	40.02	39.37	40.28	38.93	40.44	40.82	40.96	40.25
Cr#	**Cr/Cr+Al**	64.95	65.74	65.66	65.78	65.68	66.63	65.62	66.22	65.03	65.96

	Sample no	415	415	415	415						
Mg#	Mg/Mg+Fe2	41.84	41.34	41.25	42.58						
Cr#	Cr/Cr+Al	66.06	66.55	65.96	66.07						
	Sample no	419	419	419	419	419	419	419	419	419	419
Mg#	Mg/Mg+Fe2	42.09	41.47	41.87	40.54	40.79	40.88	40.81	41.67	40.99	41.67
Cr#	Cr/Cr+Al	66.28	66.69	66.88	68.52	67.26	67.89	67.96	66.98	67.26	66.91
	Sample no	418	418	418	418	418	418	418	418	418	418
Mg#	Mg/Mg+Fe2	39.09	38.32	40.12	38.97	40.19	39.33	40.21	40.11	40.8	40.68
Cr#	Cr/Cr+Al	68.04	69.36	67.88	68.46	67.81	68.81	67.49	68.84	67.93	67.24

APPENDICE F

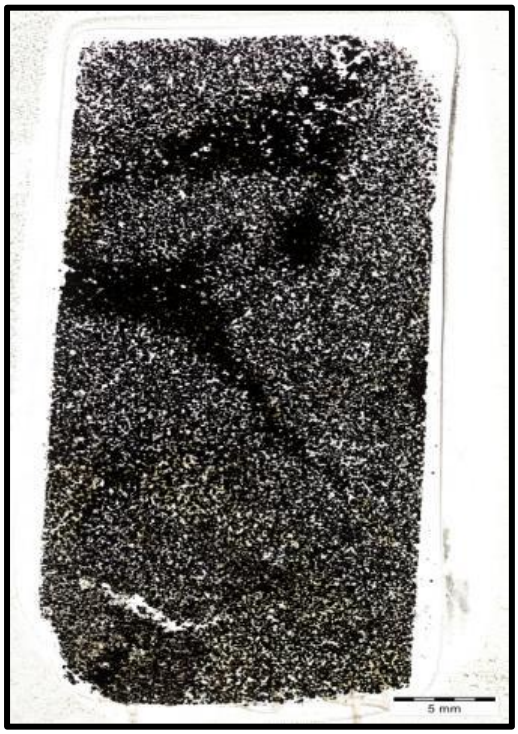
Thin section images from Saffy East and West chromitite samples

Sample 400 of Saffy East





Sample 404 Saffy East

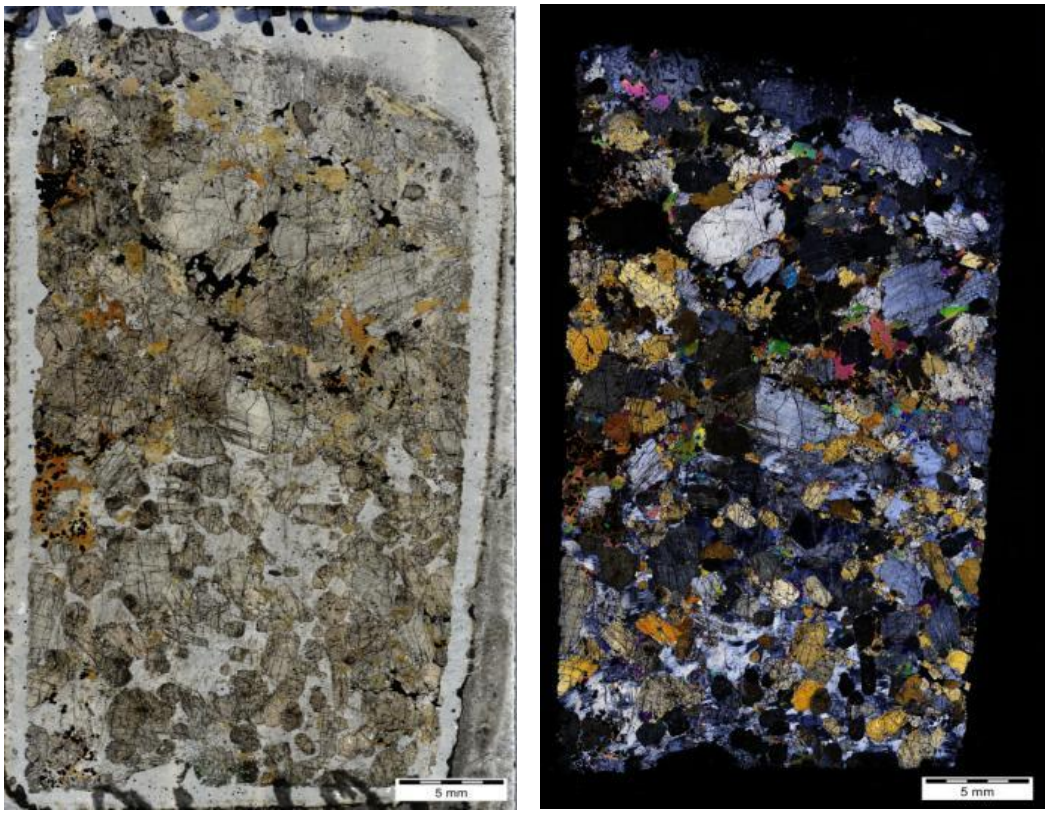




Sample 407 of Saffy East



Sample 410 (2) of Saffy East

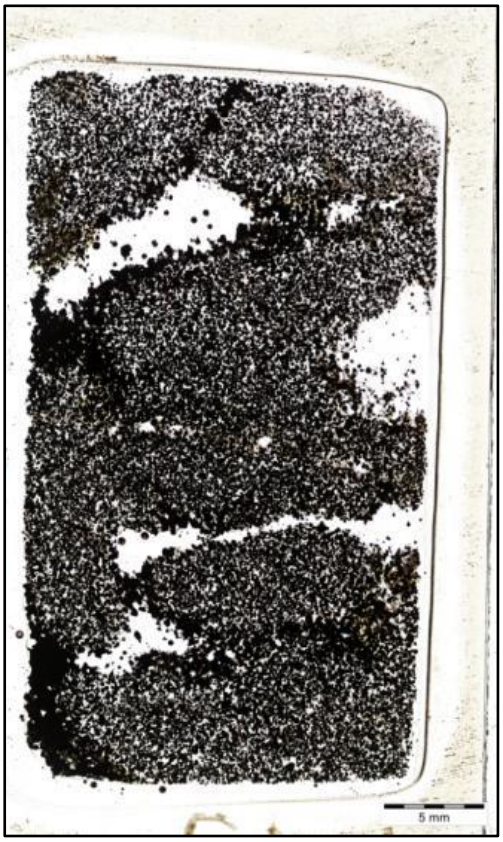


Sample 410 of Saffy East





Sample 412 of Saffy East





Sample 415 of Saffy West



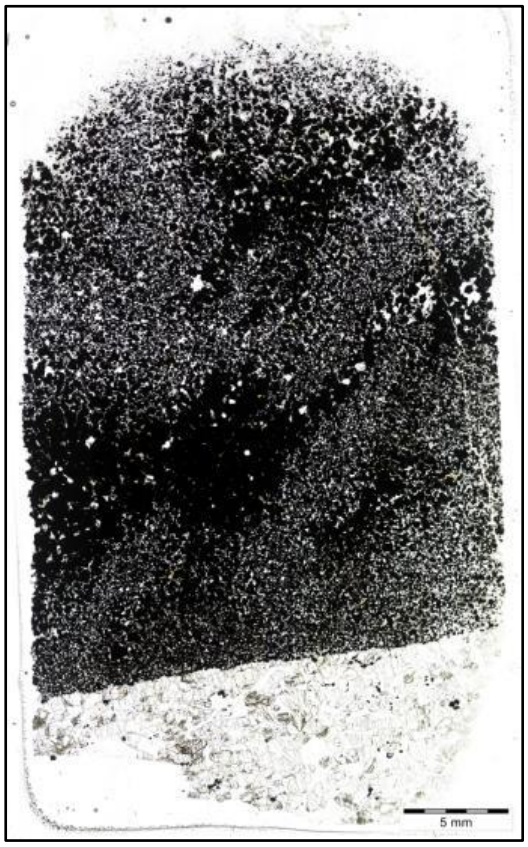


Sample 416 of Saffy West



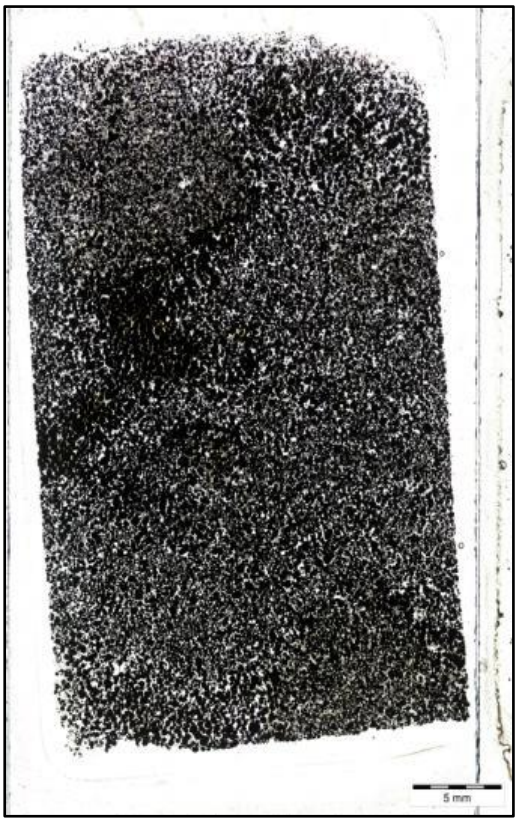


Sample 418 of Saffy West





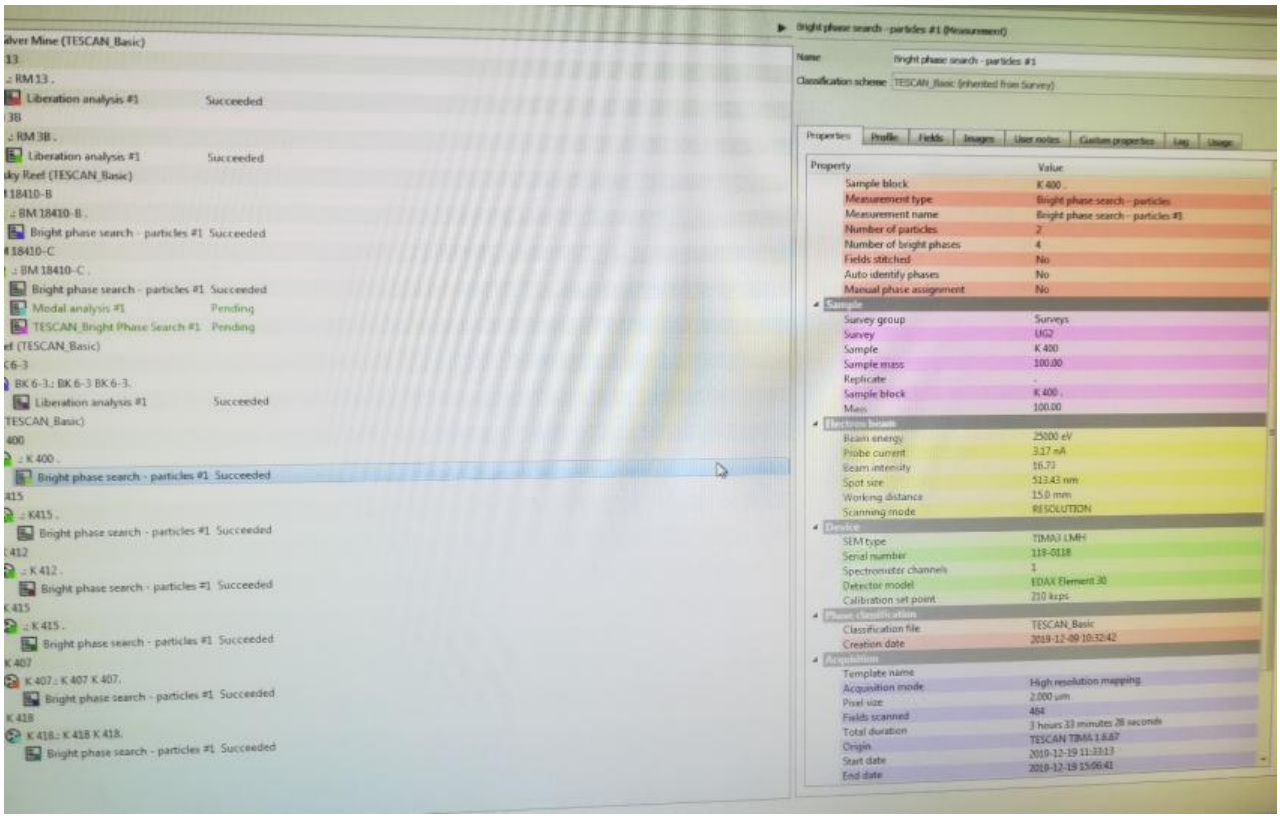
Sample 419 of Saffy West



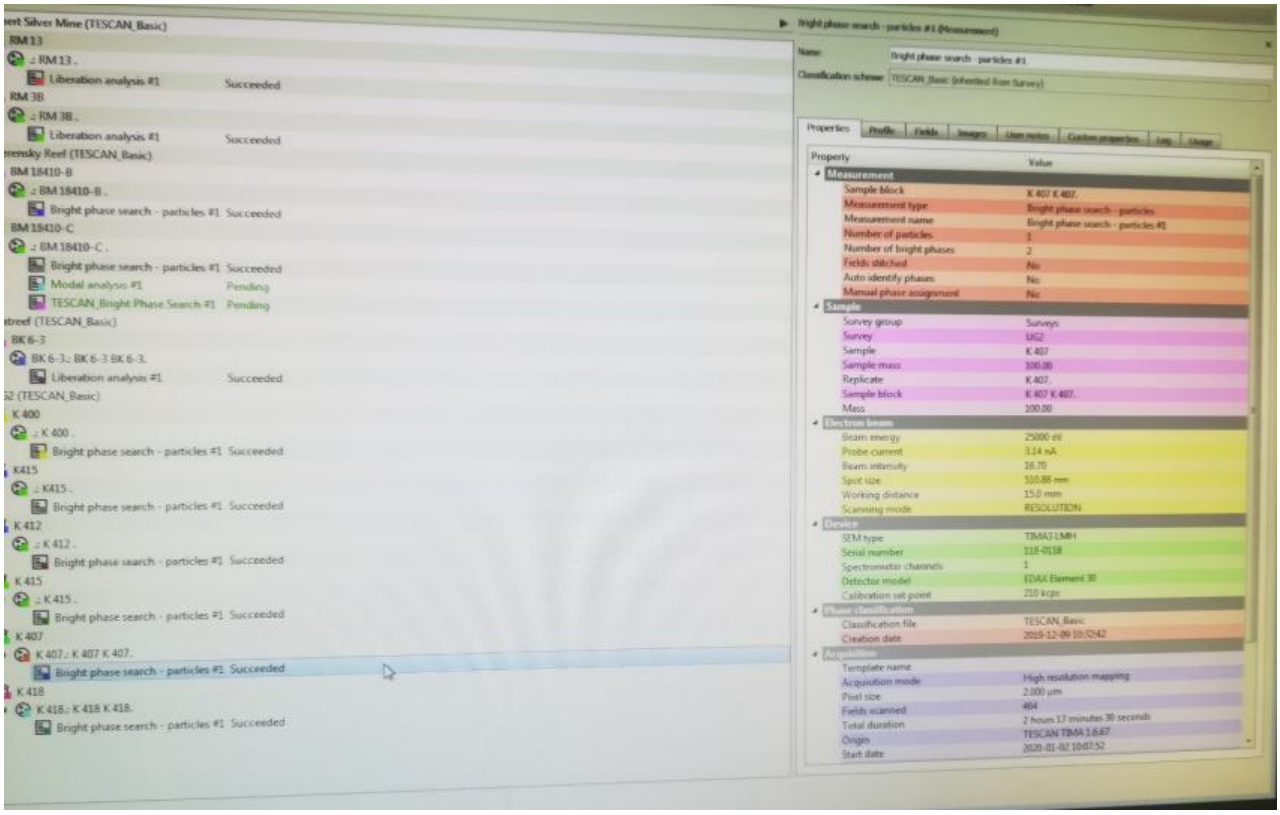


APPENDICE G

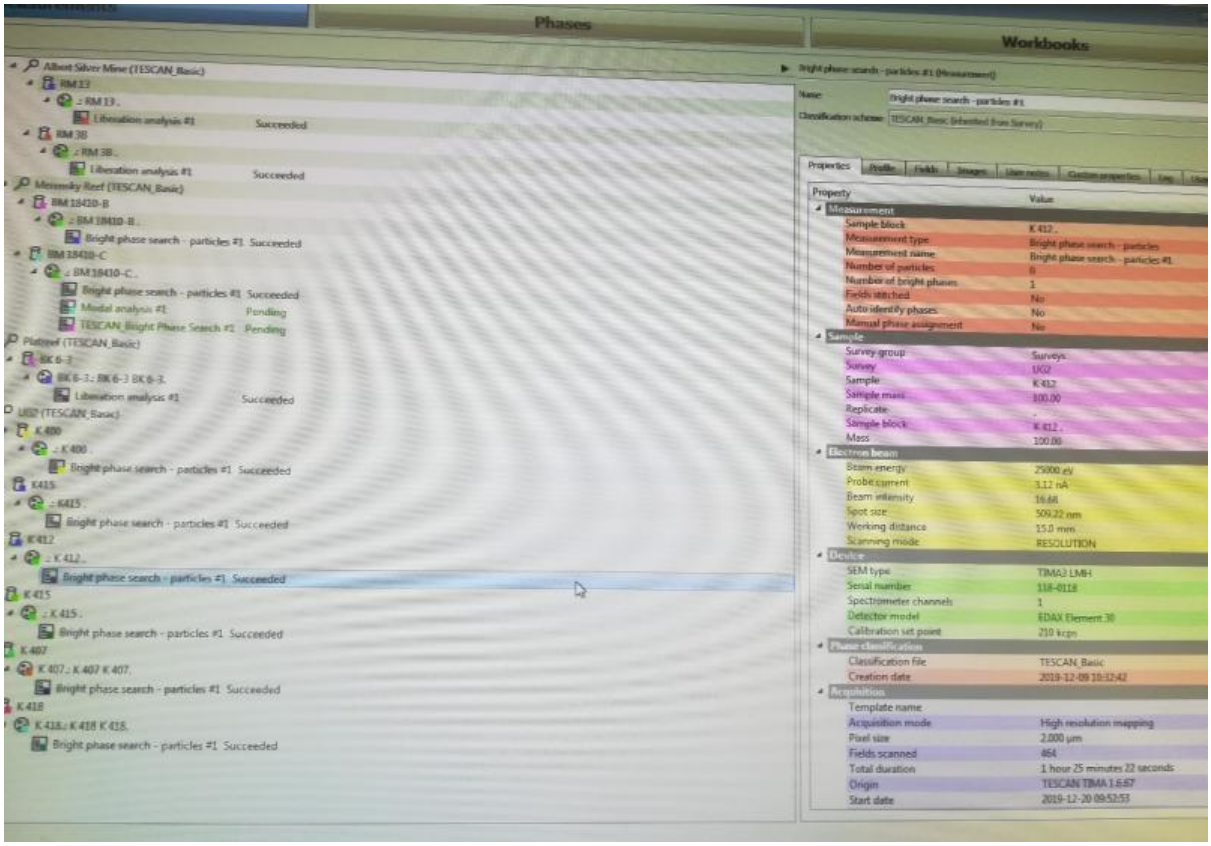
1.) Saffy East Bright Phase Search



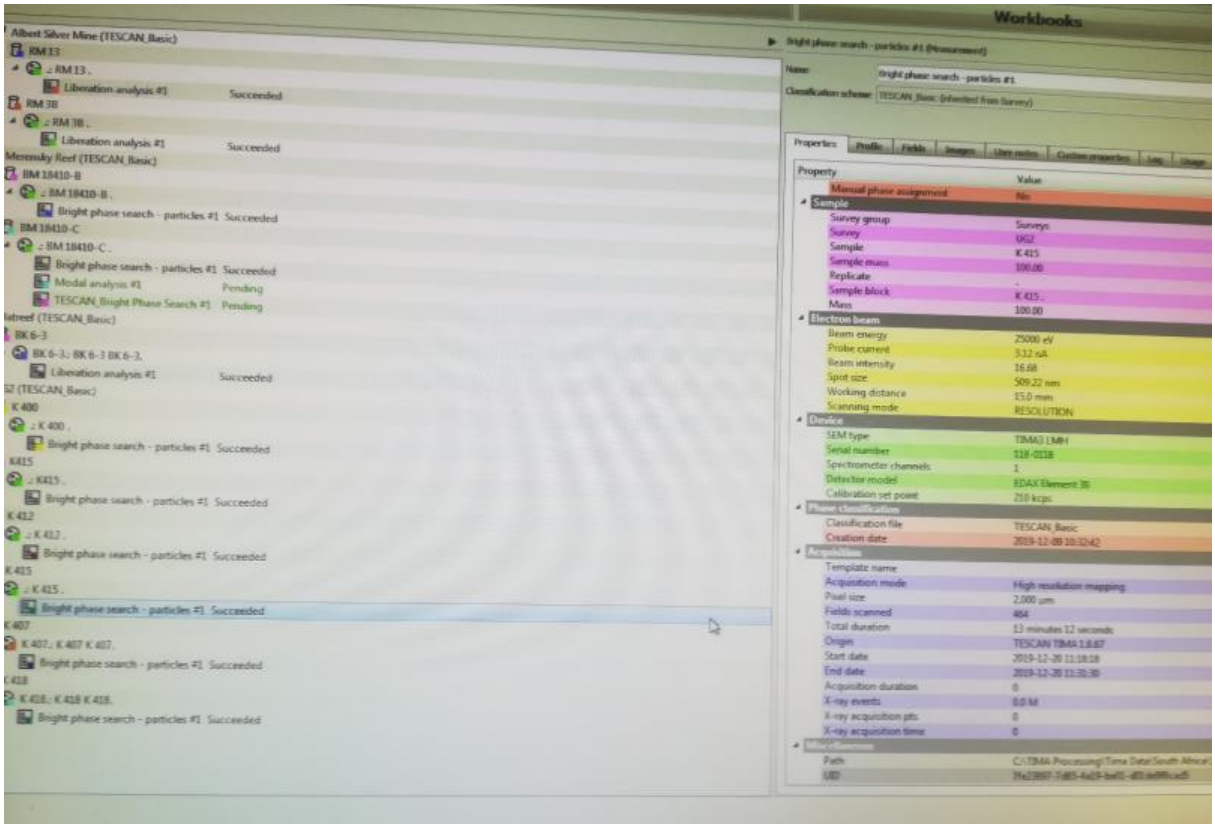
2.) Saffy East Bright Phase Search



3.) Saffy East Bright Phase Search



4.) Saffy West Bright Phase Search



5.) Saffy West Bright Phase Search

